To my father, Robert Hall,

who inspires me to be my best

and to my wife,

Traci, who would have it no other way.

DEVELOPMENT OF TEST APPARATUS FOR EXAMINING THE FRETTING FATIGUE POTENTIAL OF POST-TENSIONED, EXTERNAL TENDONS IN BOX-GIRDER DEVIATOR DUCTS

John E. Breen

Michael E. Kreger

DEVELOPMENT OF TEST APPARATUS FOR EXAMINING THE FRETTING FATIGUE POTENTIAL OF POST-TENSIONED, EXTERNAL TENDONS IN BOX-GIRDER DEVIATOR DUCTS

by

CLIFF RAYMOND HALL, B.S.

REPORT

Presented to the Faculty of the Graduate School of

The University of Texas at Austin

in Partial Fulfillment

of the Requirements

for the Degree of

MASTER OF SCIENCE IN ENGINEERING

THE UNIVERSITY OF TEXAS AT AUSTIN

DECEMBER 1990

ACKNOWLEDGEMENTS

This research program was conducted at the Phil M. Ferguson Structural Engineering Laboratory at the Balcones Research Center of the University of Texas at Austin. Funding for this research project was provided by the Texas State Department of Highways and Public Transportation.

The author would like to thank Dr. John E. Breen for his guidance and encouragement throughout this research. Thanks also to Dr. Michael E. Kreger for his friendship and insight, and for keeping me current with the Illini.

A special thanks is given to the staff at Ferguson Laboratory without whom this project could not have been completed. Thank you Pat Ball, Sharon Cunningham, Wayne Fontenot, Jean Gehrke, Laurie Golding, Wayne Little, and Blake Stasney for all you have done for me. Appreciation and encouragement go out to graduate student Karen Ryals for her help with this project and her success in its continuation. Thanks also, to Gregor Wollmann who provided me with all his knowledge, at least what he could remember, about fretting fatigue.

To the friends I have found while I was here; Chris (Chriff) Higgins, Brian (Dude, don't do it dude) Falconer, Todd (Never late for class) Helwig, Donna (Donner) Mader, Brock (Brockey) Radloff, Azez (1000 times I tell you) Hindi, Tony (Carbonara) Powers, Paco (I'll meet you there) Noyola, Jose (Environmentalist Hunter) and Maria Arrellaga, Reed and Lynn (Pearl Light and Big Car) Freeman, Brett (Ski Nautique) Phillips, and Les (Calf Buster) Zumbrunnen, thanks for making it seem like fun.

To my families, the Halls, the Winborns, and the Brockhoffs, thanks for being there when we needed you, and providing us with love, encouragement, and a place to relax.

Finally, thank you Traci for allowing me to pursue my dreams. I love you.

TABLE OF CONTENTS

CHAPTER 1 INTRODUCTION 1

1.1 General 1

1.2 Objectives 6

1.3 Scope 6

CHAPTER 2 FRETTING POTENTIAL IN EXTERNAL TENDON SYSTEMS 7

2.1 General 7

2.2 Fatigue of Post-Tensioned Concrete 7

2.2.1 General. 7

2.2.2 Post-Tensioned Concrete. 9

2.2.3 Conclusions From Previous Research. 15

2.3 Fatigue of External Tendons 19

2.3.1 Expected Problems. 19

2.3.2 Previous Studies. 19

CHAPTER 3 TEST PROGRAM DEVELOPMENT 24

3.1 General 24

3.2 Development of the Concrete Segment 24

3.2.1 Controlling Factors. 24

3.2.2 Segment Configuration. 26

3.2.3 Model Scale and Final Dimensions. 28

3.2.4 Layout of Deviator Duct. 31

3.3 Development of the Test Setup 31

3.3.1 Controlling Factors. 31

3.3.2 General Layout. 32

3.3.3 Loading Concept. 32

3.3.4 Tendon Anchorage. 36

3.3.5 Stressing Frames. 38

3.3.6 Segment Supports. 40

3.3.7 Safety Precautions. 43
3.3.8 Overall Layout. 43

CHAPTER 4 DESIGN AND CONSTRUCTION 46
4.1 Concrete Segment 46
4.1.1 Tendon Forces. 46
4.1.2 Design of the Deviator Sections. 48
4.1.2.1 Deviator Forces. 48
4.1.2.2 Deviator Reinforcement. 48
4.1.3 Design of the Box Segment. 49
4.1.3.1 Loading and Reactions. 49
4.1.3.2 Box Segment Reinforcement Design. 49
4.1.4 Fabrication of Segment. 53
4.1.4.1 Formwork. 53
4.1.4.2 Reinforcing Cage. 55
4.1.4.3 Concrete Placing. 55
4.2 Test Apparatus 58
4.2.1 Design of the Loading System. 58
4.2.2 Design of the Stressing and Anchorage Frames. 60
4.2.3 Design of the Segment Longitudinal Supports. 64
4.2.4 Design of the Segment Lateral Supports. 70
4.2.5 Fabrication and Installation of the Test Setup. 70

CHAPTER 5 TEST PROGRAM 72
5.1 Instrumentation 72
5.1.1 Strain Gages. 72
5.1.2 Other Instrumentation. 72
5.1.3 Test Equipment. 73
5.2 Post-Tensioning 75
5.2.1 Procedure. 75
5.2.2 Materials. 77

5.2.2.1 Prestressing Strand. 77
5.2.2.2 Primary Wedges. 77
5.2.2.3 Grout. 80
5.3 Fretting Fatigue Testing 80
5.3.1 Dynamic Tests. 80
5.3.2 Static Tests. 82

CHAPTER 6 SUMMARY AND RECOMMENDATIONS 83
6.1 Summary 83
6.2 Recommendations 85

APPENDIX A SEGMENT DESIGN CALCULATIONS 86

APPENDIX B TEST SETUP DESIGN CALCULATIONS 99

LIST OF FIGURES

1.1 Cross-section of Typical Post-Tensioned Box-Girder Segments 2
1.2 Typical Shapes for External Tendon Deviators (from Powell [26]) 4
1.3 Cross-Section of Deviator 5
1.4 Typical Post-Tensioned Segmental Box-Girder Span (after Long Key Bridge from Powell [26]) 5
2.1 Typical Fatigue Strength Plot (S-N Curve) 8
2.2 Strand-in-Air Failure Zone (from Paulson [25]) 8
2.3 Cracked Post-Tensioned Beam (after Wollman and Yates [35,36]) 10
2.4 Schematic Representation of Fretting Mechanism (from Yates [36]) 12
2.5 Fatigue Crack Characteristics (from Waterhouse [31]) 12
2.6 Impact of Fretting on Fatigue Life (after Waterhouse [31]) 14
2.7 Effect of Slip Amplitude on Fretting Fatigue (from Yates [36]) 14
2.8 Reduced Beam Specimens for Fatigue of Post-Tensioned Concrete (from Georgio [13]) 16
2.9 Scaled Beam Specimens for Fatigue of Post-Tensioned Concrete (from Georgio [13]) 17
2.10 Tendon Stress Condition at Deviator Contact Points (from MacGregor [19,20]) 20
2.11 Cable Systems Tested by Eibl and Voss [9,10,11]) 22
2.12 Test Setup Used by Eibl and Voss [9,10,11]) 22
3.1 Powell/Beaupre Test Setup (from Powell [26]) 25
3.2 Initial Deviator Segment Details Considered 27
3.3 Test Segment: Original Model 29
3.4 Test Segment: Original Model Modified for Easier Construction 30
3.5 Increases in Tendon Stresses Caused by Deflection of Span (after Virlogeux [30]) 34
3.6 Preliminary Loading Concepts 35
3.7 Typical Anchorage Detail for Post-Tensioned Tendons (after Jartoux and LaCroix [15]) 37

3.8 Double-Chuck Grip System for Strand Anchorage (after Lamb [17] and Paulson [25]) 37
3.9 Double-Chuck Grip System for Multi-Strand Anchor Head 39
3.10 Schematic of Strand Alignment Problem 39
3.11 Post-Tensioning Frame Attached to Concrete Buttress 41
3.12 Reactions on Deviator Segment 42
3.13 Adjustable, Frictionless Horizontal Supports for Deviator Segment 44
3.14 Schematic of Test Setup (Elevation) 45
4.1 Segment Support Conditions, (a) During Post-Tensioning, (b) During Testing 47
4.2 Deviator Reinforcement Scheme 50
4.3a Box Segment Reinforcement Layout 51
4.3b Box Segment reinforcement Schedule 52
4.4 Specimen Formwork 54
4.5 Deviator Pipe Size and Location 56
4.6 Reinforcing Cage in Formwork 57
4.7 Consolidation of Concrete During Casting 57
4.8 Loading System 59
4.9 Post-Tensioning Frame 61
4.10 Completed Post-Tensioning Frame 62
4.11 Anchor Head Attachment Plate 63
4.12 Chair for the Stressing Ram 65
4.13 Alignment Details for External Tendons with 10 Degree Deviation Angles . . . 66
4.14 Assembled Alignment Details 67
4.15 Horizontal Supports for Segment 68
4.16 Assembled Horizontal Specimen Supports 69
5.1 Test Equipment 74
5.2 Equipment for Post-Tensioning and Seating 76
5.3 Strand-in-Air Test Setup (after Paulson [25]) 78
5.4 Strand-in-Air Test Results 79
5.5 Three Piece Copper Wedge Used in the Primary Chuck 79
5.6 Grout Injection Detail (after Radloff [27]) 81

CHAPTER 1
INTRODUCTION

1.1 General

The use of segmental concrete box-girder construction in medium to moderately long span bridges is rapidly increasing throughout the United States. Recent developments have led to the use of external tendons (tendons outside of the concrete section), as opposed to traditional internal tendons (tendons contained in ducts within the webs or flanges). External tendon construction provides substantial economic savings due to a more efficient web section and simplifies construction by relieving reinforcing congestion thus allowing easier placement and better compaction of the web concrete as illustrated in Figure 1.1. Examples of this type of construction can be seen, among other places, in bridges connecting the Florida Keys and in several miles of elevated highway in San Antonio. The growing use of external post-tensioned box-girders in bridge structures creates a need for greater knowledge about the behavior of the system. Research has been performed on the strength and detailing of the tendon deviation points (known as deviators) [4,26] but little is known about the effect on the tendon of the relatively pronounced angle change in the deviator region under cyclic loading. In such a relatively new type of construction with a potential for fatigue degradation, studies should be performed under cyclic loading to ensure the long life of the system.

Since there has been limited research performed in the area of fatigue of external tendons, a review of previous research on fatigue of prestressed concrete is necessary to foresee any potential problems. Previous studies of prestressed concrete have shown that the fatigue failure of the girder is governed by the fatigue failure of the tendon. In the studies of post-tensioned concrete, premature fatigue failures in cracked sections often occurred in the tendon strands and were caused by a condition known as fretting [22,34,36]. Fretting is the surface damage caused by minute slippage between two contacting surfaces, usually metal. The damage to the material caused by fretting includes abrasive wear, corrosion, and fatigue cracking. A result of fretting, which can significantly reduce the fatigue life of the material

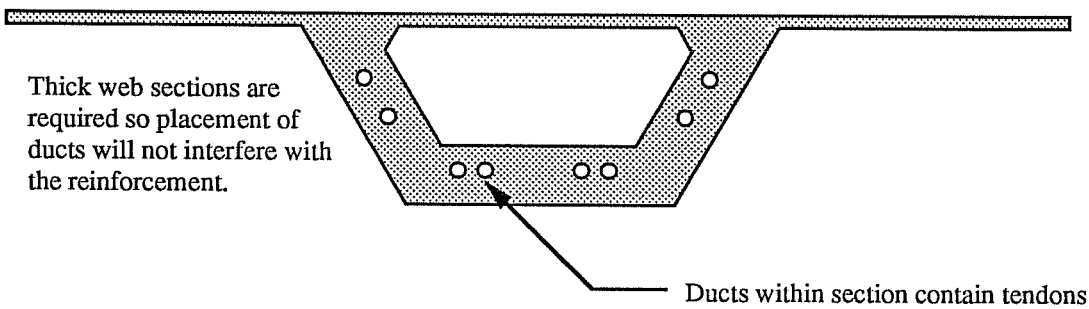

a) Section with internal tendons

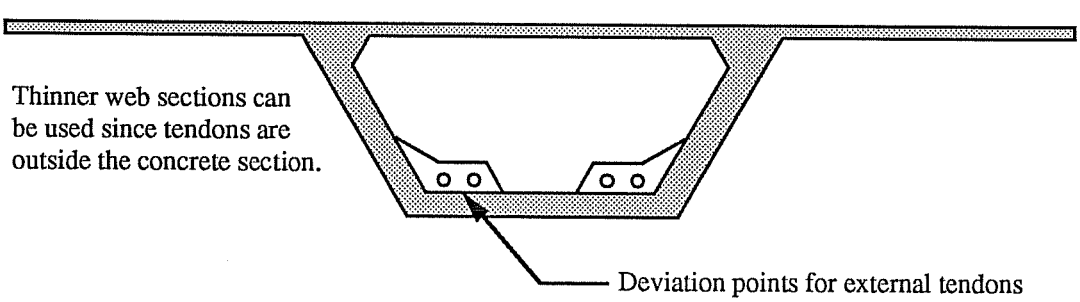

b) Section with external tendons

Figure 1.1 Cross-Sections of Typical Post-Tensioned Box-Girder Segments

through the formation and propagation of fatigue cracks in the tendon, is known as fretting fatigue. The details of an external post-tensioned box-girder system, as in typical post-tensioned girders, seemingly include many of the aspects necessary for fretting fatigue to occur in the tendon. These include fluctuating axial tendon stresses, metal-to-metal contact (tendon to duct) under a high contact pressure, and slip potential.

The external post-tensioned box-girder maintains the draped profile of the tendons by passing the tendons through a series of deviators. There are three common deviator configurations used for external tendons; the diaphragm (see Figure 1.2a), the rib or stiffener (see Figure 1.2b), and the saddle or block (see Figure 1.2c). Each of these deviator types are reinforced concrete projections which are cast monolithically with the girder section and contain curved rigid ducts (typically metal) to allow the external tendon to pass through (see Figure 1.3) [26]. During post-tensioning, the tendon comes into contact with the duct. Upon completion of post-tensioning, the tendons, which are usually encased in polyethylene pipes running from the anchorage zones to the tendon deviators, are typically grouted for corrosion protection along their entire length. Figure 1.4 illustrates the layout of the tendons, deviators, and anchorage zones in a typical span. The overall system is considered unbonded for design purposes since the majority of the tendon is not bonded to the concrete section and the stresses in the tendon are largely independent of the stresses in the adjacent concrete section [26]. Because the deviators are the only attachment points, other than the anchorage zones, of the tendon to the concrete section, the deviators are locations of high stress concentrations on the tendon. With respect to the tendon the deviators also represent an area of two (or more) contacting surfaces of high local transverse contact pressure, and an area of potential slip during cyclic loads - conditions necessary for fretting to occur. This report documents the initial phase of a research project intended to explore this potential problem. The focus of this report is on the development of a test method for studying fretting fatigue in external tendons of box-girders.

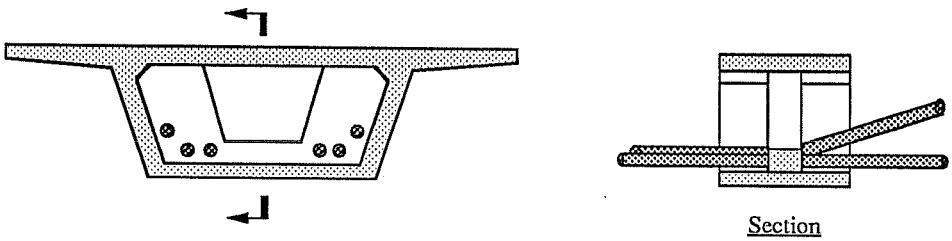

a) Diaphragm deviator

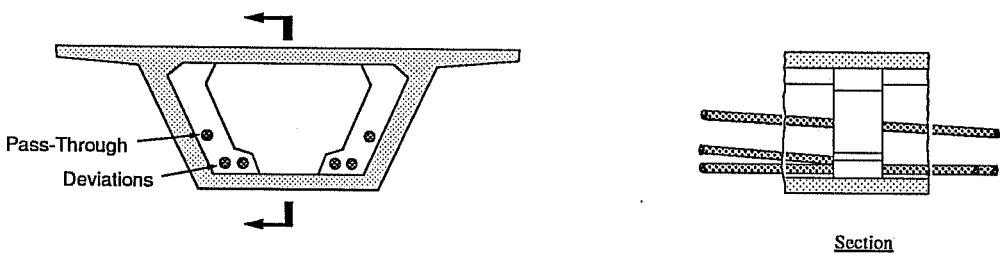

b) Rib or stiffener deviator

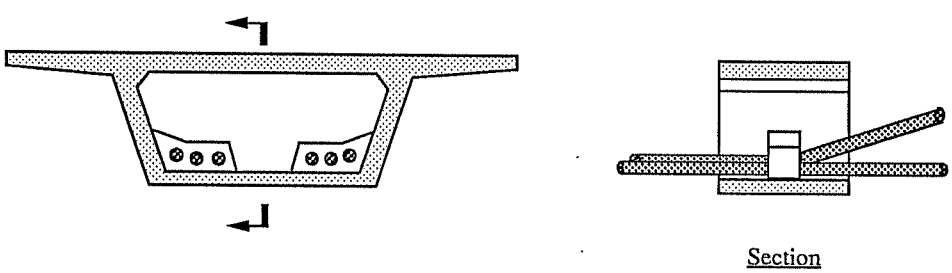

c) Saddle or block deviator

Figure 1.2 Typical Shapes for External Tendon Deviators (from Powell [26])

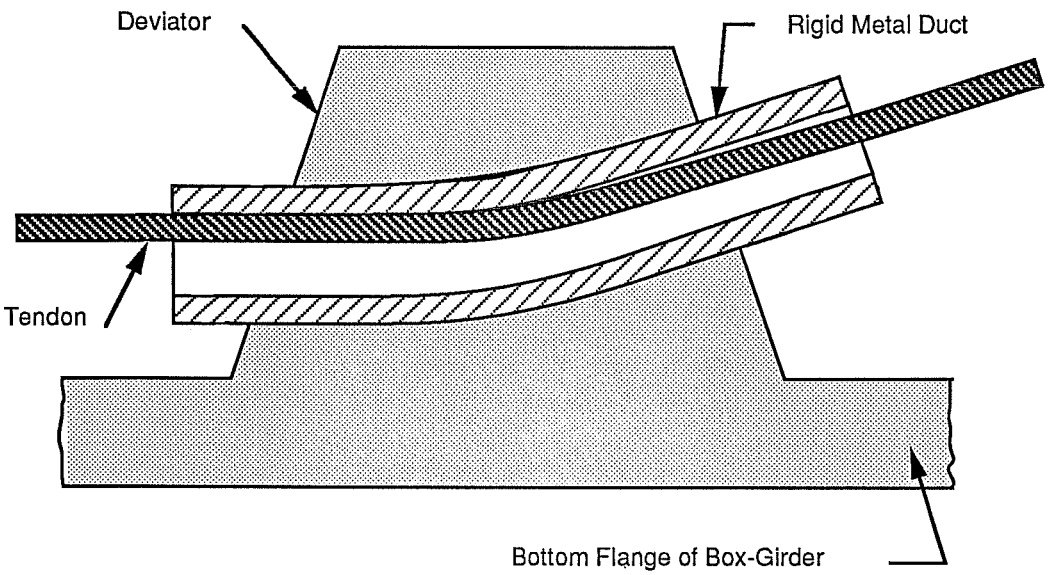

Figure 1.3 Cross-Section of Deviator

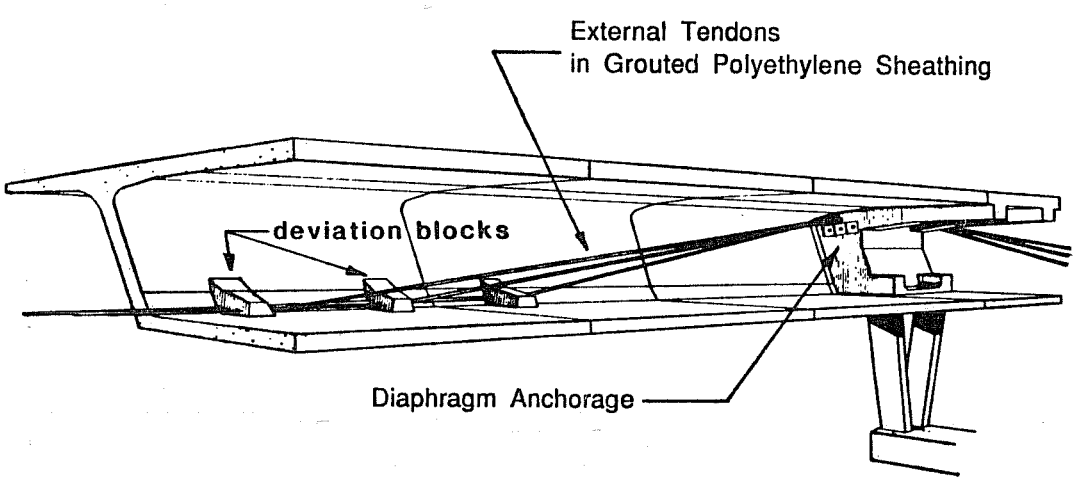

Figure 1.4 Typical Post-Tensioned Segmental Box-Girder Span
(after Long Key Bridge from Powell [26])

1.2 Objectives

The objectives of this research are

1) to update current research on fatigue of external post-tensioned box-girders,
2) to devise a test method to be used in the study of the effects of fretting fatigue at the deviators of external post-tensioned box-girders,
3) to design and construct a test set-up that will enable these future studies to be performed.

1.3 Scope

This report focuses on the development and construction of a test setup to be used in the study of external post-tensioned tendons under fatigue loading. Chapter 2 presents a brief background on fretting fatigue, previous research on fatigue of post-tensioned beams, and the fatigue problems to be expected in the external tendons. Also a summary of the limited research reported on fatigue in external tendons is presented.

Chapter 3 covers the development of the testing method, specimen, and set-up, while Chapter 4 covers the design and construction of the specimen and test set-up. Chapter 5 explains the required instrumentation and equipment as well as the stressing and testing procedures. Finally, a summary of the report along with some recommendations for future testing, are presented in Chapter 6 and the design calculations for the concrete segment and the test setup are included in Appendices A and B respectively.

CHAPTER 2
FRETTING POTENTIAL IN EXTERNAL TENDON SYSTEMS

2.1 General

This chapter presents a brief review of results and conclusions from previous pretensioned and post-tensioned beam tests pertinent to external tendon construction, a brief introduction into fretting fatigue, and a literature review update on fatigue of external tendons. The interested reader is referred to Yates [36], Wollmann [35], and Diab [8] for an extensive review of fretting fatigue, fatigue of pretensioned concrete, and fatigue of post-tensioned concrete and to Powell [26] for the state-of-the-art of external post-tensioning.

2.2 Fatigue of Post-Tensioned Concrete

2.2.1 General. Fatigue is the failure of a material after a number of repeated load cycles at a stress level below the level which would cause failure if the load was applied statically. The fatigue mechanism begins with the initiation of a surface crack at a stress concentration (which can be caused by local pressures, surface flaws, cracks, or even welds) under fluctuating stresses. The mechanism continues with the propagation of the initial surface crack until the crack grows to a critical depth and brittle fracture occurs. As the range of the fluctuating stress increases, the growth rate of the crack increases also. The stress range where there is no crack propagation is known as the endurance limit. A typical plot of fatigue strength (stress range, S) versus fatigue life (number of load cycles, N) is shown in Figure 2.1. These plots are typically referred to as S-N curves and are plotted on a log-log scale.

Early research on fatigue of prestressed concrete did not distinguish post-tensioned concrete from pretensioned concrete and all the focus was on pretensioned concrete. The fatigue life of pretensioned concrete has been shown by various researchers to be directly related to the fatigue life of the prestressing tendon [12,24]. Therefore, strand-in-air tests (fatigue tests performed on a single isolated strand) can be used to predict the fatigue life of a pretensioned concrete beam - cracked or uncracked. Figure 2.2 shows n S-N plot from the

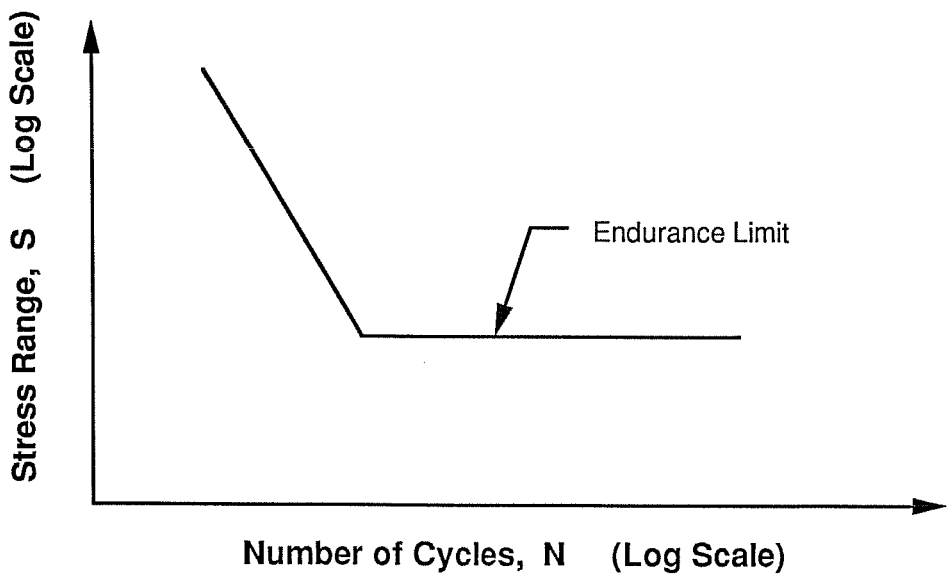

Figure 2.1 Typical Fatigue Strength Plot (S-N Curve)

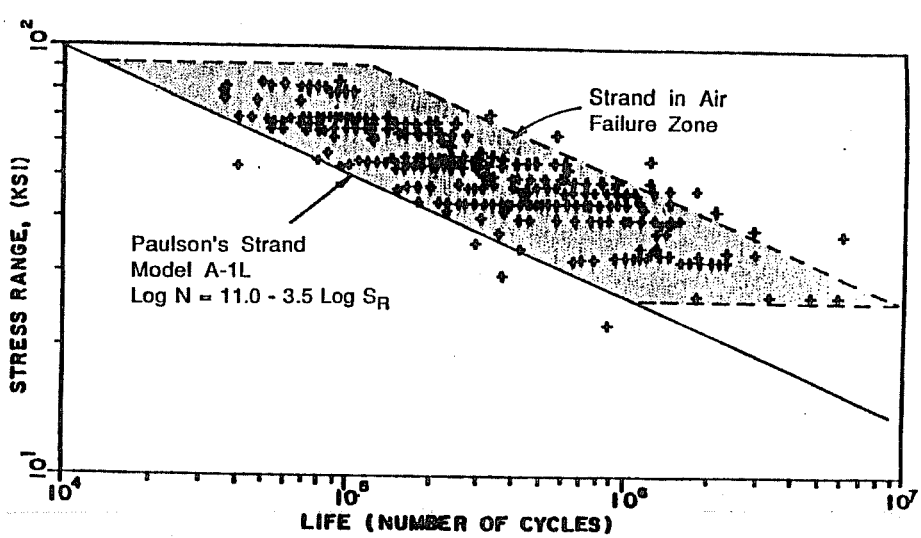

Figure 2.2 Strand-in-Air Failure Zone (from Paulson [25])

results of over 700 strand-in-air tests compiled by Paulson [25] and gives a recommended lower five percentile fracture design model for the fatigue life of prestressing strand. Recently, however, considerable research has been performed which suggests that the fatigue life for post-tensioned concrete is substantially lower than that predicted for pretensioned concrete.

2.2.2 Post-Tensioned Concrete. As research progressed to the study of post-tensioned concrete, a disturbing trend was observed which was not found in pretensioned concrete. When cracked sections of post-tensioned concrete were tested under fatigue loading (fatigue is generally not a problem in uncracked sections), the tendons failed prematurely. After considerable investigation of the details and failures, a number of conditions were cited as the cause for these premature failures.

The details involved in post-tensioning often involve a metal duct which forms a void for inserting the tendon into the concrete after it is cured. This duct is usually curved to develop lateral forces for load balancing. When the tendon is stressed it bears along the inner radius of the duct, causing contact between the individual strands, and between the tendon and the duct (see Figure 2.3a) [35]. This varies significantly from a pretensioned girder where the strands are completely surrounded by concrete eliminating the possibility of contact. Cracking in a prestressed beam increases the localized stress in the tendon significantly as shown in Figure 2.3b. These increased local stresses tend to cause debonding of the post-tensioned tendon and provide a place for slip of the tendon to occur. The contact between the tendon and duct (as well as the contact between individual strands) coupled with the increased local stresses and the relative slip between the tendon and duct (or between strands), produces severe abrasions which can initiate surface cracks. Under a cyclic load, these surface cracks can propagate until brittle fracture occurs at a reduced fatigue life. This process is known as fretting fatigue.

Fretting is the surface damage caused when two elements, usually metal, are in contact under a high contact pressure and minute slippage occurs under repeated oscillations. The consequences of fretting action are wear, corrosion, and fatigue cracking. Several mechanisms of fatigue crack initiation have been attributed to the fretting process [5,16,32].

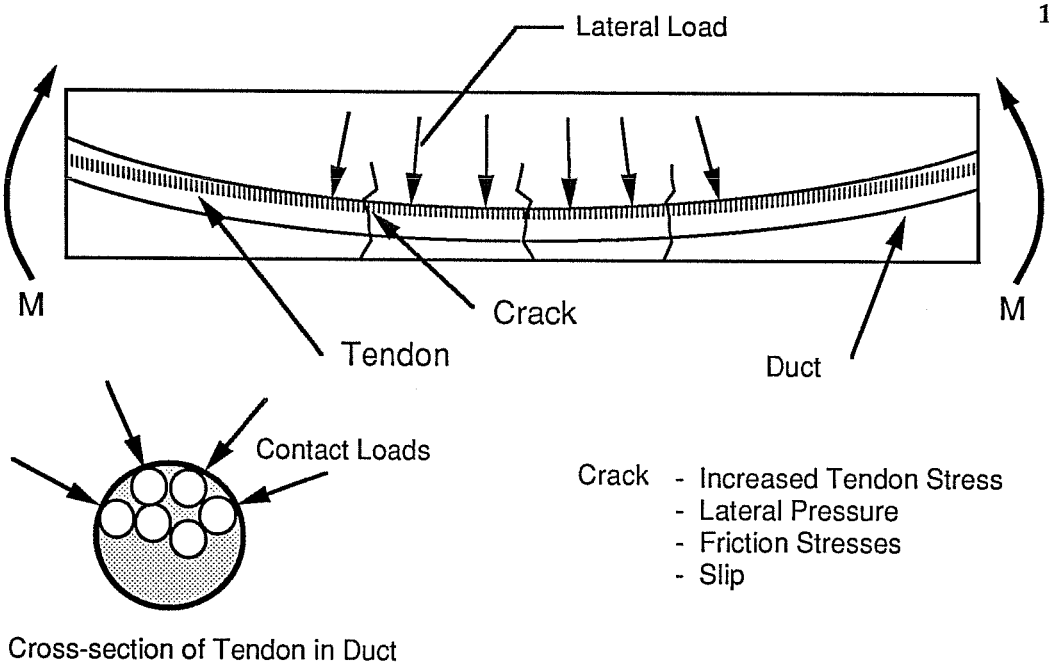

a) Tendon Contact in Post-Tensioned Beam

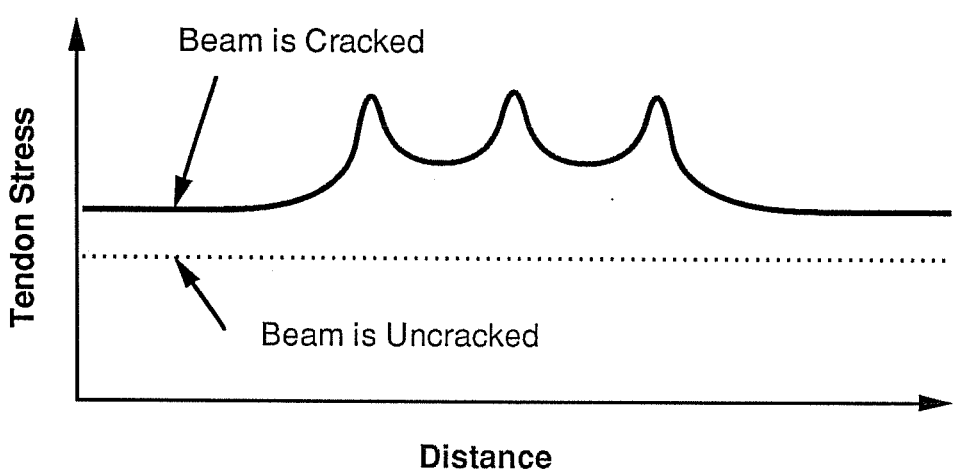

b) Tendon Stress Concentrations at Cracks

Figure 2.3 Cracked Post-Tensioned Beam (after Wollmann and Yates [35, 36])

Although there appears to be disagreement about some of the aspects of fretting, there is a general consensus about the mechanism which is predominant in post-tensioning tendons. This mechanism is known as asperity contact initiation and is illustrated in Figure 2.4 [36]. The two materials are under a high contact force, Q, that produces high local stresses at the points of contact (asperities) since the contact areas are very small. As the metals slip the protective oxide film on the surface is worn off and the material fuses together due to the high clamping force (a process known as cold welding). With each additional slip these "welds" are broken and reformed [36]. Additionally, loose particles are formed which oxidize and increase in hardness. These particles abrade the contacting surfaces as the materials continue to slip relative to each other [17]. Cracks initiate due to a combination of the abrasions and the surface stresses resulting from the asperity contacts, and the existing stresses in the material.

Crack behavior under fretting conditions varies greatly from that of normal fatigue as illustrated in Figure 2.5. The normal fatigue crack initiates along a slip plane (Stage I) and for only a relatively short distance. Soon after initiation, the crack propagates (typically along a grain boundary) perpendicular to the fluctuating stress (Stage II). In fretting conditions the locations of surface stress concentrations and crack initiations shift as the material slips until eventually a crack begins to propagate through the material [33]. This crack starts on an inclined path corresponding to a plane of principal tension which results from the complex surface stress condition. The crack continues on this path until it extends outside the area of influence of the surface stresses (Stage I) [36]. After the crack has grown out of the area of surface stress influence it follows a path perpendicular to the axial stresses similar to normal fatigue (Stage II).

Fracture under fatigue conditions occurs when a crack reaches a critical depth and unstable crack growth occurs causing brittle fracture in the material. In elements where fatigue life is dominated by crack propagation (such as thick plates) fretting will not affect the finite life of the elements. However, fretting could reduce the endurance limit of such an element since cracks would initiate at lower stress ranges than under normal fatigue conditions. In thin elements (such as the wires in prestressing strand) the critical crack depth may be less than the transition length from the initiation phase (Stage I) to the propagation phase (Stage

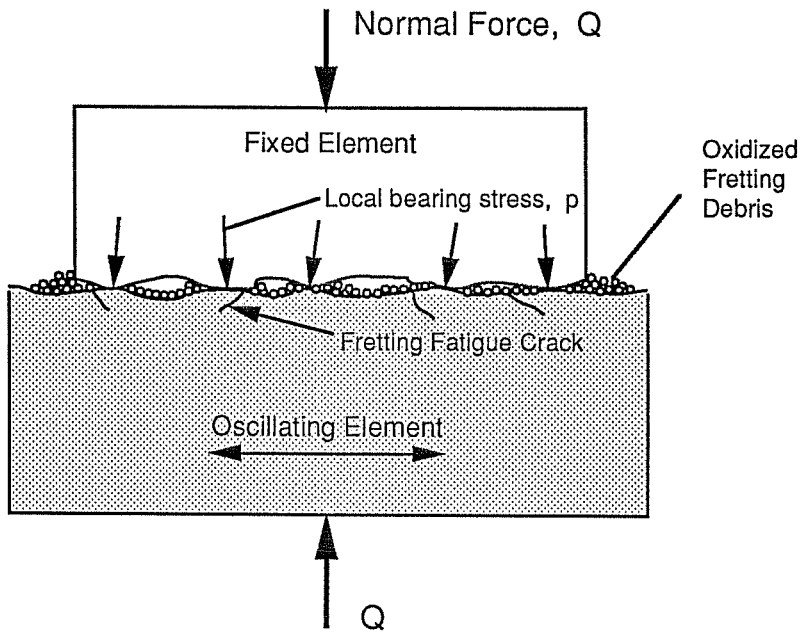

Figure 2.4 Schematic Representation of Fretting Mechanism (from Yates [36])

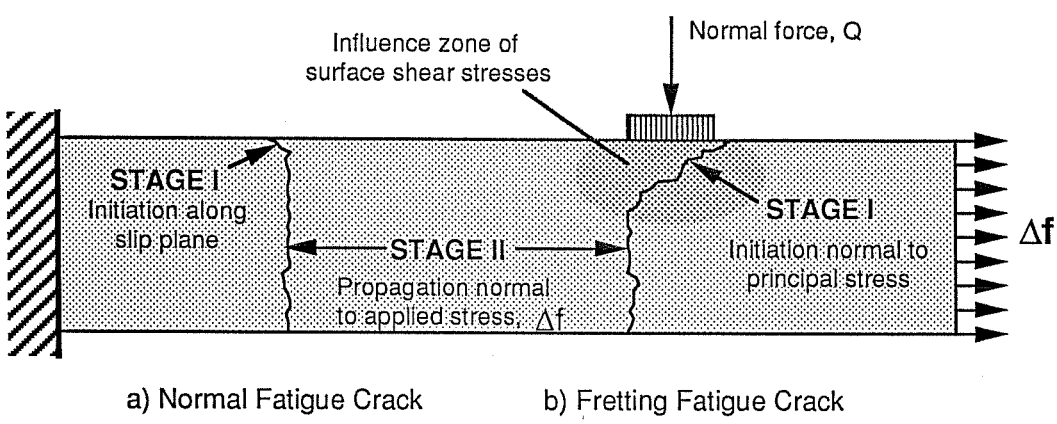

Figure 2.5 Fatigue Crack Characteristics (from Waterhouse [31])

II) and fatigue life would depend on crack growth in the initiation phase [36]. For elements where fatigue life depends on crack initiation (ie. fretting on thin elements) a reduction in the finite life of the element is expected. Also, similar to the thick element, early crack initiation in the element is expected to produce a lower endurance limit [31]. This phenomenon is demonstrated by the shifts in the S-N curves from normal fatigue to fretting fatigue of elements as illustrated in Figure 2.6.

There are many different factors that have an influence on fretting fatigue and most of them are interrelated. A few of the more important variables applying to fretting of post-tensioned tendons are discussed below.

Stress Range: Stress range has a similar effect on fretting fatigue as it does on normal fatigue, that is a reduction in fatigue life as stress range is increased. It has been observed in some situations that if the stress range is low enough cracks will initiate but not propagate to failure [31]. This trend, however, has not been shown to be applicable to such thin elements as prestressing wire.

Slip Amplitude: The amount of slip occurring between the materials affects the fretting fatigue life in a unique way (see Figure 2.7). Fretting fatigue life will decrease with increasing slip amplitude until a point is reached where slippage is large enough that the surface cracks are worn away [16]. A lower limit for fretting wear has been established where the slip amplitude exceeds the range of elastic deformation on the surface. A lower limit has not been established for fretting fatigue, however, since fretting fatigue has been reported to occur at slip amplitudes that are almost immeasurable [16].

Lateral Pressure: An increase in lateral pressure has been found to increase the crack growth rate and reduce the fatigue life [5]. However, the effect of lateral pressure on tendons is difficult to isolate since the lateral pressure is dependant on the stress in the tendon, local curvature of the duct, the duct size, and the tendon arrangement in the duct [35].

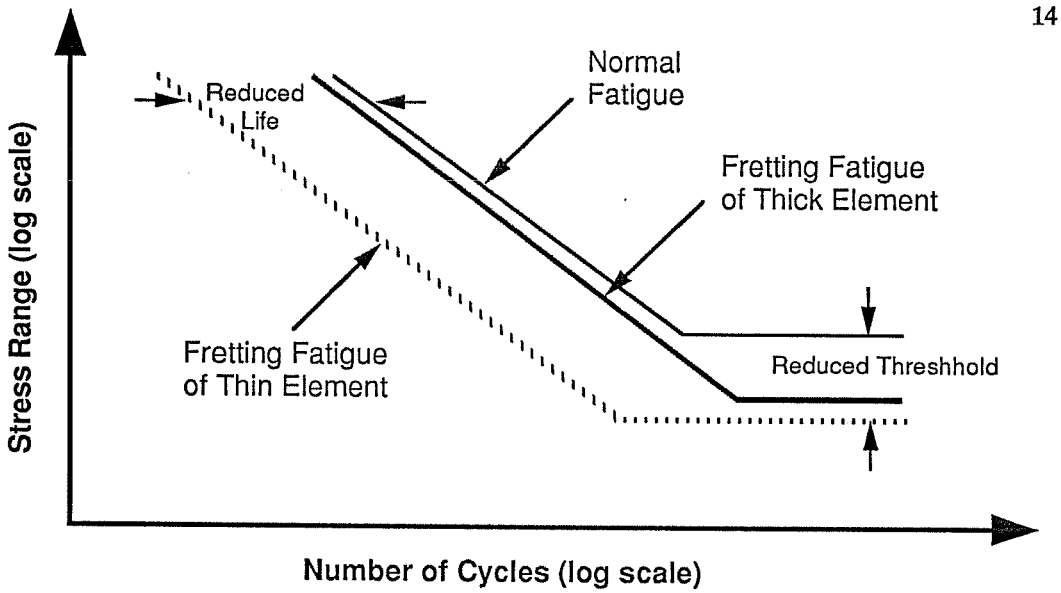

Figure 2.6 Impact of Fretting on Fatigue Life (after Waterhouse [31])

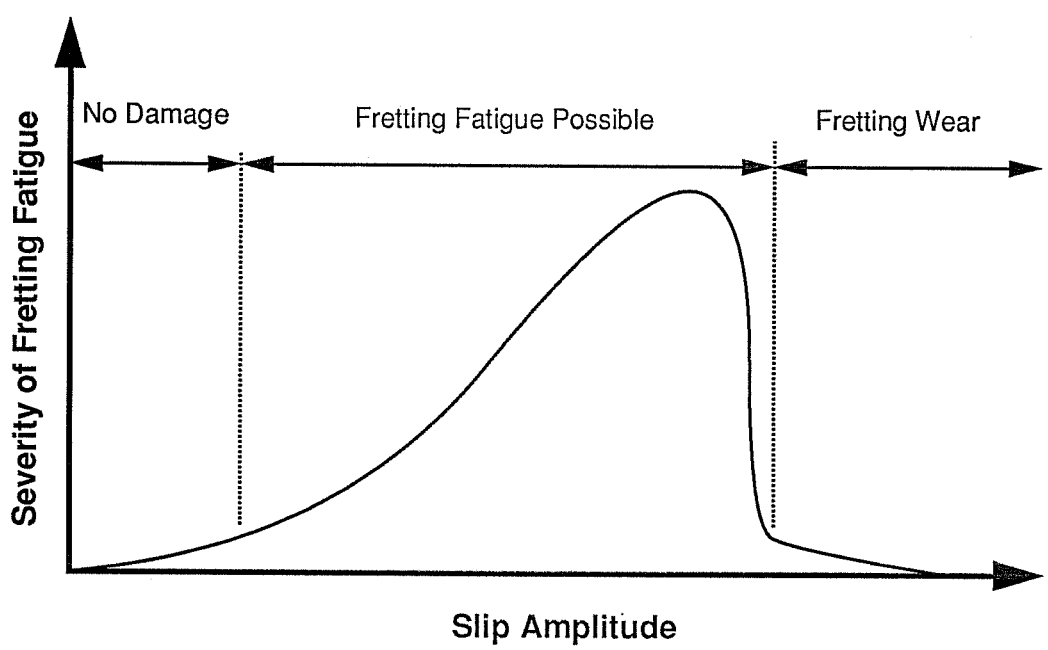

Figure 2.7 Effect of Slip Amplitude on Fretting Fatigue (from Yates [36])

Material Properties: Harder surfaces will resist fretting damage better than softer materials. Metal-to-metal contact has the biggest impact on post-tensioned tendons and metal-to-concrete (or grout) has little impact on fretting fatigue [23,24].

Environment: The presence of oxygen has been found to reduce the fretting fatigue life, while the influence of corrosive agents in the environment on fretting fatigue has been found to be insignificant [31,36]. The effects of other factors such as humidity and temperature are unknown for carbon steels [36].

It should be noted that the influence of these effects was obtained by isolating each variable in the tests. In real situations all of the variables are interrelated and influence each other and the worst combination of them will cause fracture [35].

2.2.3 Conclusions From Previous Research. There has been many different types of tests performed to study the effects of fatigue on post-tensioned girders. These tests typically consisted of scaled girder specimens or reduced beam specimens and the tendons were either draped parabolically or with a constant curvature along the specimen, or were locally deviated at two drape points. The tendon types varied between researchers and they consisted of single wires, single strands, multiple wires, or multiple strands. Figures 2.8 and 2.9 show a few examples of the tested specimens. This section presents the general conclusions from the following studies.

1. Large-scale girder specimens tested by Rignon and Thurlimann [28].
2. Large-scale girder specimens and reduced beam specimens tested by Oertle, Thurlimann, and Esslinger [22,23].
3. Small-scale girder specimens tested by Muller [21].
4. Reduced beam specimens tested by Yates [36].
5. Reduced beam specimens tested by Wollmann [35].
6. Large-scale girder specimens tested by Diab [8].
7. Large-scale girder specimens tested by Georgio [13].
8. Reduced beam specimens tested by Trinh [29].

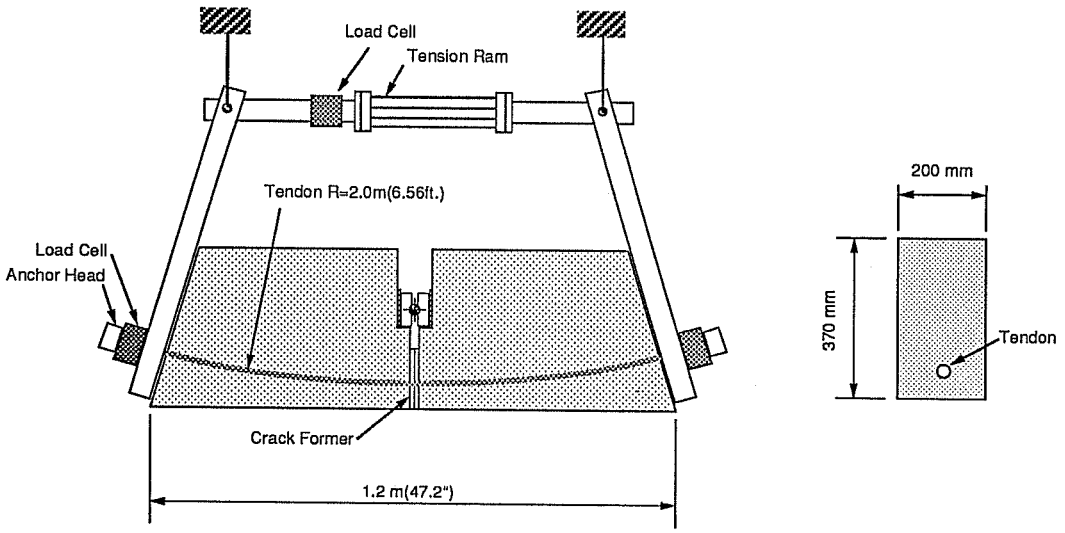

a) Oertle, Thurlimann, and Esslinger Test [22]

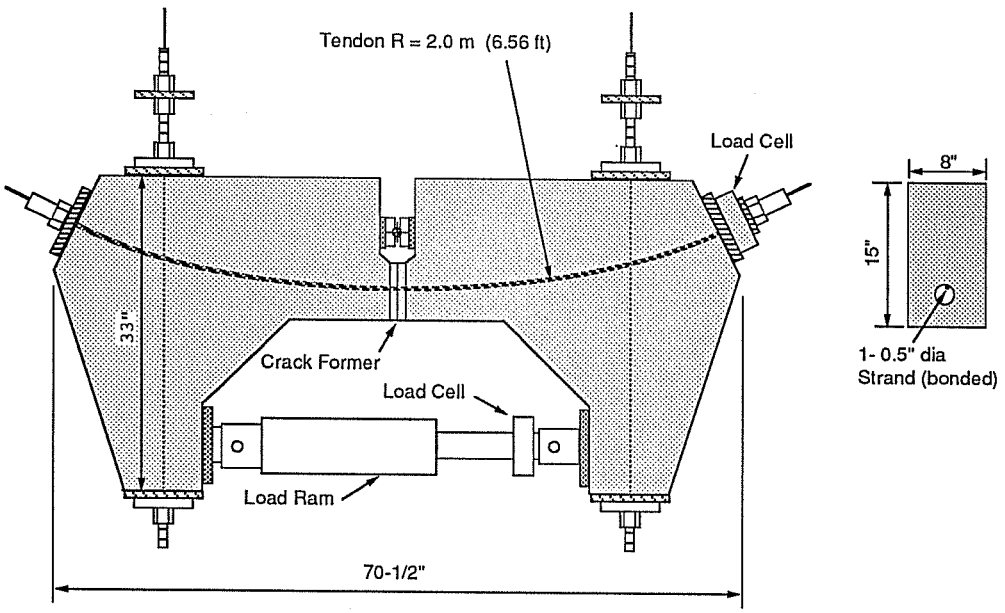

b) Yates Test [36]

Figure 2.8 Reduced Beam Specimens for Fatigue of Post-Tensioned Concrete (from Georgio [13])

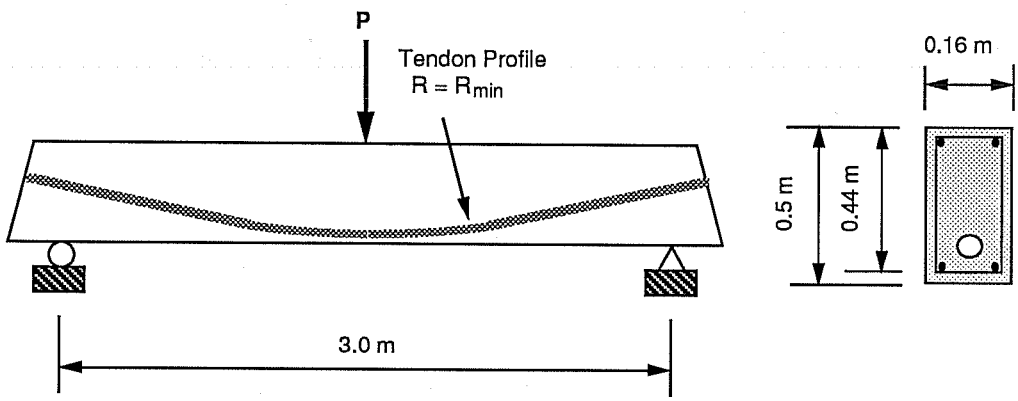

a) Beams Tested by Muller [21]

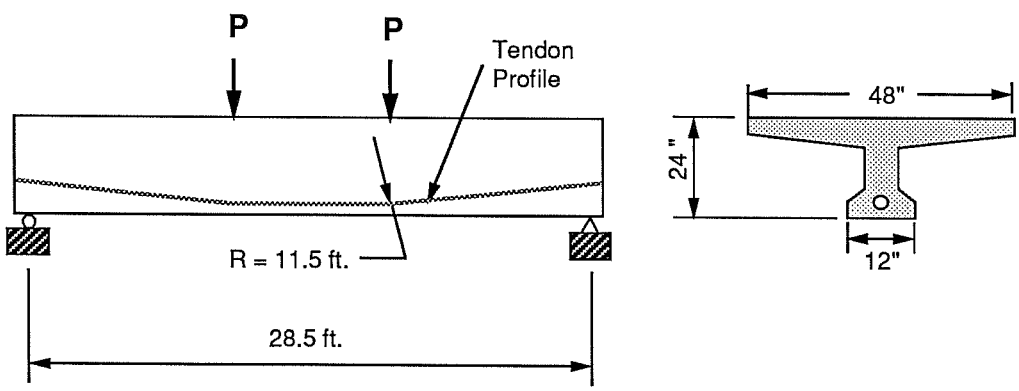

b) Beams Tested by Diab [8]

Figure 2.9 Scaled Beam Specimens for Fatigue of Post-Tensioned Concrete (from Georgio [13])

All of the studies showed a similar pattern of wear in the post-mortem investigations. The ducts were found fractured at the crack locations, indentations were found due to strand (or wire) rubbing against the duct and against adjacent strands (or wires) when multiple strands (or wires) were used. Fracture usually occurred in the curved region of the tendon and was caused by fretting. In tests using two drape points to obtain the tendon profile, fracture occurred at the drape points Fatigue life of cracked post-tensioned beams was found to be severely reduced due to fretting fatigue. If the girder remains uncracked however, fretting fatigue is not a problem. It was also discovered that for an ungrouted tendon, wear was observed similar to the grouted tendons, but fracture occurred away from the wear location. It is suspected that the slip amplitudes were large enough to exceed the upper limit of fretting, so fretting fatigue was not a problem [23].

There was a difference found between tendon failure in a plastic duct and tendon failure in a metal duct. Overall, the tendons in the plastic ducts showed an improved, although still reduced, fatigue life over the tendons in the metal ducts. The tendons in the metal ducts typically fractured due to the strand or wire rubbing against the duct. The tendons in the plastic duct typically fractured due to fretting between adjacent strands or wires or between individual wires in a strand. The tendon often wore through the plastic duct but did not fail due to this contact. One test was run using epoxy-coated strands and was found to have a better fatigue life than the uncoated tendon because the epoxy had to be worn away before fretting could occur [35].

There were a few general conclusions made with regard to all tests. As stated in the discussion on fretting fatigue contact pressure is an important factor in fatigue life. In post-tensioned girders contact pressure is a function of many variables including, radius of curvature of the duct, ratio of duct area to tendon area, and strand arrangement. By increasing the radius of curvature or the ratio of duct area to tendon area the contact pressure will decrease and fatigue life will increase [8,13,29,35,36]. Also, a strand twisted within the tendon may cause concentrated contact pressures and result in premature failure of the strand [35].

2.3 Fatigue of External Tendons

2.3.1 Expected Problems. By examining the results of the studies on fatigue of post-tensioned girders a trend is apparent that is likely to exist in external tendons as well. The external multiple strand tendon has strand to duct contact under a high contact pressure at the deviators. These deviators are similar to the drape points in the post-tensioned beams except that they are the only locations (besides the anchorage points at the ends of the tendon) where the tendon is attached to the concrete section. The tendon undergoes a concentrated angle change at the deviator by using a duct with a small radius of curvature. This angle change produces a change in force in the tendon through friction between the tendon and the duct during the stressing procedure. This force transfer occurs over a short length with high lateral forces combining with the friction forces to induce high surface shear on the tendon at the contact points (see Figure 2.10) [19]. As the system undergoes continued fluctuations in loads (thousands of cycles), it is expected that the tendon will begin to experience minute unmeasurable slippage in the deviator region. Under continued load fluctuations or under the influence of an overload, the grout is expected to deteriorate allowing additional slip to occur. The high lateral pressures and surface shears on the tendon, coupled with the potential for tendon slip, are the necessary conditions for fretting fatigue and a reduction in fatigue life.

2.3.2 Previous Studies. Since the use of external post-tensioned girders and the findings of reduced fatigue life in cracked post-tensioned girders are relatively recent, there has been limited research performed in the area of fretting fatigue on external post-tensioned tendons. In tests on a three-span externally post-tensioned segmental box-girder model, **MacGregor** [19], reports that the service load stress increases in the tendon were measured at less than 2 ksi in all spans. This value would be far below the endurance limit for normal uniaxial tension fatigue of prestressing strand. Also, after five consecutive load cycles the stress response remained constant indicating that the tendons did not slip at the deviators. Since the scope of this study was the strength and ductility of the model, a large number of load cycles were not applied. Slip was observed at twice the load required for decompression (about four times the design load), which suggests loss of bond between tendon and duct can occur due to a previous overload.

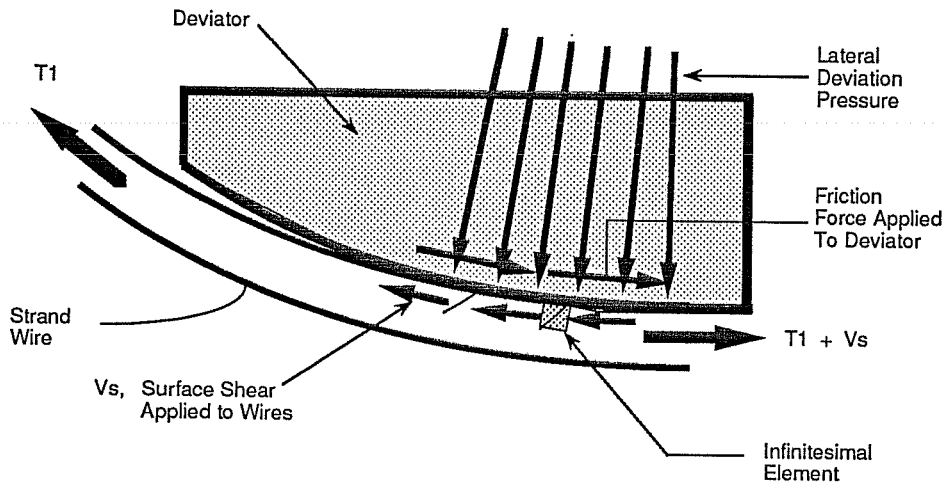

a) Deviator / Tendon Forces

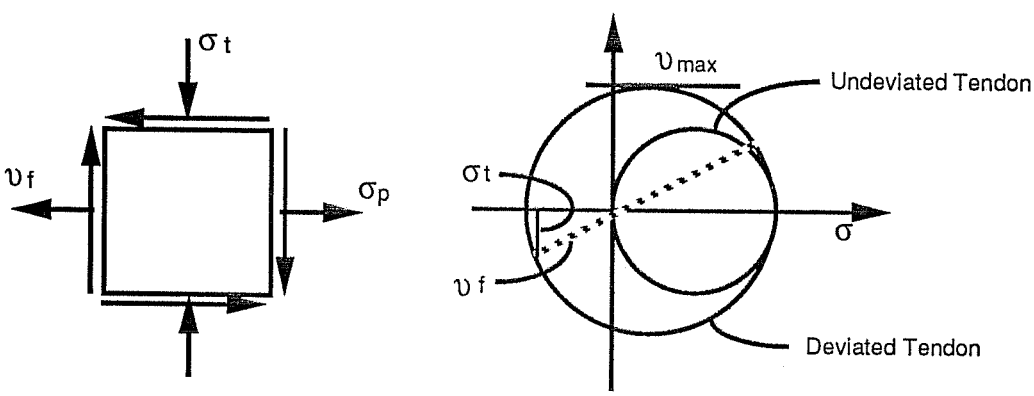

σpt = tendon stress

σt = lateral deviation stress

υf = shear stress from friction forces $\approx \mu \bullet \sigma t$

$\upsilon_{max} > \upsilon f$

b) Stress Condition at Infinitesimal Element

Figure 2.10 Tendon Stress Condition at Deviator Contact Point (from MacGregor [19,20])

In further tests on MacGregor's three-span bridge model, **Hindi** [14], grouted the tendon to the concrete section at the pass-through points as well as in the deviators. This additional bonding increased the ultimate strength and ductility of the model. There was also a larger tendon stress increase discovered at service loads. This stress increase was found to be slightly less than 4 ksi which indicates that possible future design details may produce higher stress ranges in the tendon at service load conditions. Note also that the tendon stress increase is inversely related to the bridge stiffness and will vary from bridge to bridge.

Tests by **Eibl and Voss** [9,10,11] were performed to study the effects of three different types of cable systems (see Figure 2.11) at the deviators under fatigue loading. Type 1 consisted of 7 mm dia. wire strands in a polyethylene duct surrounded by wax, type 2 was similar to type 1 except there was an additional metal cover inside the plastic duct, and type 3 consisted of 15 mono strands, held apart in a polyethylene duct with the space around them grouted with mortar. An illustration of the test layout is shown in Figure 2.12. The radius of curvature was 4 m (12.3 ft.) and the deviation angles ranged from 0.5 to 6 degrees. The setup geometry was designed so the tendon would achieve 0.4 mm (1/64 in.) displacement at the deviation saddle during testing. This relative lateral displacement of the tendon along the saddle was determined from analysis of two bridges Eibl and Voss designed assuming there is no friction between the tendon and the saddle. The tendon was cycled under 2.5 million load cycles with an amplitude of 35 N/mm^2 (5 ksi) and a maximum stress of $0.7f_{pu}$. Eibl and Voss also reported the expected stress range in the tendon at service load conditions to be 15 N/mm^2 (2.2 ksi) [9].

The following results were reported.

- All cables showed satisfactory behavior (no fatigue problems due to fretting).
- For deviation angles greater than 4 degrees, the deviation saddle acted as a fixed support after many thousand cycles.
- Friction loss during stressing was about 1% of the initial prestress load in the tendon.
- Type one cables showed a noticeable deformation on the inner surface of the plastic duct due to contact pressures.

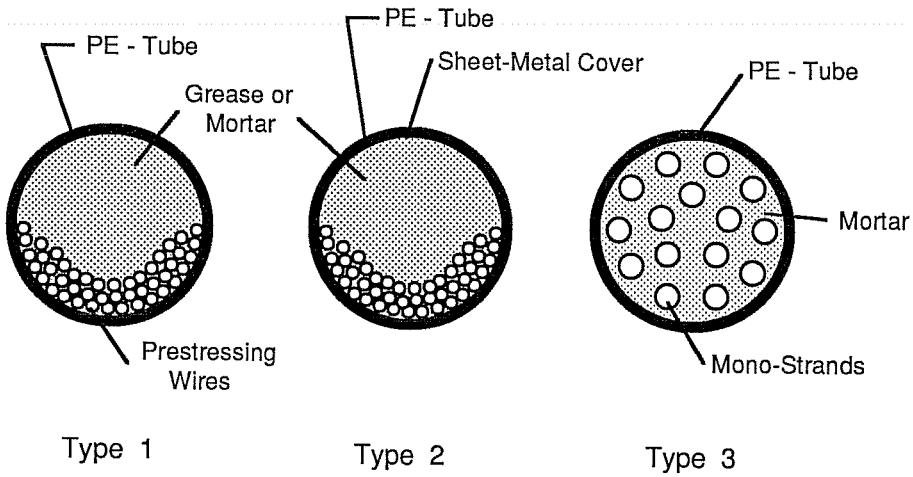

Figure 2.11 Cable Systems Tested by Eibl and Voss [9,10,11]

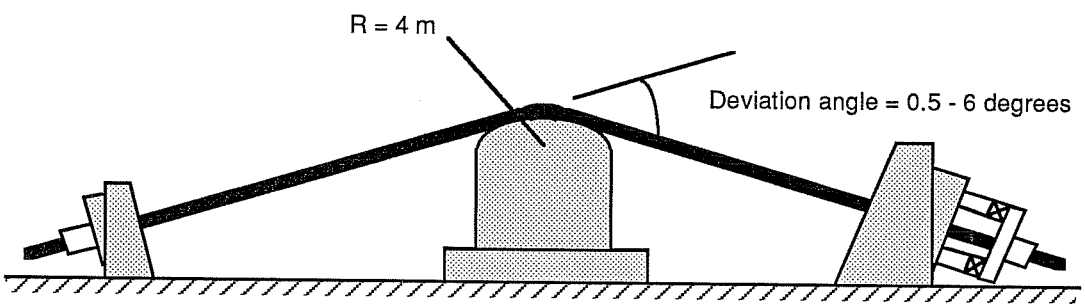

Figure 2.12 Test Setup Used by Eibl and Voss [9,10,11]

Care must be taken when applying these results to other cable systems, especially those commonly used in the U.S. where the tendon is in direct contact with a metal duct. In the test on the type one and two cable systems the cable is essentially unbonded. This situation is similar to the unbonded internal tendon test by Oertle, Thurlimann, and Esslinger [23], where it is suspected that fretting fatigue did not occur due to slip amplitudes being too large. In the type 3 cable system, the strands were held apart, which eliminates strand to duct and strand to strand contact.

To date, there have been no fatigue studies reflecting the details typically used in the U.S. for post-tensioned external tendons used in segmental box-girders. As stated earlier, internal post-tensioned tendons have exhibited a reduction in fatigue life due to fretting fatigue. This is brought on by large contact stresses between the tendon and the duct (as well as between adjacent strands in the tendon), large local stresses in the tendon, and relative slip of the tendon (or individual strands). Although the level of stress reversals in external tendons should be significantly below those of internal tendons, the external tendons also are subject to these same potential fretting fatigue initiators in the tendon deviators. This is sufficient cause to explore the possibility of fretting fatigue problems in the tendons at the deviators. Therefore, studies are needed to determine whether the conditions which might produce fretting fatigue play a significant role in typical external tendons.

CHAPTER 3
TEST PROGRAM DEVELOPMENT

3.1 General

In studying the behavior of deviation saddles, Powell and Beaupre [4,26] constructed a test setup for testing external tendon deviators under static loading. This setup, shown in Figure 3.1, was used as the core of the test setup for studying fretting fatigue potential in external post-tensioned tendons. The Powell/Beaupre setup was designed for testing deviator segments of 1/5 to 1/3 scale of actual size. The tendons were stressed by typical post-tensioning methods and then additional stress was introduced statically by jacking the anchorage frames outward from the concrete buttresses until the deviator failed. The concrete buttresses, which are anchored to the laboratory floor with tensioned rods, provide shear friction resistance capable of developing a total horizontal reaction of up to 460 kips from the post-tensioning tendons [26].

3.2 Development of the Concrete Segment

3.2.1 Controlling Factors. Several factors had to be considered while designing a model to be used for examining fretting fatigue of external tendons in box-girder deviators. These factors included:

1. The segment must fit into the Powell/Beaupre setup, since this test setup is to be used as the core of the fretting fatigue setup.
2. The segment details must be representative of a typical box-girder deviator segment.
3. The fluctuating stresses must follow a similar load path to reach the tendon as would occur in an actual segmental bridge span.
4. Since a number of segments are to be tested, they should be relatively easy to construct.

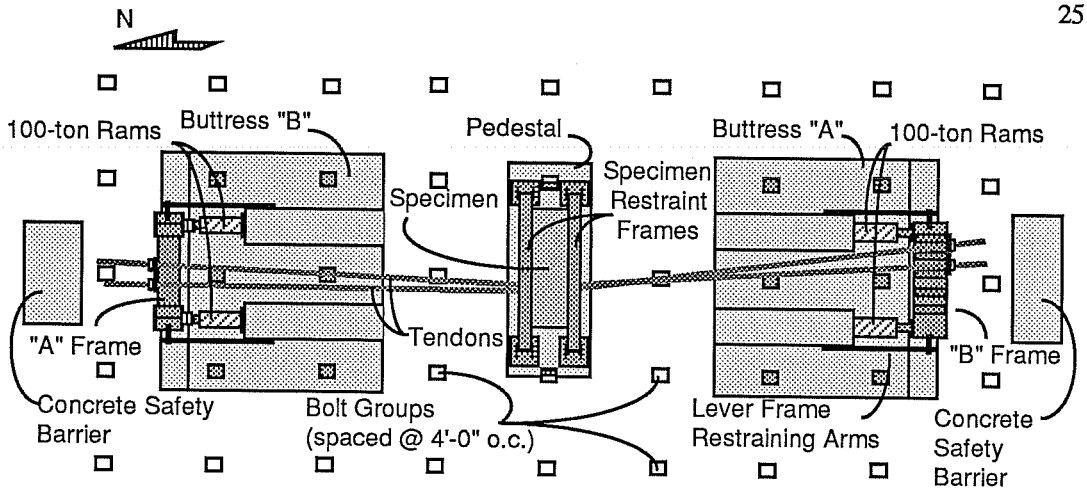

a) Plan

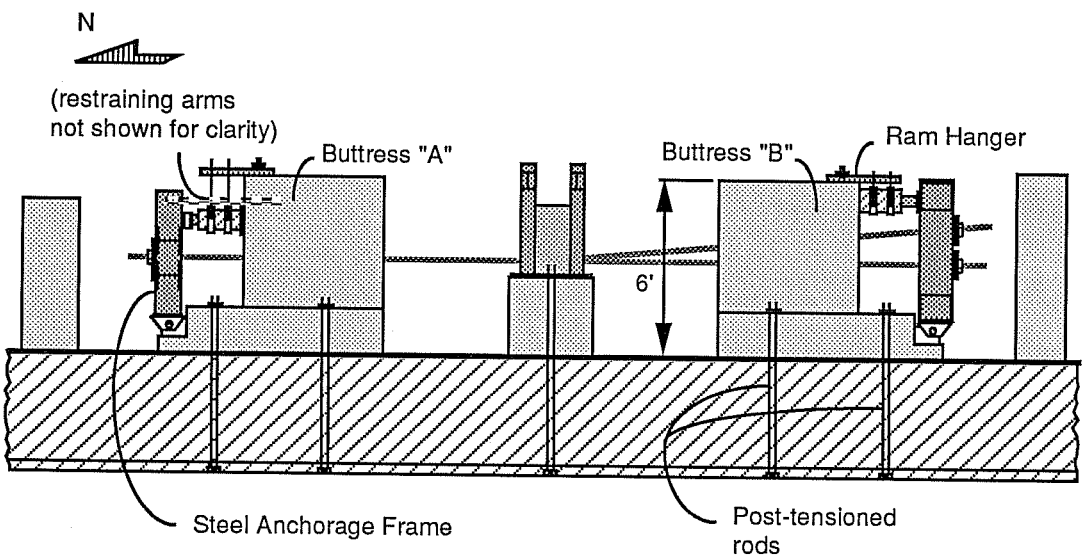

b) Elevation

Figure 3.1 Powell/Beaupre Test Setup (from Powell [26])

3.2.2 Segment Configuration. A few details of the segment configuration were determined from the characteristics of fretting fatigue and its potential in external tendons. These details included the number of tendons and the amount of bridge segment required for examining fretting fatigue in external tendons. If fretting were to occur, it would likely occur in all tendons simultaneously; therefore, it would only be necessary to test one tendon to obtain adequate results for the entire span. Also, since fretting is most likely to occur in the deviator duct, only the deviator segment of the girder is required. Because the concern is not for testing the deviator capacity, the only additional restraint was maintaining the correct load path of the fluctuating tendon stresses. In order to achieve fluctuating stresses in the tendon to closely simulate the correct load path as in a prototype bridge, it was decided that the cyclic load would be applied by moving the segment up and down with a hydraulic ram. This is explained in greater detail in Section 3.3.3.

After the previous conclusions were made, the next step was to determine some general details of the deviator portion of the segment. These included the deviator duct orientation and the number of deviators to be used. Figure 3.2 shows four of the deviator duct orientation details considered. In Detail 1 the tendon enters the duct on a vertical angle on the side of the dead end anchorage and leaves the duct horizontally towards the live anchorage or stressing end. This detail would work well in the Powell/Beaupre setup since the stressing frames are set up to anchor the tendons in such a manner and it closely represents the tendon/deviator detail of one half of a typical span. However, this detail is unsymmetrical and would produce an unbalanced situation. Detail 2, where the tendon enters and exits the duct with the same angle, was considered as a more symmetrical detail and is similar to Detail 1 in a rotated plane. These details only represent half of the span, however, and were discarded for models that would be more representative of the tendon/deviator configuration of the entire span. Therefore, a segment using two deviators was considered. The first double-deviator segment considered, Detail 3, was actually two independent segments (similar to Detail 1) back-to-back with a frictionless surface between them. Because this detail would be difficult to test it was rejected and Detail 4 was selected. Detail 4 uses two deviator ducts within one segment separated by a short gap. The tendon enters the first deviator on an angle and exits horizontally. The tendon then enters the second deviator horizontally and exits on an angle.

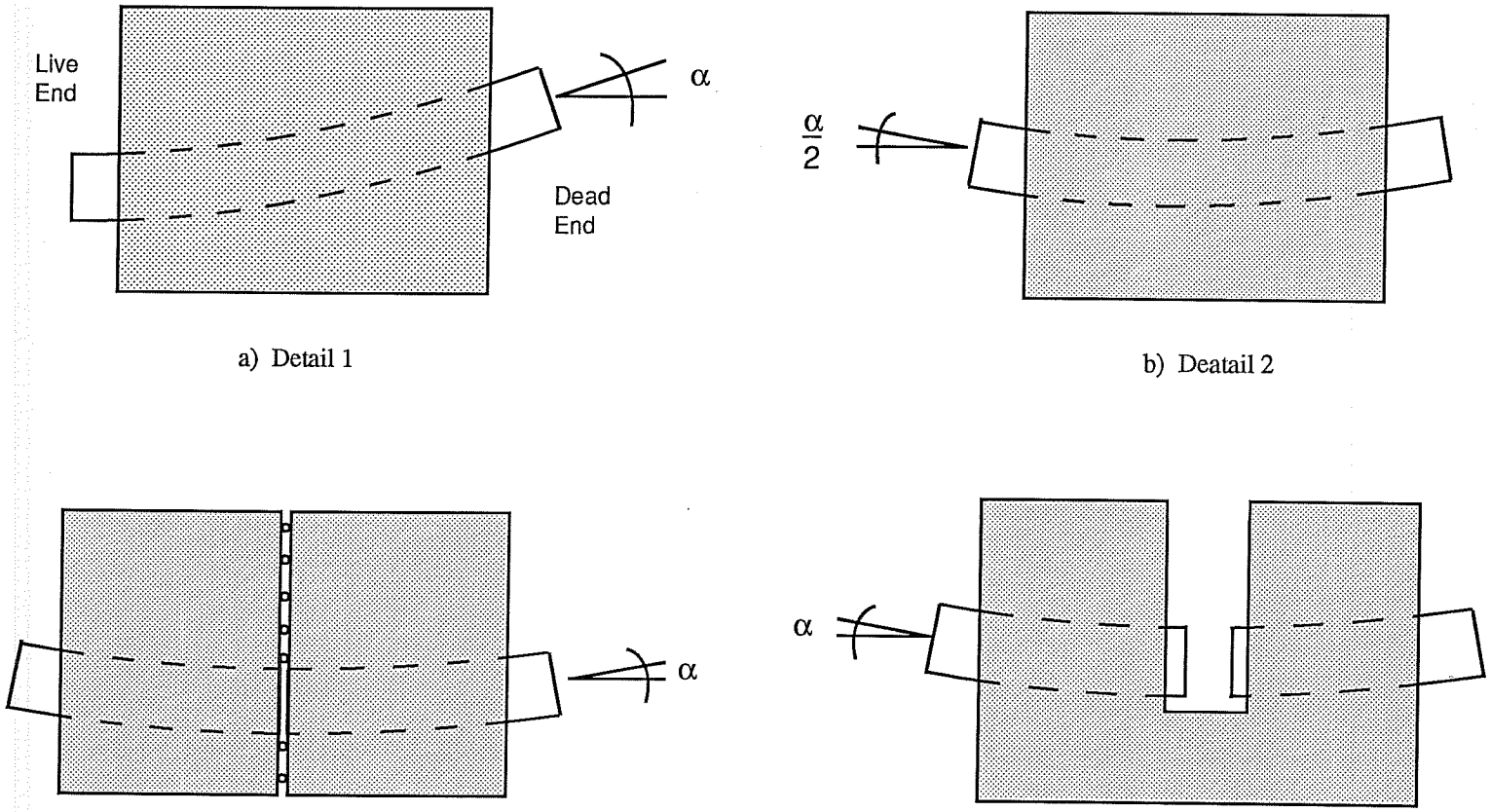

a) Detail 1

b) Deatail 2

c) Detail 3

d) Detail 4

Figure 3.2 Initial Deviator Segment Details Considered

This detail represents closely the tendon/deviator arrangement found in typical segmental bridge spans except that the usual long length between deviators is greatly shortened. In addition, Detail 4 is symmetric. Only vertical deviation angles were considered for the alignment of the duct, since including an additional horizontal angle in testing would not add any effects additional to what would be found if the angle was considered as in the principal plane of the tendon deviations.

Once the orientation and the number of deviator ducts was determined, the final design of the model could be decided. The isolated deviation block is the most commonly used deviator detail in existing externally post-tensioned bridges in the U.S. [26]. Therefore, a detail similar to the deviation block detail was chosen. The idea of using a single large solid block with a duct passing through for the segment was considered. This was quickly discarded because the load used to apply the fluctuating tendon stresses would then be applied directly to the top of the deviator, which differs greatly from actual loading conditions. To achieve the proper load path, the load should be applied to the top flange of the segment and flow down through the webs into the deviator and tendon. Since a full size box-girder segment would be too large for the test setup and only one deviator could be tested at a time, a model box-section using a center deviator was considered (see Figure 3.3). The cyclic load would be applied on the top flange and follow the correct load path to the tendon. The deviators are similar to actual deviator details except they are not attached to the web; however, the close proximity of the web should compensate for any differences. This detail was then modified slightly for construction purposes to achieve the test segment (see Figure 3.4). The top flange was removed and the web and deviator sides were sloped to allow the formwork in the void area to be removed more easily. The cyclic load would now be applied directly to the webs, but this would not change the load path to the deviator and tendon.

3.2.3 Model Scale and Final Dimensions. Upon examination of the capacity of the Powell/Beaupre setup it was found that a full scale tendon (12 - 1/2 in. strands stressed to $0.75f_{pu}$) could be used. Therefore, the final model would have to be a full-scale deviator segment for one tendon. The final dimensions of the segment, shown in Figure 3.4, are a result of typical details of box-girder deviators, the limits of the test setup, and the materials available.

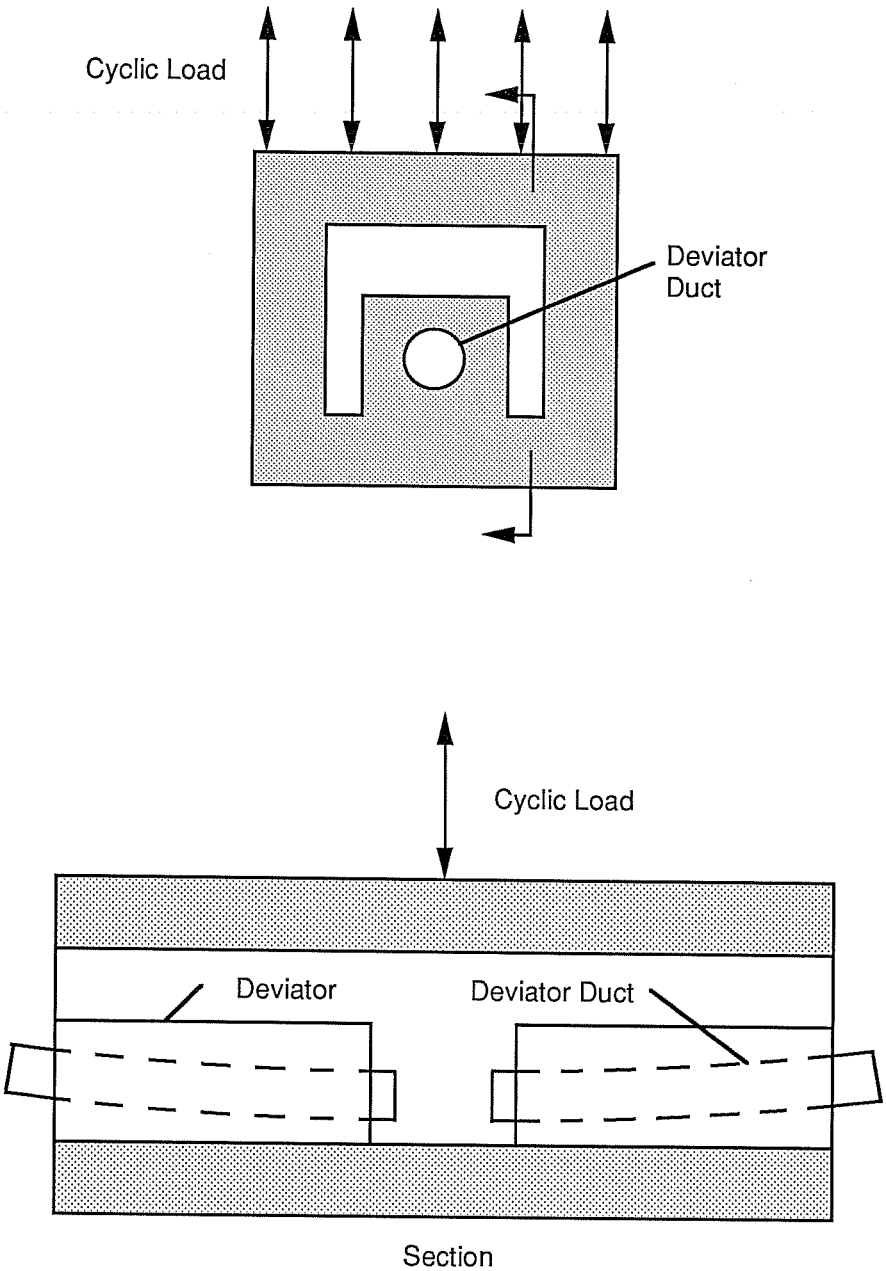

Figure 3.3 Test Segment: Original Model

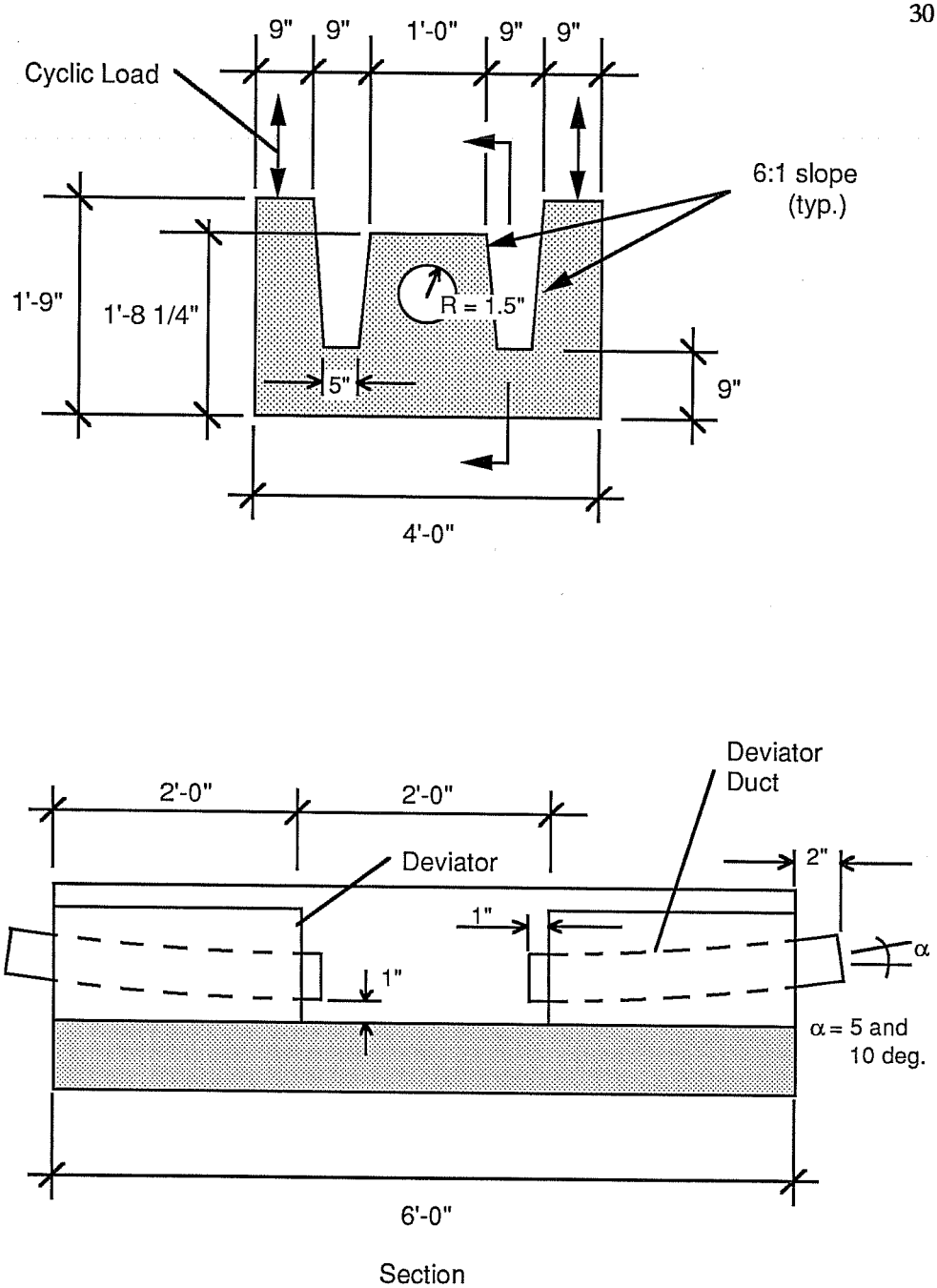

Figure 3.4 Test Segment: Original Model Modified For Easier Construction.

Typical deviators used throughout the U.S. were found to be anywhere from 1.5 to 3 feet long. Since the deviator ducts used in this research were extra deviator ducts donated by Prescon Corporation and pre-bent to various radii, the length of the deviator was limited. The typical length of duct was 27 inches long which allowed for a maximum deviator length of 24 inches. This length is well within the range of typical deviator lengths. The width and height of the deviator were selected to allow for adequate concrete cover around the duct and to be representative of typical deviator block details. The gap between deviators was also set at 24 inches to allow enough room for instrumentation and grouting techniques. This results in a segment with an overall length of six feet. The web thickness and bottom flange depth of nine inches, were chosen from typical box-girder segments. Finally, a six to one slope was chosen on the web and deviator sides to allow for easier formwork removal. Descriptions and illustrations of the deviator and box segment reinforcement are presented in detail in Section 4.1.2.2 and 4.1.3.2 respectively.

3.2.4 Layout of Deviator Duct. As stated previously the duct dimensions were limited to those of the duct donated. The duct consists of 3 inch standard galvanized metal pipe (3 in. inside diameter with 0.25 in. wall thickness). These pipes are standard for deviating tendons of the magnitude to be used in this specimen. Typical deviation angles used in actual bridge spans can range from less than one degree to over 12 degrees. Powell [26], in her prototype model shows horizontal deviation angles from 0.8 to 3.7 degrees and vertical deviation angles from zero to 8.2 degrees. Therefore, tendon angle deviations of 5 and 10 degrees were chosen as representative of actual deviation angles. Deviation ducts were then chosen from the pipes available based on the deviation angle plus a two to three degree overbend, which is standard practice to help compensate misalignment problems. The final duct angles selected were approximately 8 and 10 degrees.

3.3 Development of the Test Setup

3.3.1 Controlling Factors. The primary objective in designing the test setup was determining a system to safely test external tendons under fatigue conditions that represent, as close as possible, the conditions that would occur in an actual external post-tensioned box

girder. To achieve this objective it was necessary to consider several factors which influenced the design of the test setup. These factors included:

1. All stresses, static and dynamic, must be applied following similar techniques or load paths as would occur in an actual segmental girder.
2. Fatigue tests involving exposed external tendons with typical strand anchorages (chucks and wedges that grip the strand) usually fail in the grip region due to the stress concentrations and indentations caused by the wedge teeth. Therefore, a cyclic load must be applied in a manner that will produce a fatigue failure in the tendon away from the anchorage (grip) region.
3. Since contact pressure is a function of deviation angle, the setup must allow for segments with various deviation angles.
4. A high lateral force capacity test setup previously constructed at Ferguson Laboratory for statically testing deviation saddles by Powell and Beaupre [4,26] should be utilized if possible. The setup could be modified to facilitate "correct" loading patterns of the specimen.
5. Because the energy stored in an unconfined highly stressed post-tensioned tendon presents a potentially dangerous situation, the setup must have sufficient safety precautions to protect the testing crew and general lab personnel.

3.3.2 General Layout. An applied axial load method similar to that used by Powell and Beaupre was considered for testing the tendons under a fatigue loading. This would be accomplished by using the 100-ton capacity rams to repeatedly push outward at the top of the anchorage frames and then release them back, producing cyclic stresses in the tendon. This method was abandoned due to concerns about achieving the right load path for the fluctuating stresses and because of the likely possibility of failure in the grip region since the maximum displacement would occur in this region. A system, therefore, had to be devised that could be easily adaptable to the Powell/Beaupre setup with limited modifications.

3.3.3 Loading Concept. The fluctuating tendon stress in a segmental bridge occurs when the girder deflects under repeated traffic loading. This deflection causes the

tendon to undergo additional stresses (see Figure 3.5). Therefore, it was decided that the fluctuating tendon stress should be applied in a manner that simulates the deflection of a segment of a bridge. This would be accomplished by using a hydraulic ram to displace the segment vertically.

Several methods of accomplishing this task were considered. The segment could be pushed down from the top or pulled down from underneath (see Figure 3.6a and b). The test procedure using these methods (Methods (a) and (b)), would be as follows:

1. Temporary supports would be required below the segment to support the dead load of the segment before the tendon is stressed and above the segment to support the segment during stressing procedures.
2. As the tendon is stressed the dead load supports below the segment would be removed.
3. After the tendon is stressed to the mean stress level, the ram would push or pull downward on the segment until the peak tendon stress is reached.
4. The stressing supports on the top of the segment would then be raised far enough to allow the segment to move upward freely, but would be kept close enough to act as a safety device in the event of catastrophic failure of the tendon.
5. Fluctuating stress levels would be applied by cycling the ram between preset levels.

If the segment was inverted it could then be pushed up from the bottom or pulled up from the top (see Figure 3.6c and d). The test procedure using these methods, (Methods (c) and (d)), would be as follows:

1. Temporary supports are required below the segment to support the dead load of the segment before the tendon is stressed and to support the segment during stressing procedures.
2. After the tendon is stressed to the mean stress level, the ram would push or pull upward on the segment until the peak tendon stress is reached.
3. The segment supports would then be lowered far enough to allow the segment to move

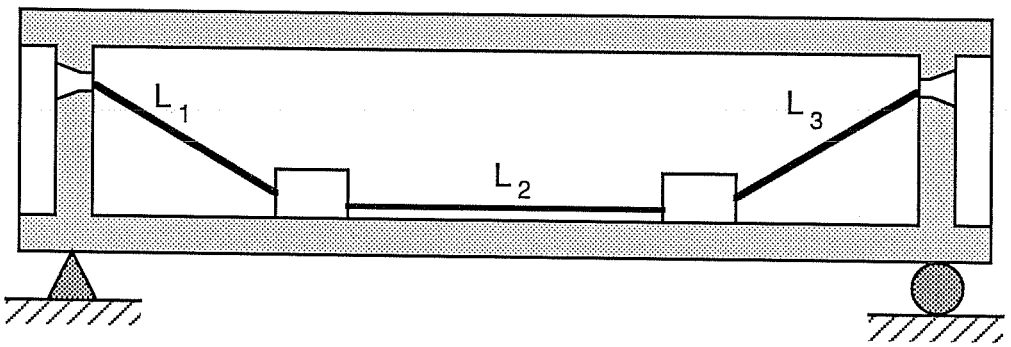

a) Initial Tendon Length With No Applied Load

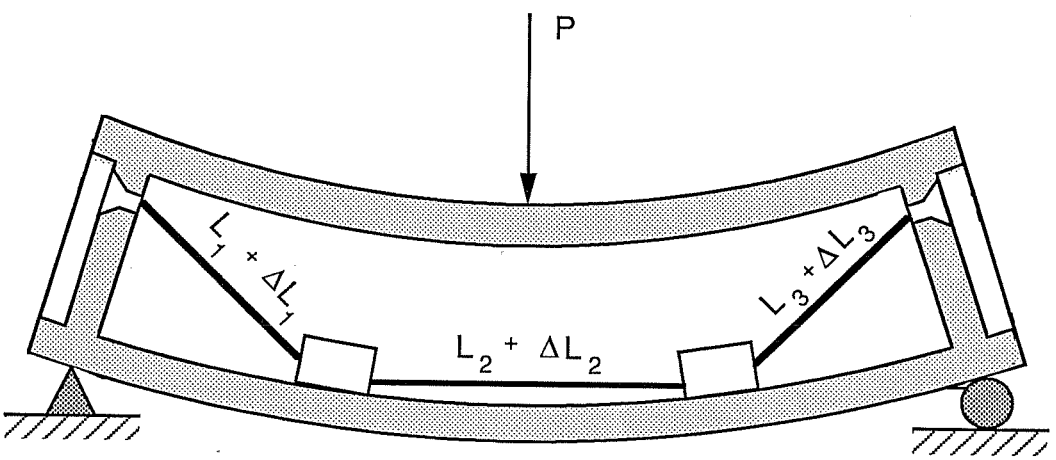

b) Elongation of Tendons Due to Deflection

Figure 3.5 Increase in Tendon Stresses Caused By Deflection of Span (after Virlogeux [30]).

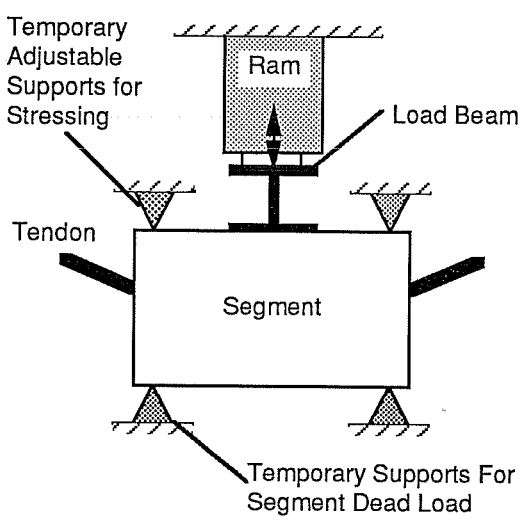

a) Center-hole ram supported from above.

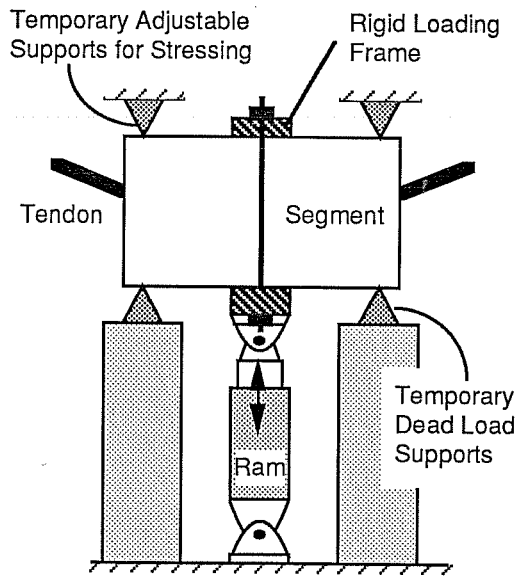

b) Loading ram anchored to the floor.

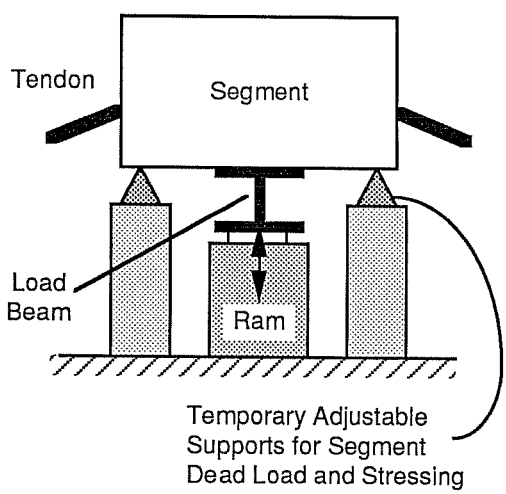

c) Center-hole ram anchored to the floor.

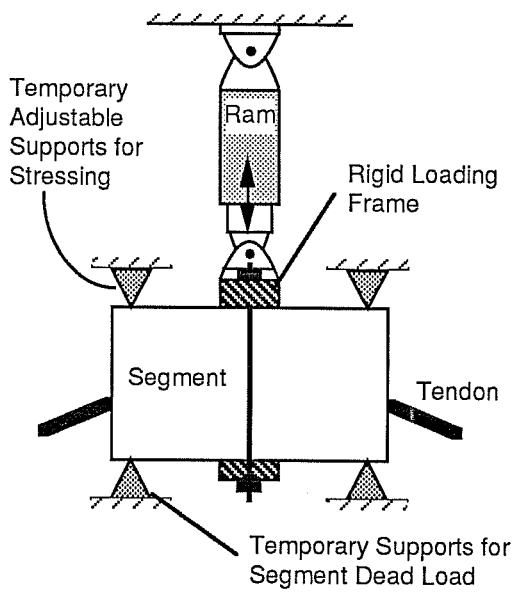

d) Loading ram supported from above.

Figure 3.6 Preliminary Loading Concepts

downward freely but would be kept close enough to act as a safety device in the event of catastrophic failure of the tendon.

4. Fluctuating stress levels would be applied by cycling the ram between preset levels.

Methods (a) and (b) present a more difficult testing process since adjustable supports are required on the top and bottom of the segment. These methods were quickly rejected. The main differences between Methods (c) and (d) lie in the type and location of the ram. Method (c) would use a center-hole ram in compression that would sit on the floor and push upward on the segment. This method would require a simple beam to transfer the load from the ram to the webs. Method (d) would use a ram in tension that would have to be suspended from a frame and pull up on the segment. This method would require an additional frame mechanism so that the ram could apply the load through the segment webs. Although the center-hole compression rams available were not specifically designed for fatigue loading, the extra time and materials needed to construct the frames for the tension ram made the tension ram less desirable. Therefore, method (c) was chosen as the most practical loading method.

3.3.4 Tendon Anchorage. In a typical box-girder span the external tendons are anchored with wedges gripping the strands in an anchor head. The anchor head and strands in the anchorage zone are then grouted (see Figure 3.7) for corrosion protection and to prevent fatigue failure of the strand in the grip area due to stress concentrations and indentations from the wedge teeth. It was envisioned that a number of tests would be performed using this loading system. Therefore, a method to re-use the anchor head was highly desirable. Since grouting of the tendons in the anchorage region would make re-use of the anchor head difficult, alternative anchorage methods had to be considered. Lamb [17] and Paulson [25] had tested single prestressing strands in fatigue using varying types of a double-chuck grip system. The double-chuck grip system consists of a primary chuck with wedges that protrude from the top of the chuck and a secondary chuck and wedge device that snugs up against the protruding wedges (see Figure 3.8). The primary wedges are made of a soft material to help prevent stress concentrations and indentations from the wedge teeth. Good results were achieved in Lamb's tests with copper wedges and in Paulson's test with layers of

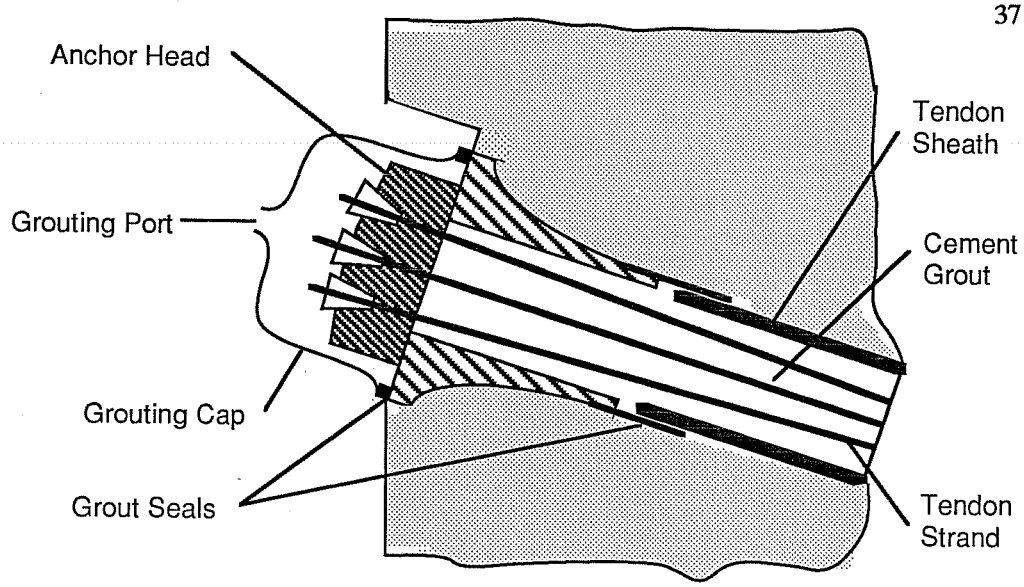

Figure 3.7 Typical Anchorage Detail for Post-Tensioned Tendons (after Jartoux and LaCroix [15])

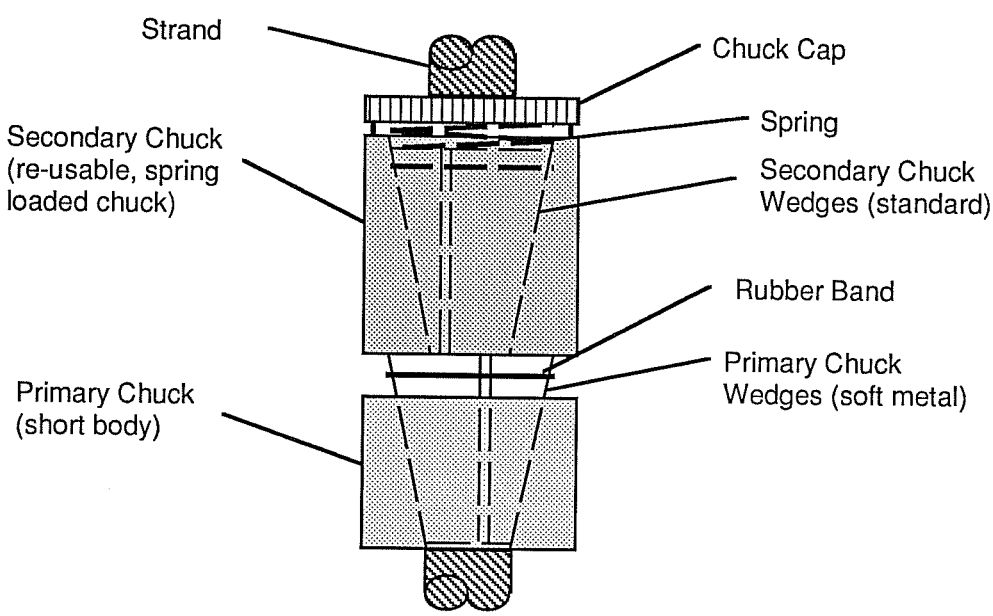

Figure 3.8 Double-Chuck Grip System for Strand Anchorage (after Lamb [17] and Paulson [25])

aluminum foil between the strand and standard steel wedges. The secondary chucks will share the tensioning load with the primary chucks but under a cyclic load only the primary chucks carry the fluctuating stresses; therefore, the secondary chucks can use standard steel wedges. The secondary chucks also help to prevent slippage of the strand in the primary (soft) wedges by forcing the soft wedges further into the primary chuck which results in larger clamping forces on the strand. The double-chuck method was selected because these systems have had some success and are relatively simple to implement. These grip methods were first tried on single strand specimens in a test setup developed in a previous research program at Ferguson Laboratory to ensure their success. These tests are reported in more detail in Section 5.2.

This system was modified slightly to utilize an anchor head as the primary chuck. A standard 12 strand anchor head could not be used in this system however, because the secondary chucks would interfere with adjacent secondary chucks. Therefore, a larger anchor head capable of gripping 37 strands was required to fit the secondary chucks properly (see Figure 3.9). A problem arose from this anchorage method because the angles of the holes in the anchor head and the required tendon angles do not allow the individual strands to properly align (see Figure 3.10a). Most of the strands would have to kink at the end of the anchor head in order to achieve the proper alignment to correctly intersect the segment deviator (see Figure 3.10b). This kink would become a location of high stress concentrations and would likely cause premature failure of the tendon. To alleviate this problem an alignment detail was required to gather the strands after they leave the anchor head forcing the change in angle at a location where high stress concentrations can be prevented from causing premature tendon failure. This is accomplished, as illustrated in Figure 3.10c, by using a greased aluminum pipe to gather the strands and divert their angles. The aluminum should be soft enough to prevent fretting and the grease helps reduce friction.

3.3.5 Stressing Frames. Due to the type of detail selected for the test segment (tendon entering and exiting the segment on an angle) and the details required for anchoring the tendon (37 strand anchor head rather than a 12 strand head) the anchorage frames used in the Powell/Beaupre setup could not be utilized. New frames therefore, had to be designed to be used for stressing and anchoring the tendon and to allow for tendon angles of varying

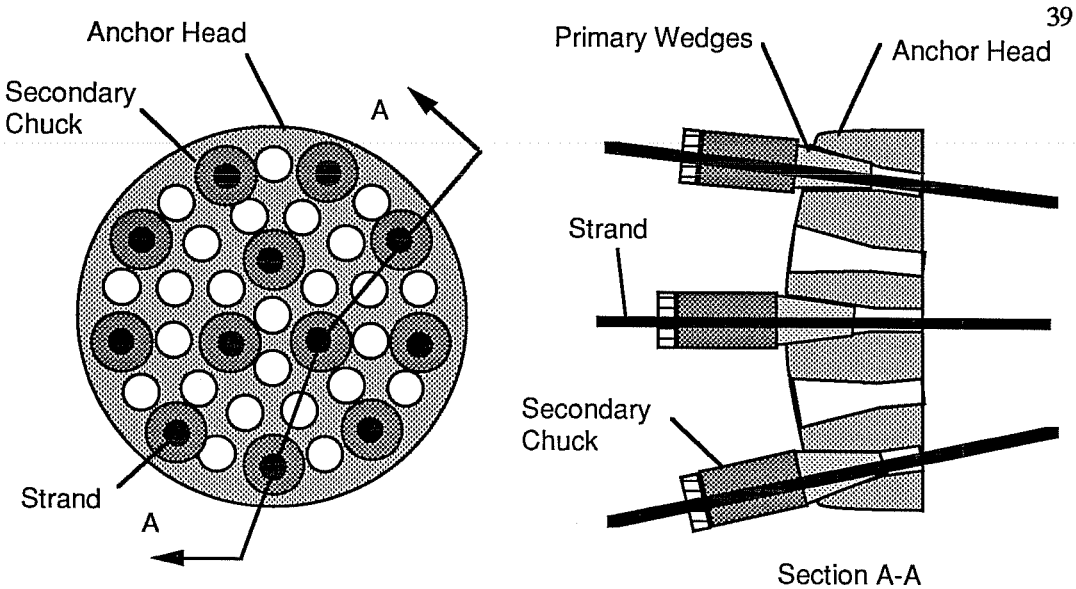

Figure 3.9 Double-Chuck Grip System for Multi-Strand Anchor Head.

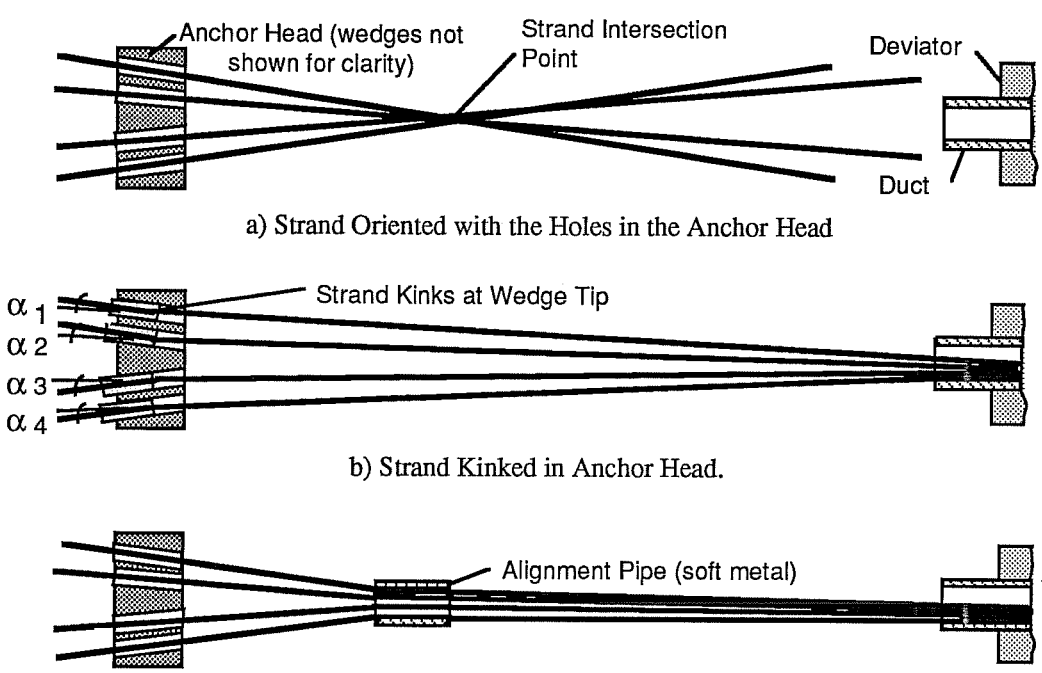

Figure 3.10 Schematic of Strand Alignment Problem.

degrees. This was accomplished by using plates with circular holes cut out of the center and bolted to the stressing frame. The anchor head is then temporarily attached to a short length of pipe which is cut to the required tendon angle and welded to the plate. This system allows for using interchangeable plates with varying angles and reuse of the anchor heads. For simplicity the new stressing frames would be attached directly to the concrete buttresses. These frames have to transfer the load to the buttresses and be stiff enough to prevent excessive prestress loses in the tendon due to frame deflection. A schematic of the stressing frames is shown in Figure 3.11.

3.3.6 Segment Supports. In Section 3.3.3, the need for vertical supports of the segment during stressing was discussed. These supports need to be strong enough to carry the entire vertical load from the tendons during prestressing. The support must also be adjustable, or a portion of the support removable, to allow for unencumbered vertical movement of the segment during testing. There is also a need for horizontal supports to prevent lateral movement of the segment. When the tendon is stressed it will elongate. As it is pulled through the deviator, the friction forces between the tendon and the duct, resulting from the angle change of the tendon, will cause the segment to move with the tendon unless it is resisted. This friction will also cause a loss of stress in the tendon across the deviator and produce an unbalanced loading condition (see Figure 3.12a). To resist these forces and maintain the proper alignment of the segment, longitudinal supports are required at both ends of the segment (these supports are represented by reaction forces $R_{long.}$ in Figures 3.12a and 3.12b). Any misalignment of the duct, the segment, or the stressing frames, can cause additional unbalanced loading in any direction. Therefore, it is also necessary to provide lateral supports on each side of the segment (these supports are represented by reaction forces $R_{lat.}$ in Figures 3.12a and 3.12b) to maintain the segment alignment. Since the segment will be moved vertically to apply the stress fluctuation in the tendon, these supports must be essentially frictionless in the vertical direction.

Because the distance between the two concrete buttresses is approximately 12 feet and the segment length is six feet, there was only a limited area at each end of the segment to install the longitudinal supports. This area was too small to use supports attached to the

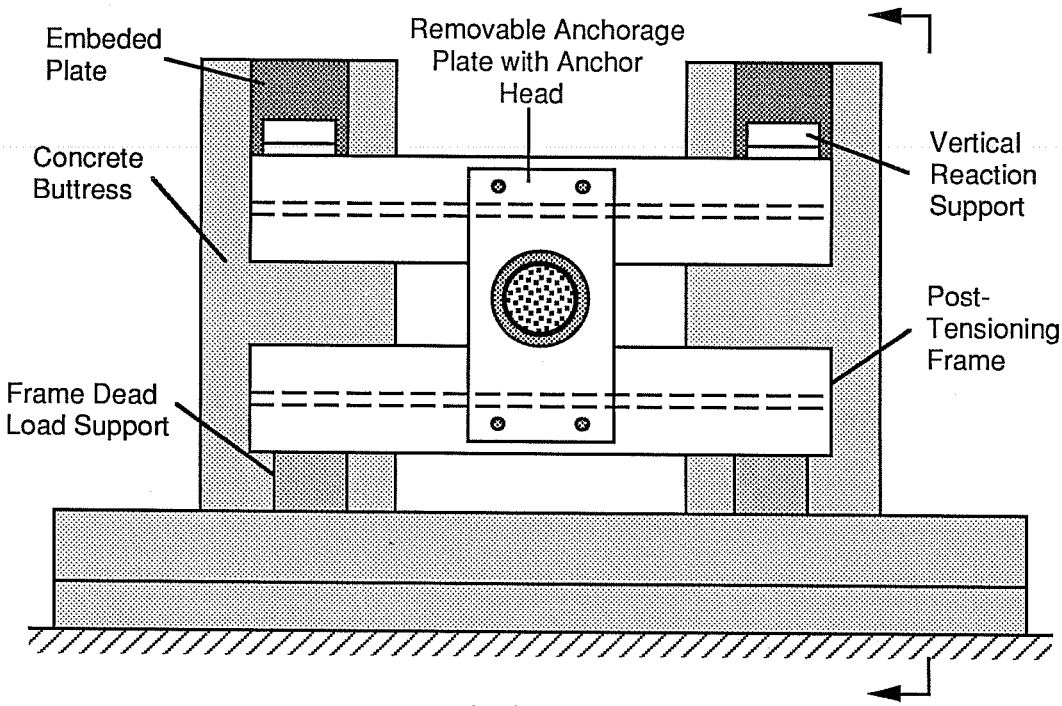

a) Elevation

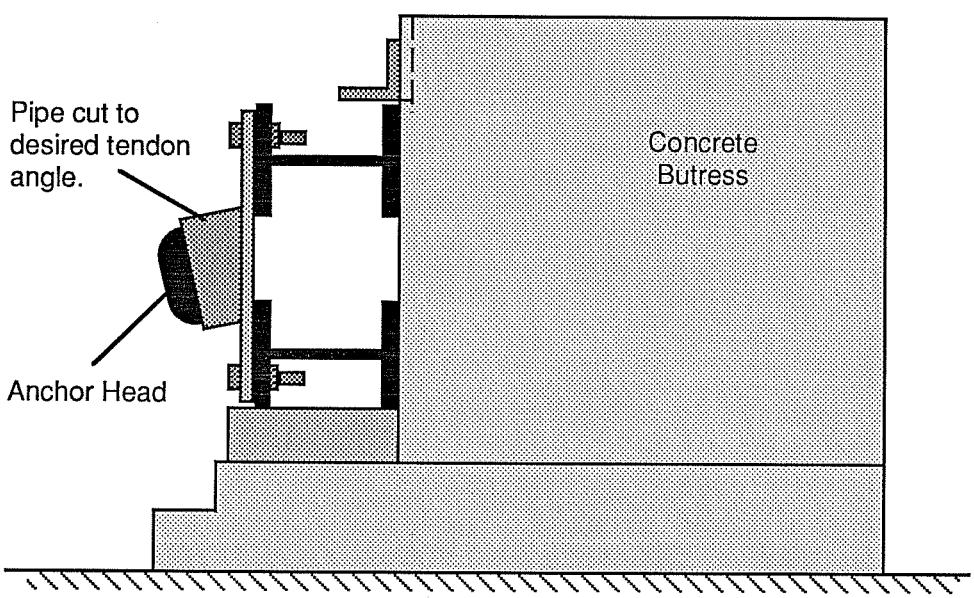

b) Section

Figure 3.11 Post-Tensioning Frame Attached to Concrete Buttress.

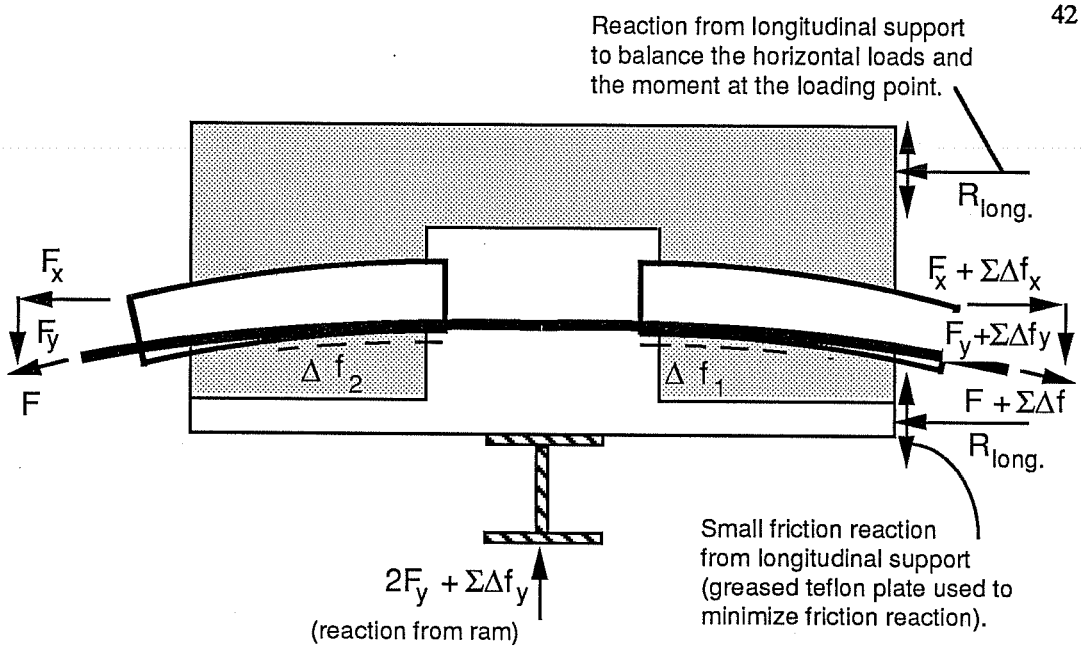

a) Reactions from Tendon, Testing Ram, and Longitudinal Supports - Elevation View.

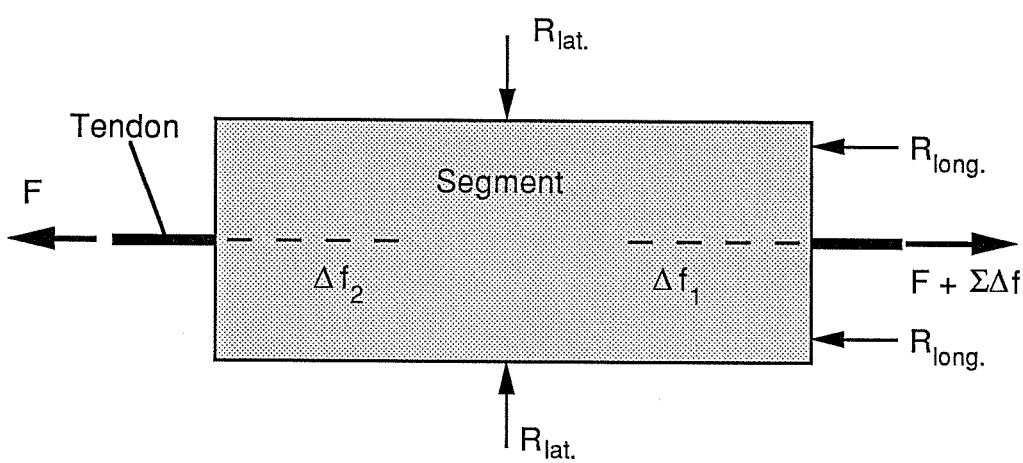

b) Longitudinal and Lateral Support Reactions - Plan View.

Figure 3.12 Reactions on Deviator Segment

floor; therefore, the longitudinal supports were designed to be anchored to the concrete buttresses. These supports had to be adjustable to support segments of varying tendon angles (thus varying segment elevations) and to allow placement of the segment into the test setup. In addition it was important that they be essentially frictionless. The longitudinal support system consists of frames anchored to the concrete buttresses, with adjustable steel plates bearing against the segment. These plates can be adjusted vertically along the frame as well as horizontally (see Figure 3.13a). The plates use a teflon sheet coated with grease, sandwiched between the concrete and steel to reduce the friction between the segment and the support. The lateral supports do not have the space restrictions that the longitudinal supports have and can easily be anchored to the floor. Since the reactions on the lateral supports are much lower than those on the longitudinal supports, single columns with adjustable steel plates were used for these lateral supports. These lateral supports are adjustable and essentially frictionless in the same manner as the longitudinal supports (see Figure 3.13b).

3.3.7 Safety Precautions. A wall made of three large concrete blocks discarded from a previous research project at Ferguson Laboratory was constructed behind the tendon anchorage frames. This wall was erected as a safety precaution to prevent the chucks or strand from shooting out of the anchor head in the event of tendon failure. A wooden box was constructed around the open area between the buttresses and this concrete wall to contain the strands and prevent them from whipping under this type of tendon failure. The tendon is housed in a section of steel tube (TS 6 x 6 x 1/4) in the open area between the concrete buttresses to prevent whipping of the tendon in this area as well. The steel tube used is large enough to allow movement of the tendon during testing without any interference.

3.3.8 Overall Layout. The final test setup layout incorporates only the concrete buttresses from the Powell/Beaupre setup. Both the specimen pedestal and the stressing frames from the Powell/Beaupre setup were removed. New stressing and anchorage frames were required as well as adjustable vertical supports and adjustable frictionless horizontal supports for the segment. Figure 3.14 shows a schematic of the final test setup.

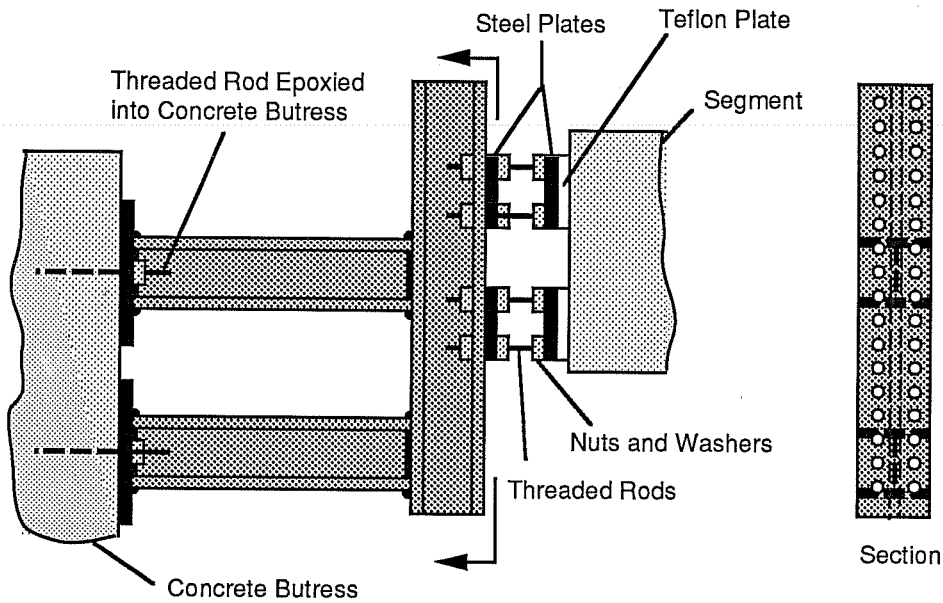

a) Longitudinal Support

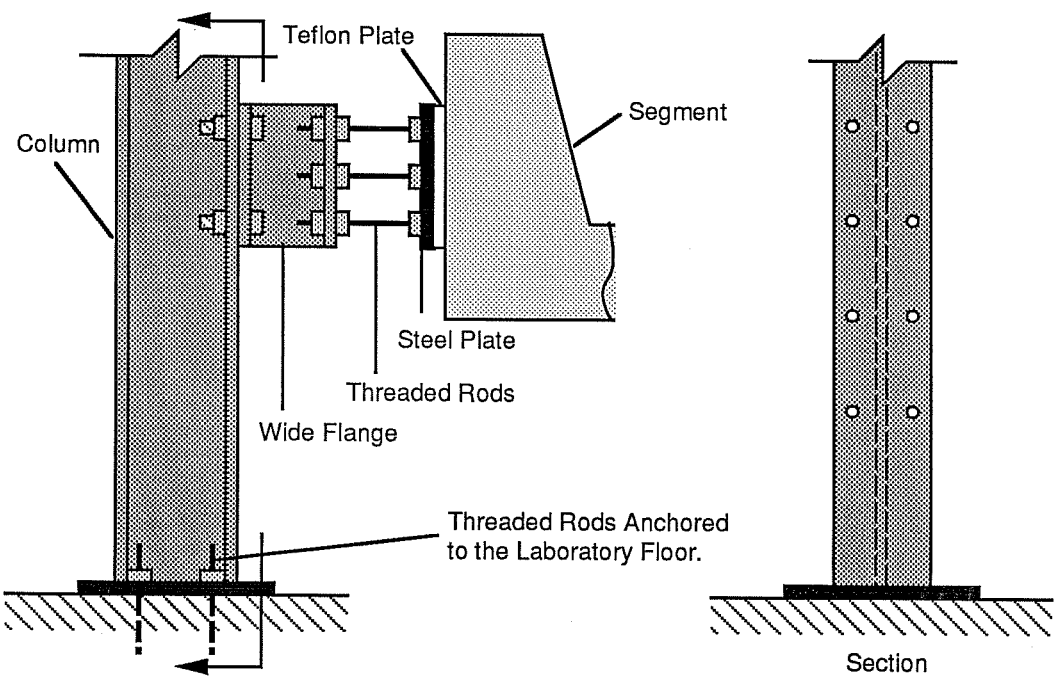

b) Lateral Support

Figure 3.13 Adjustable, Frictionless Lateral Supports for Deviator Segment

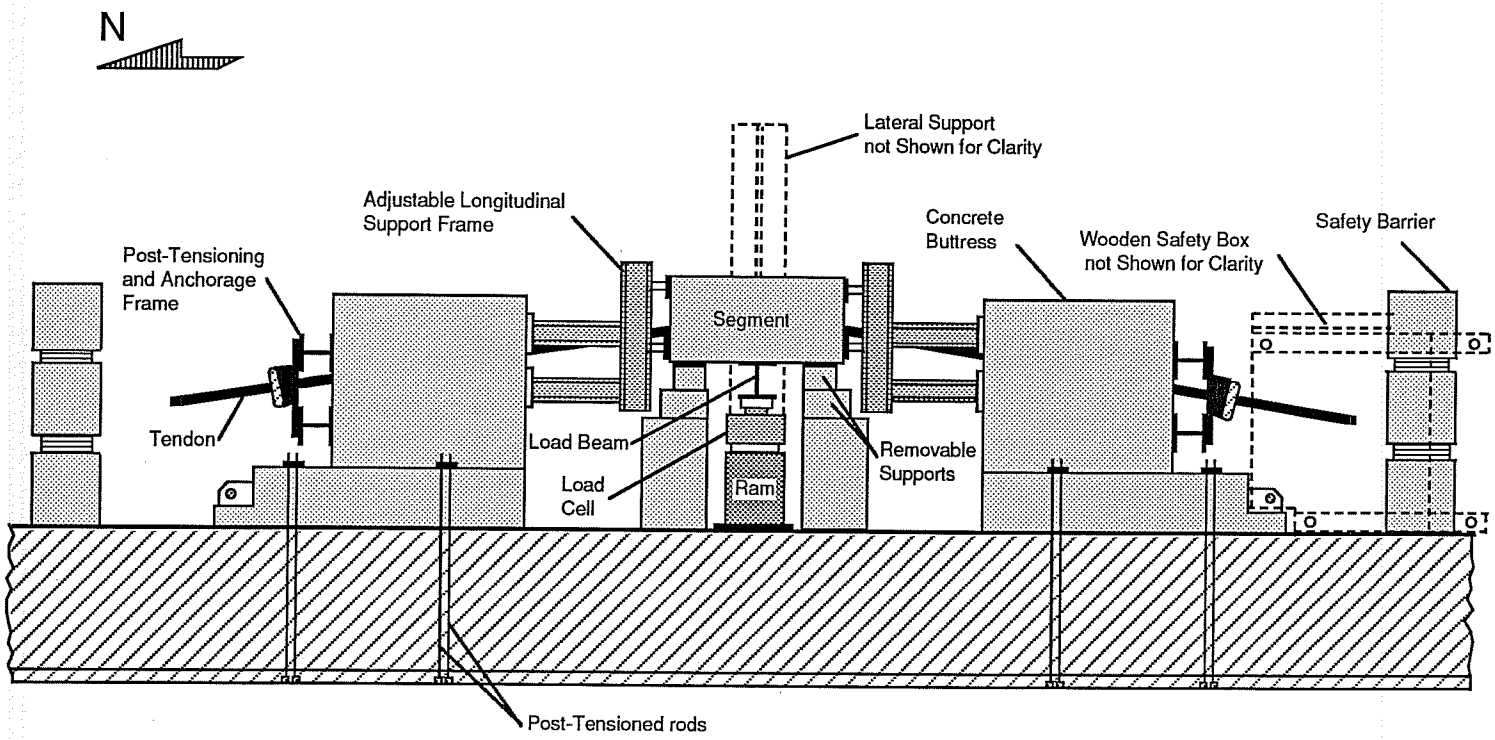

Figure 3.14 Schematic of Test Setup (Elevation).

CHAPTER 4
DESIGN AND CONSTRUCTION

4.1 Concrete Segment

4.1.1 Tendon Forces. The load on the concrete segment is the equilibrant of the vertical component of the tension in the tendon. Because the segment has different support conditions during initial post-tensioning and during testing (see Figure 4.1), the maximum tendon stress during each stage must be computed and used with the proper support condition when designing the specimen. Conservatively, the segment was designed for both of these support conditions using the maximum tendon stress resulting from either condition.

During post-tensioning, the tendon will be initially stressed to $0.75f_{pu}$. Due to the layout of the strands (12 strands in a 37 strand anchor head) and the anchorage method (double-chuck grip system), the strands must be stressed individually. Tendon stress losses are expected from seating of the wedges into the anchor head and from friction across the deviator. Special seating steps were developed to minimize the former. A center-hole ram located at the midpoint of the segment will then fluctuate the segment vertically to produce an additional stress range in the tendon to a design maximum stress range of 24 ksi. This design maximum stress range, although much higher than the expected tendon stress range in a prototype structure, was used for determining the loads on the specimen. The purpose for using such a high stress range is explained in detail in Section 5.2. Since the strands are to be stressed individually, the seating losses will somewhat reduce the tendon stress during post-tensioning. This final effective stress during post-tensioning will be the minimum stress during the cyclic load testing. The design maximum tendon stress during testing was assumed to be the full initial stress of $0.75f_{pu}$ (203 ksi), plus the design maximum stress range (24 ksi). Thus a maximum tendon stress of 227 ksi was used to design the segment. Seating losses were conservatively neglected during design.

In the segment design, friction across the deviator was considered in determining the horizontal and vertical reactions. The following equation was used in

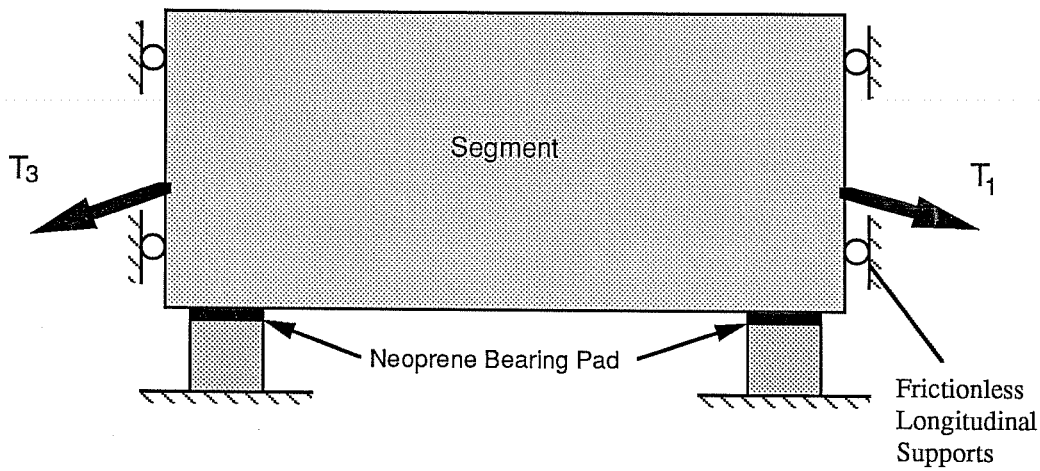

a) Simply Supported Vertically at Ends from Concrete Blocks.

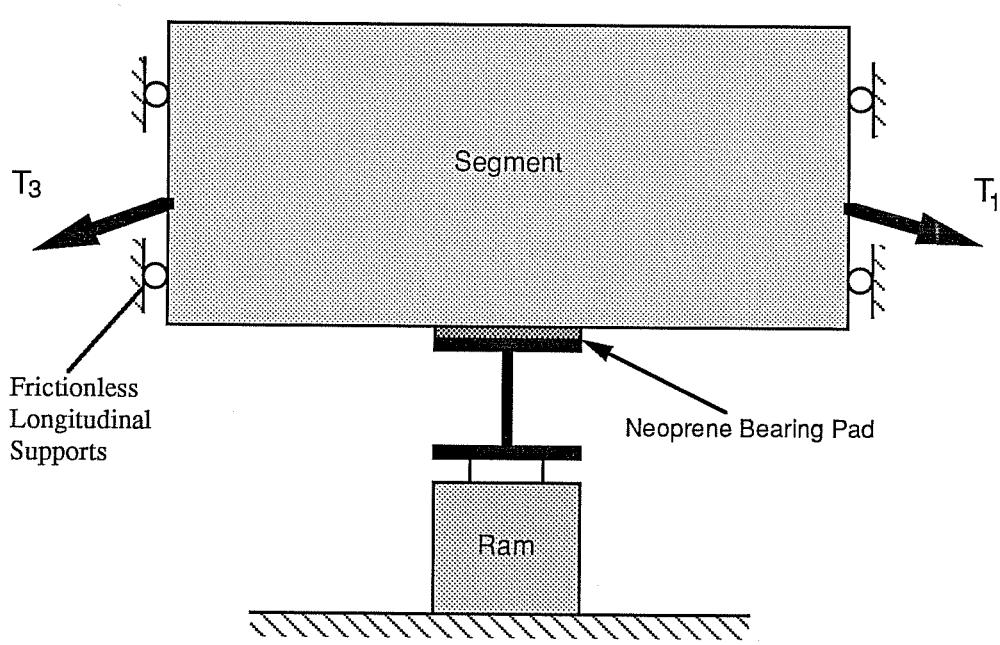

b) Vertically Supported at Middle From Load Beam.

Figure 4.1 Segment Support Conditions, (a) During Post-Tensioning, (b) During Testing.

calculating the change in tendon stress due to friction losses.

$$T_{n+1} = T_n e^{-(\mu\alpha + KL)}$$

μ is the curvature coefficient of friction, α is the angle of curvature of the duct (radians), K is the wobble coefficient of the duct, and L is the length of the curved duct in feet. Typical accepted values of μ and K for rigid steel duct are, μ = 0.15 - 0.25, and K = 0.0002 [18]. Radloff [27], found values of μ = 0.12 - 0.28 in friction tests using curved deviators with angles of 6 and 12 degrees. Therefore, in calculating the friction losses to size the restraining systems, K was taken as 0.0002, and due to the variation of μ, a very conservative value of μ = 0.5 was chosen. Appendix A presents the tendon forces and their calculated values during post-tensioning and testing as well as all design calculations for the segment.

4.1.2 Design of the Deviator Sections.

4.1.2.1 Deviator Forces. The stresses from the tendon must be carried by the deviator into the overall segment. The tension in the tendon combined with the friction forces across the deviator produce tension forces pulling down on the deviator and shear forces across the deviator. All of the calculations required to design the deviators, including the loads acting on the deviator, are presented in Appendix A. The vertical reaction used in the design of each deviator was 3.01 kips/inch, and the horizontal reaction is 2.86 kips/inch.

4.1.2.2 Deviator Reinforcement. The methods used for designing the local deviator reinforcement are from Beaupre's suggested design for block deviators [4] and from the AASHTO Standard Specifications for Highway Bridges [1]. 5000 psi compressive strength concrete and Grade 60 reinforcement were used in the design. A load factor of 1.26 was used in design resulting from the ultimate tendon stress (from the manufacturer) divided by the maximum design tendon stress, $1.06f_{pu} / (0.75f_{pu} + 24)$.

The reinforcement scheme was adapted from Beaupre's [4] block deviator reinforcement layout. This scheme uses loop bars to carry the direct tension and outer stirrups to carry the horizontal shear and distribute any cracking that may occur. The final design of the deviator reinforcement called for eight sets of loop bars and stirrups. Due to space limitations the outer stirrups used were not closed. However, they were hooked around longitudinal bars for anchorage. This allowed for the loop bars and stirrups to be located in the same plane. The spacing for this reinforcement was about 3 inches. The reinforcement layout and schedule for the deviator section of the segment is shown in Figure 4.2.

4.1.3 Design of the Box Segment.

4.1.3.1 Loading and Reactions. The webs and flange of the specimen must carry the stresses from the deviator to the lateral and vertical supports. There are two separate support conditions that the specimen was designed for; one during stressing and one during testing. All of the calculations required to design the segment (computation of loads, reactions, and concrete reinforcement design) are presented in detail in Appendix A.

4.1.3.2 Box Segment Reinforcement Design. The methods used for designing the reinforcement are from the AASHTO Standard Specifications [1]. Concrete with 5000 psi compressive strength and Grade 60 reinforcement were used in the design. A load factor of 1.26 was also used. The final reinforcement layout for the box segment of the specimen is shown in Figure 4.3a and the reinforcement schedule is shown in Figure 4.3b. This reinforcement scheme consists of two longitudinal # 6 bars in each web (four total per specimen) near the bottom of the specimen to resist the moments on the specimen during stressing. Two longitudinal # 7 bars are located in the flange at the interface of each web and the flange (four total per specimen) to resist the moments occurring during testing. To resist the shear forces occurring during stressing and testing, 13 - # 3 closed stirrups at 6 in. spacing were used in each web. Additional reinforcement was used in the lateral direction to transfer the load from the deviator to the web and to help distribute cracking. These consist of 13 - # 6 bars near the bottom of the flange and 13 - # 3 bars near the top of the flange spanning from web to web.

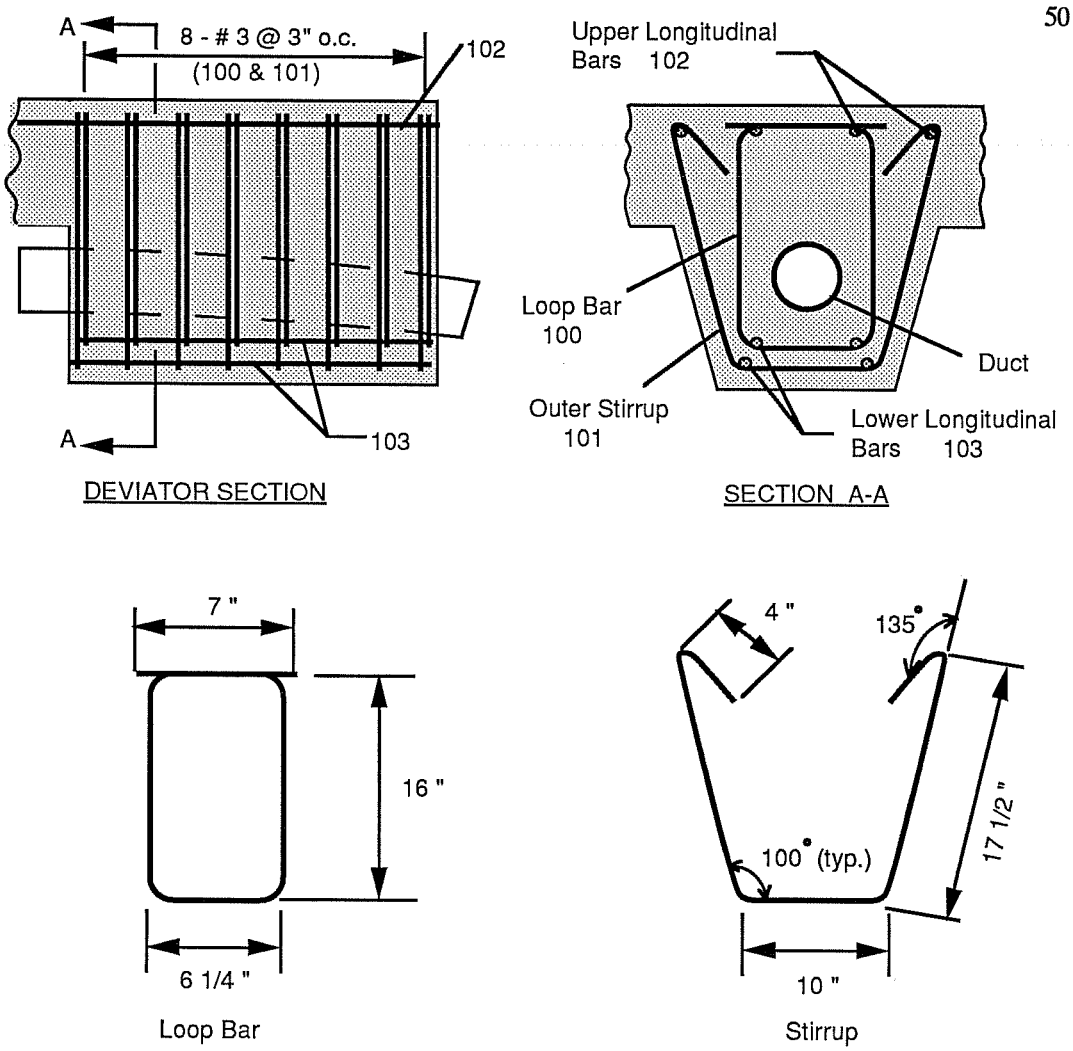

Bar No.	Bar Type	Bar Size	Total Length	Bars Required per Deviator
100	Loop	# 3	52 "	8
101	Stirrup	# 3	53 "	8
102	Straight	# 3	70 "	4 / specimen
103	Straight	# 3	22 "	4

Figure 4.2 Deviator Reinforcement Scheme.

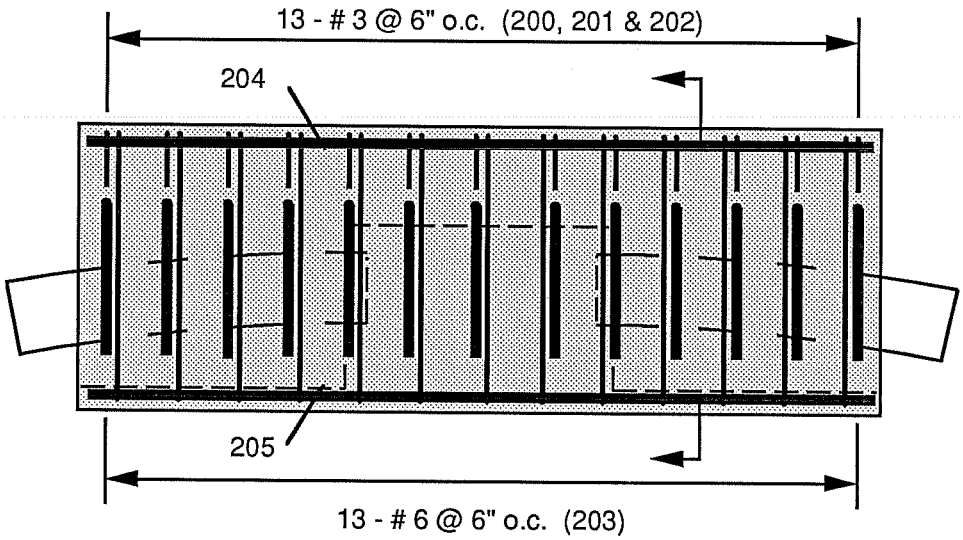

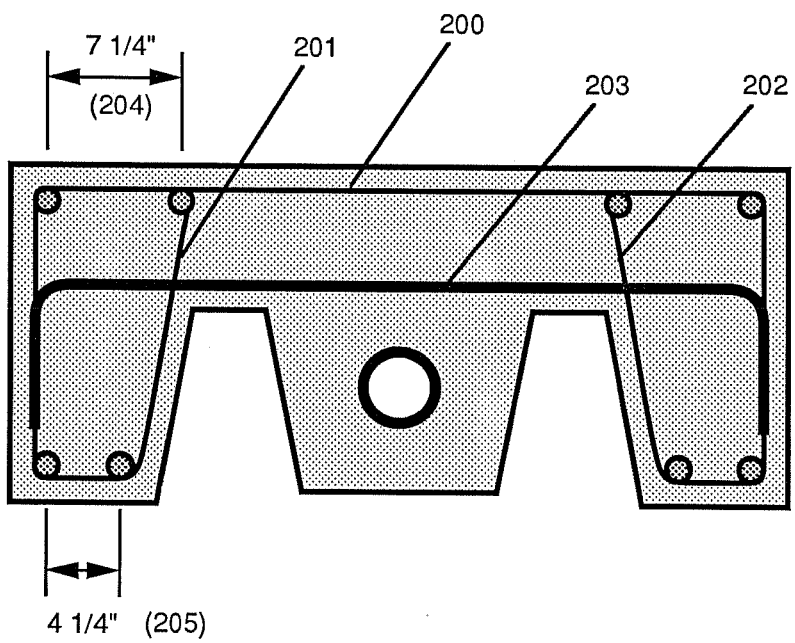

SECTION

Figure 4.3a Box Segment Reinforcement Layout.

Bar No.	Bend Type	Bar Size	Total Length	Bars Required
200	A	# 3	55 "	13
201	B	# 3	60 "	13
202	C	# 3	60 "	13
203	D	# 6	63 "	13
204	Straight	# 7	70 "	4
205	Straight	# 6	70 "	4

Bend Types (all dimensions out-to-out)

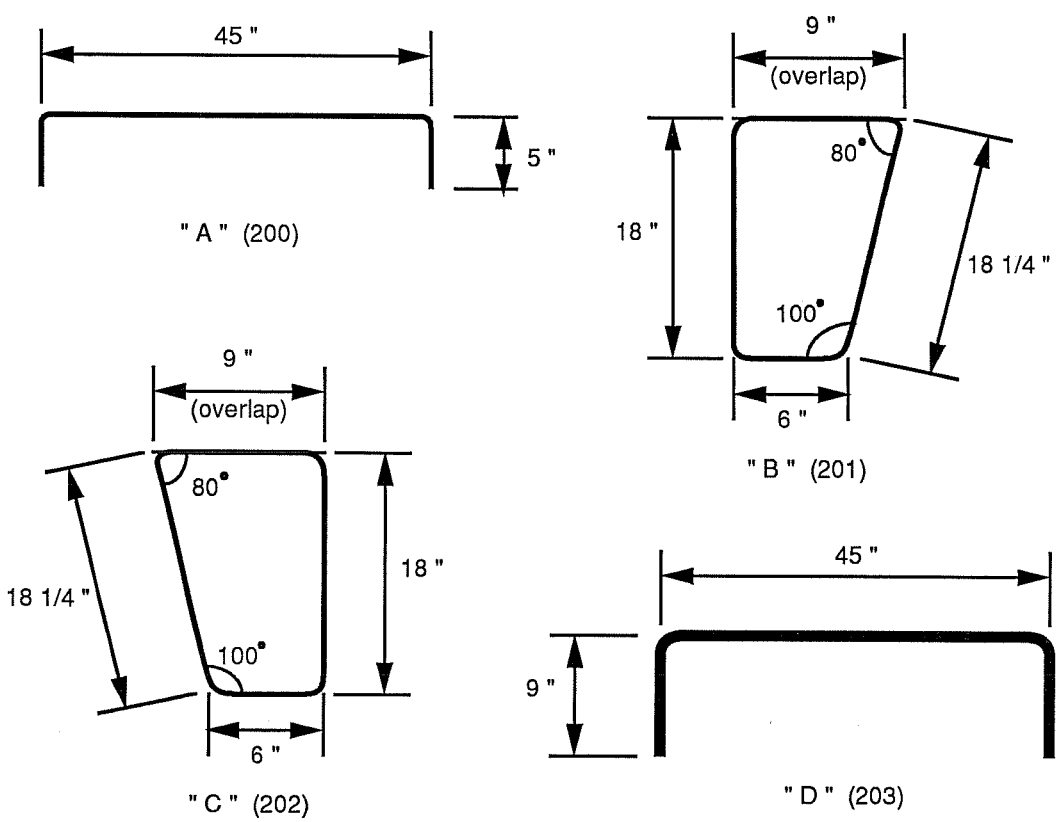

Figure 4.3b Box Segment Reinforcement Schedule.

4.1.4 Fabrication of Segment.

4.1.4.1 Formwork. The specimen forms consist of several units which can be assembled and disassembled easily. These units are made from 3/4 in. plywood and 2x4 in. lumber. Figure 4.4a shows the completed assembled form units. The formwork was designed to allow unrestricted removal of the specimen from the forms and to be reusable for all deviation angles. The side units run the length of the specimen and were bolted to the form base. The end forms consist of two units with each covering half the width of the specimen. Half units were used so they would be easy to assemble and disassemble around the duct extending out from the deviator. A square gap was cut into each unit to allow fit-up around the protruding duct. These units bolt to the form base using slotted connections, to the side units, and to each other. Bracing was extended from the side units and the end units to the form base to prevent the upper portion of the units from bulging outward.

The voids between the web and the deviator were created using forms extending along the length of the specimen and bolted to the form base. These units have a vertical slope of 6:1 to allow the specimen to be removed easily. The void between the deviators was created using a polystyrene block shaped to fit between the longitudinal void form units. A cylindrical area was carved out of the polystyrene block at each end to allow the deviator duct to extend outside the concrete. Polystyrene was used because it could be removed easily from a tight space by chipping it out. The polystyrene block was covered in heavy plastic to prevent deterioration of the block from contact with the concrete or the form oil. The polystyrene block was then positioned into the form and the edges sealed with silicone sealant.

All of the wooden forms were covered with several coats of lacquer and allowed to dry. Slab bolsters, 1 1/2 in. high to allow for adequate cover on the reinforcement cage, were nailed to the form base. All units were assembled, except for the end units, and all gaps were sealed with silicone before the cage was placed into the formwork. Immediately before the reinforcement cage was placed into the forms, the forms were oiled to allow them to be removed from the hardened concrete easily. The reinforcing cage was then set onto the bolsters and tied down. After the cage and ducts were in place, the end units were aligned and

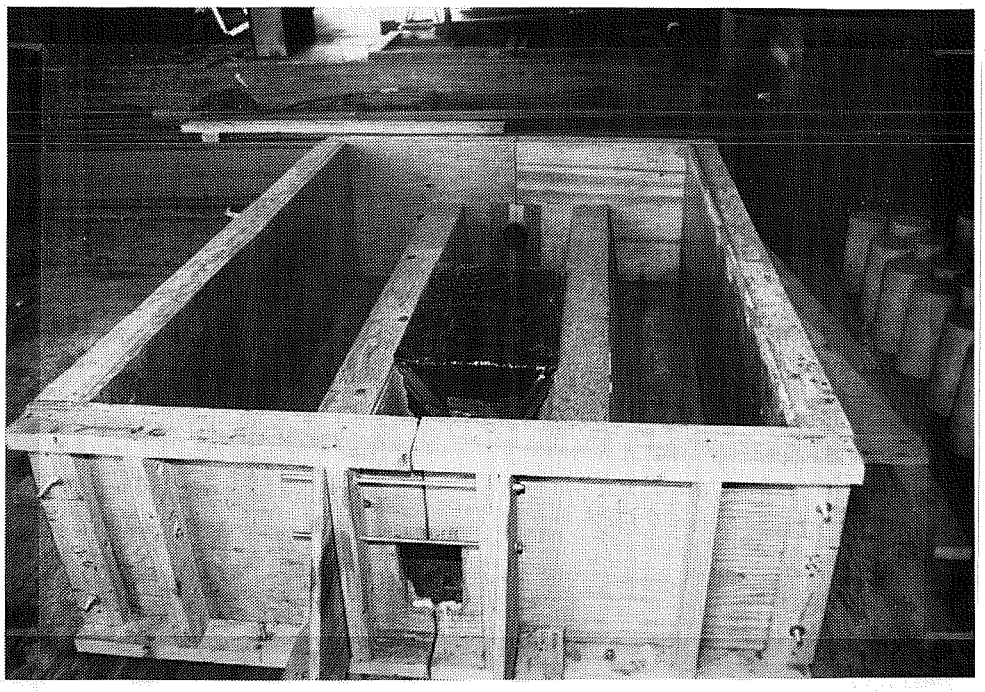

a) Assembled Form Units

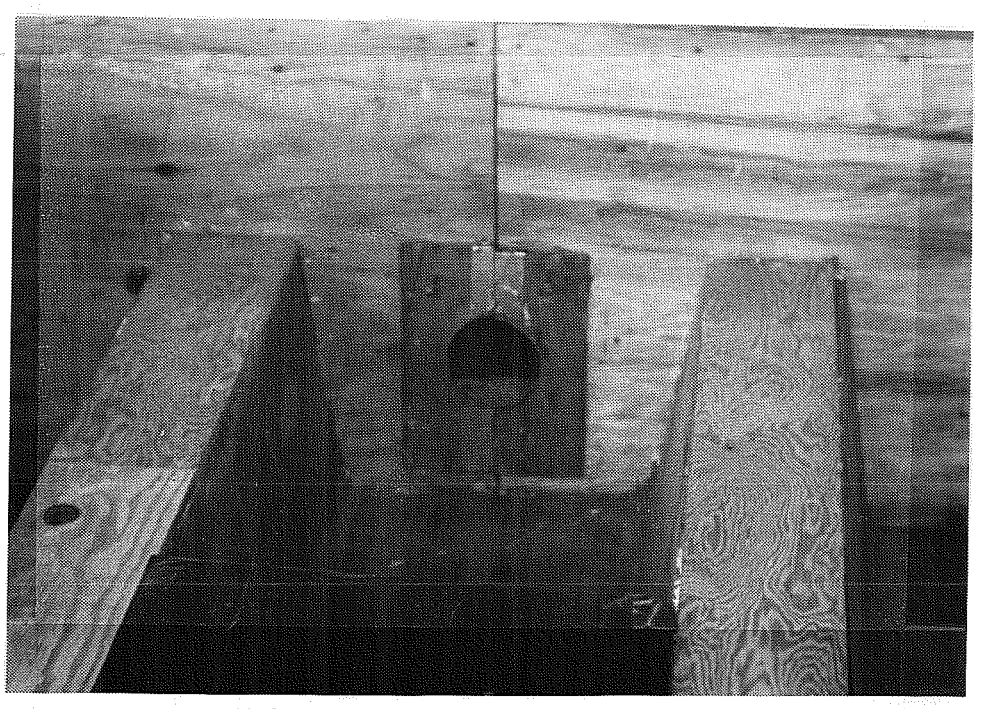

b) Close-Up of Deviator Pipe Cut-Out Detail

Figure 4.4 Specimen Formwork

bolted up. Two thin wooden sheets of plywood (1/4 in. thick) with precut half circles, were then placed around each duct and fastened to the inside of the end forms to fill up the square gap in the end unit. Figure 4.4b shows this cut-out form fastened to the form units without the deviator pipe. The gaps between the end units and the other forms, and between the duct and the forms were then sealed with silicone.

4.1.4.2 Reinforcing Cage. All reinforcement was ASTM A615 Grade 60 and was delivered pre-bent to specified dimensions. The cage was constructed by first tying the loop and stirrup bars (schedule 100 and 101) of the individual deviators to the short (22 in., schedule 102) # 3 straight bars. The two deviator cages were then tied to the long (70 in., schedule 103) # 3 straight bars to form one cage. Two separate web cages consisting of the web shear reinforcement (schedule 201 and 202) tied to the top and bottom longitudinal reinforcement (schedule 204 and 205) were then constructed. The three individual cages were then aligned in their proper positions and connected by tying the lateral reinforcement to the web and deviator cages. The completed cage was then placed into the forms and the ducts were inserted.

One end of each deviator duct was wedged into a cylindrical hole, 3 1/2 inches in diameter and 1 in. deep, in the ends of the polystyrene block. The center of this hole is 2 3/4 in. below the top of the block. The opposite end of the duct rested on a small piece of # 3 reinforcement (about 7 in. long) which was tied across the deviator loop bars. Measured downward from the top of the loop bar reinforcement, this bar is located 14 7/8 in. for a 10 degree deviation angle and 13 11/16 in. for a 5 degree deviation angle. The dimensions and placement location of the deviator pipe are shown in Figure 4.5. Once the deviator pipe was properly aligned, it was then tied to the cage with plastic cable ties to prevent misalignment during concrete placing. The finished reinforcing cage sitting in the forms with the deviator duct in place is shown in Figure 4.6.

4.1.4.3 Concrete Placing. Concrete with a target 28 day compressive strength of 5000 psi and a maximum aggregate size of 3/4 in. was delivered from a local ready-mix supplier. The fresh concrete was placed in two lifts from a bucket using an

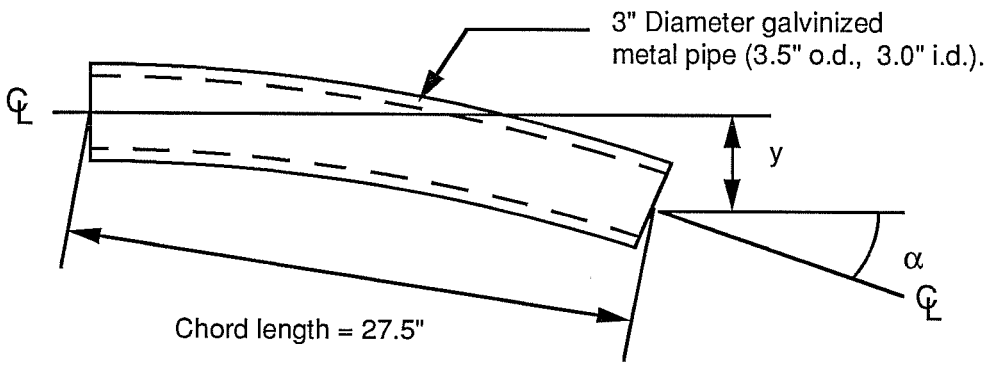

Tendon angle = 5 deg. → α = 8 deg. → y = 1 15/16 "

Tendon angle = 10 deg. → α = 13 deg. → y = 3 1/8 "

a) Deviator Pipe Dimensions.

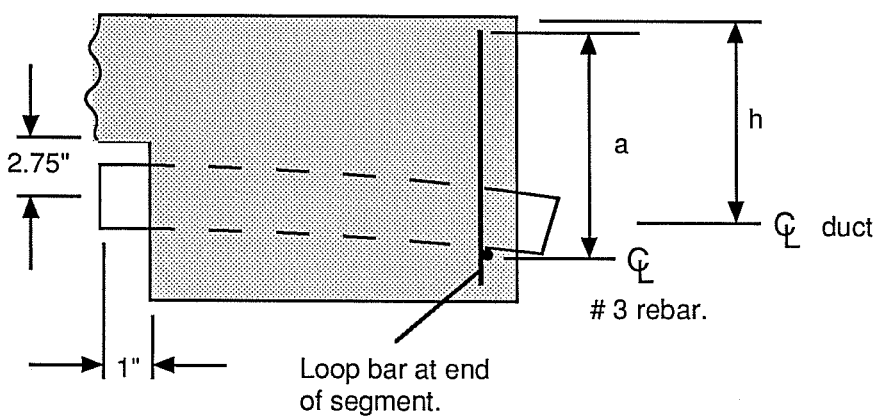

Tendon angle = 5 deg. → h = 13 11/16" → a = 13 9/16"

Tendon angle = 10 deg. → h = 14 7/8" → a = 14 9/16"

b) Deviator Pipe Location in Segment.

Figure 4.5 Deviator Pipe Size and Location.

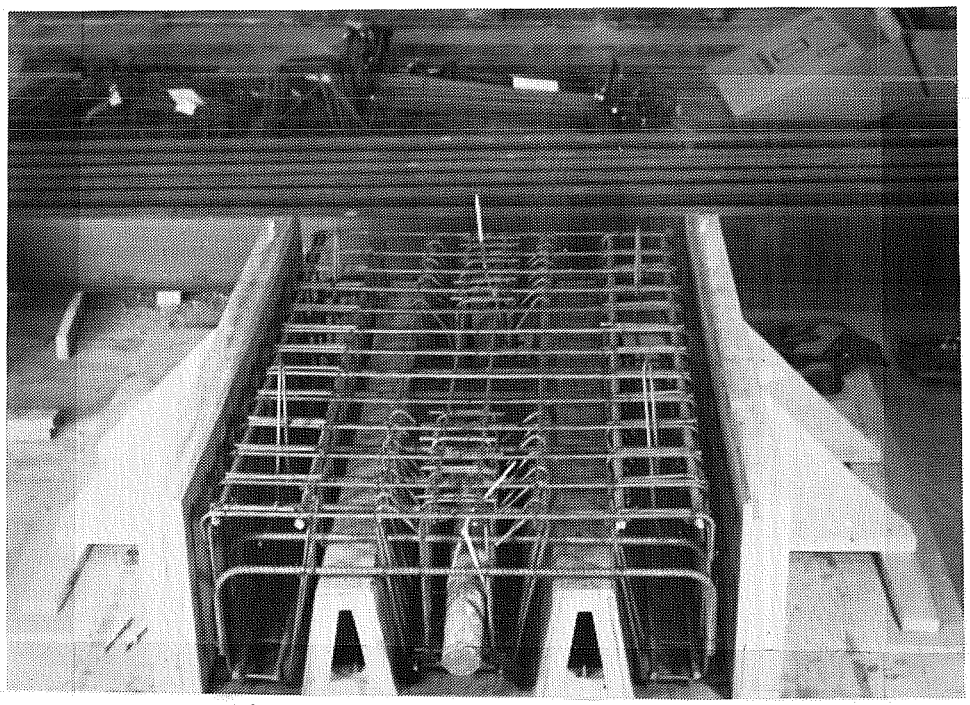

Figure 4.6 Reinforcing Cage in Formwork.

Figure 4.7 Consolidation of Concrete During Casting.

overhead crane. Consolidation of the concrete was achieved using 3/4 in. and 1 in. roundhead internal vibrators (see Figure 4.7). Several test cylinders were also fabricated. The exposed concrete of the specimen was finished using hand trowels.

About two hours after casting the specimen was covered with wet burlap and enclosed in sheets of plastic. The moist curing was continued for four days and then the forms were removed. The test cylinders were cured in a similar manner as the specimen. The concrete cylinders were tested under uniaxial compression at 7 and 28 days. The average compressive strengths were 6293 psi and 7046 psi respectively.

4.2 Test Apparatus

4.2.1 Design of the Loading System. The loading system consists of a center-hole ram with maximum dynamic pressure capacity of 3 ksi, a piston area of 49.3 in^2, and a stroke of 12 inches. The maximum dynamic load capacity of the ram is 148^k (pressure capacity multiplied by piston area). Figure 4.8 illustrates the loading system used for introducing fluctuating stresses into the tendon. The ram sits on a bearing plate attached to the floor. A two inch plate with countersunk holes was positioned between the ram piston and a 200^k load cell. A one inch plate with countersunk holes was set between the load cell and the load beam. The load beam uses a swivel support system where it rests on the one inch plate. Finally, elastomeric bearing pads were placed on the top of the beam where it bears on the specimen. All of the necessary calculations for designing the load system are presented in Appendix B.

The load beam was designed as a simply supported beam with a concentrated load applied at the center. Due to space limitations between the floor and the specimen, separate load beams had to be used for the two deviation angles. The final sizes selected were; W8x58 for the 5° angle, and W12x65 for the 10° angle. Each beam required stiffeners for the design of the elastomeric bearing pads. These pads were used to provide a simply supported end condition between the beam and the specimen and were designed using AASHTO [1] provisions. The final sizes required were; plain pad 1/4 x 8 x 9 in. for the W8 beam, and plain pad 1/4 x 9 x 12 in. for the W12 beam. The hardness of all pads used was 70 durometer.

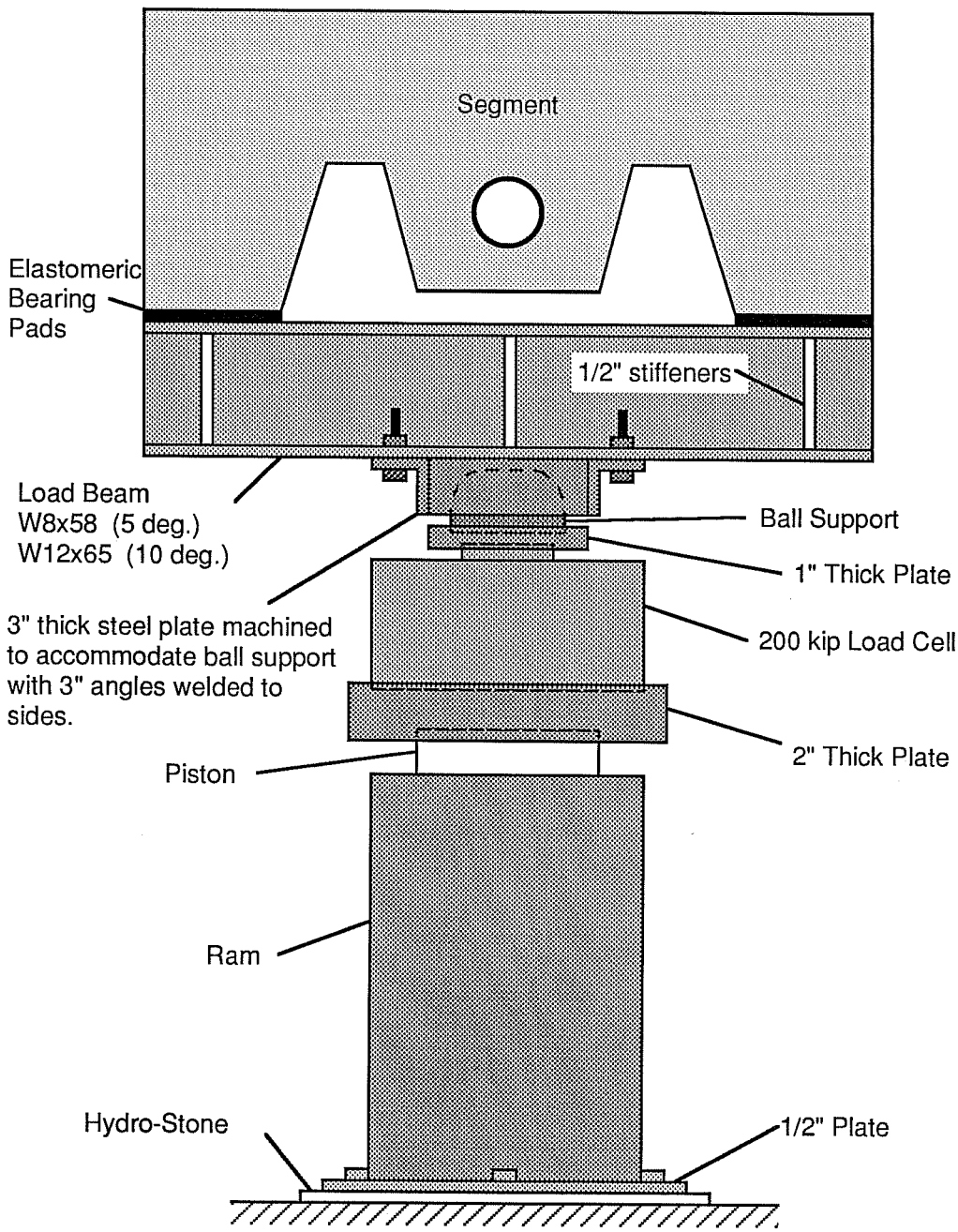

Figure 4.8 Loading System.

4.2.2 Design of the Stressing and Anchorage Frames. The stressing and anchorage frames had to be designed to transfer the load from the anchorage system to the concrete buttresses. They also had to allow for tendons of varying angles to pass through the frames. The frame consists of two W12x106 beams connected by four 1 in. stiffener plates (see Figure 4.9 and 4.10). Two of these stiffener plates are located under the anchor head and are used to stiffen the anchor head attachment plate. A filler plate, 1 x 12 x 12 in. with an 8 in. hole cut through the center, was welded flat across these stiffener plates to provide direct bearing from the anchor head attachment plate. The other two plates are located near the ends of the beams. The beams were designed to act together as a simply supported beam. The anchor head attachment plate (see Figure 4.11) is supported along its length by the stiffener plates. The bolts attaching the anchor plate to the beams are designed for shear from the vertical component of the tendon force.

Elastomeric bearing pads were used to give the beams simply supported end conditions and were designed using AASHTO [1] provisions. These neoprene pads required two internal steel reinforcing plates. The pads used were 1 1/8 x 12 x 12 in. with 5/16 in. thick neoprene external layers, one 3/8 in. thick neoprene internal layer, and two gauge 20 steel shims.

The anchorage and stressing frames had to be supported in the vertical direction as well. When the tendon is stressed an upward load will be applied to the frames from the vertical component of the tendon force. Initially, a support welded to the steel plates embedded into the concrete buttresses was considered for resisting the upward force. However, during design it was determined that the embedded studs anchoring the plate could not resist the forces and an alternative design was required. Therefore, a vertical restraint system was designed which anchors the frame to the concrete base (see Figure 4.10b). Two C12x20.7 sections were bolted to the lower beam at each end of the frames using 8 - 5/8 in. diameter A325 bolts. These channels were then bolted to similar channel sections that were welded to 1 in. plates anchored to the concrete buttress base. Two 6 in. high concrete blocks were used to support the dead load of the frame while these supports were being bolted up. The anchor plates were attached to the base by 4 - 5/8 in. diameter, A-193, B-7 rods that were epoxied into

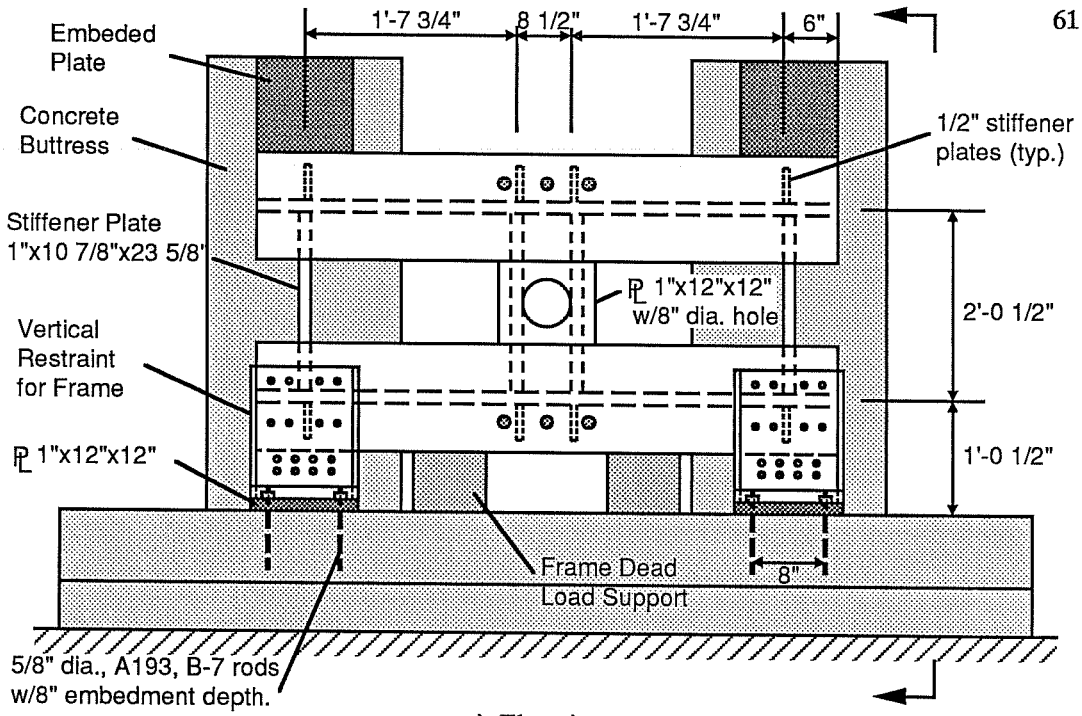

a) Elevation

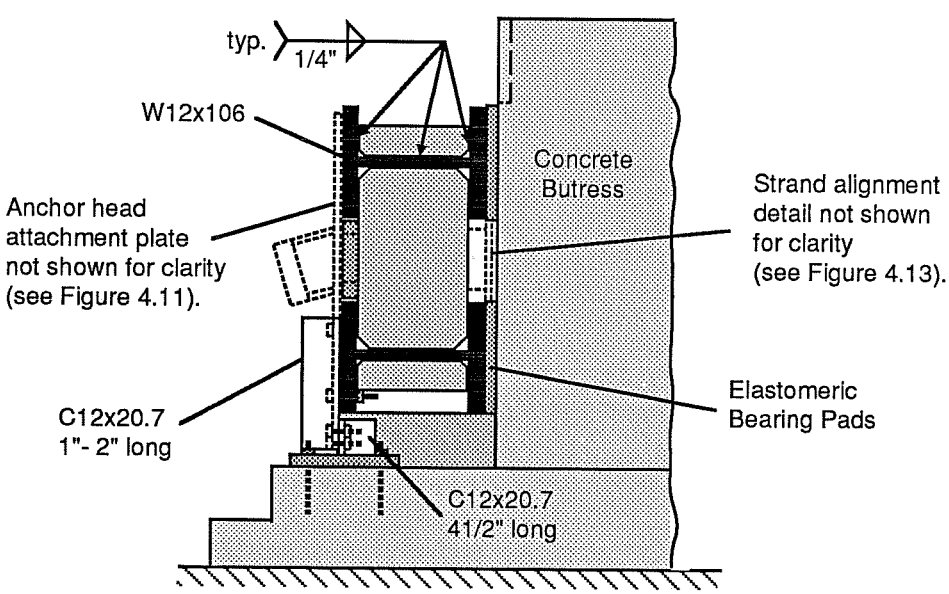

b) Section

Figure 4.9 Post-Tensioning Frame Attached to Concrete Buttress.

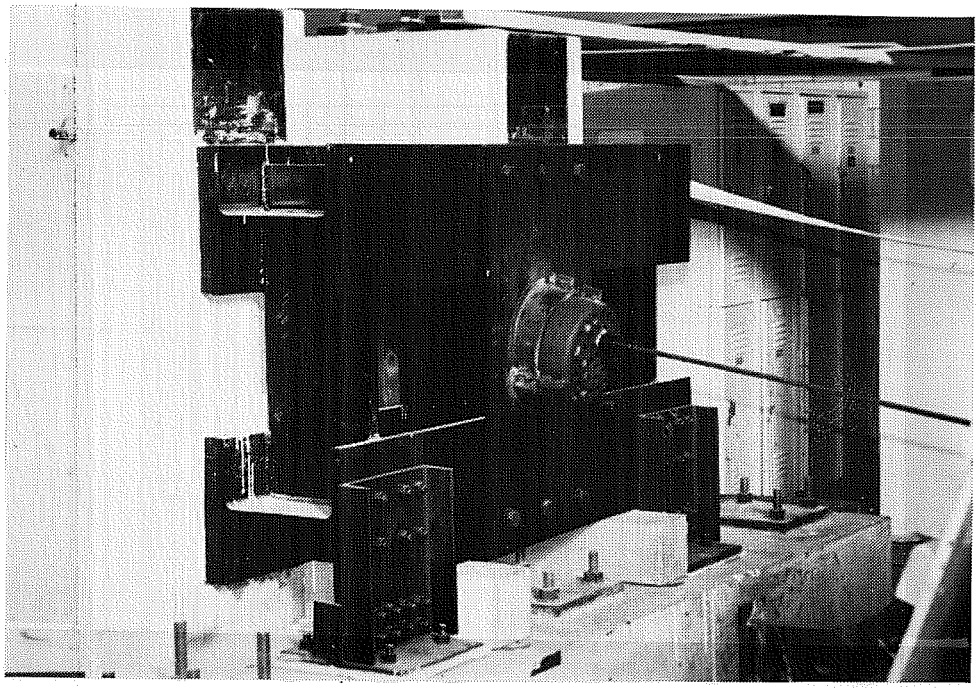

a) Post-Tensioning Frame with Anchor Head Attachment Plate - Dead End

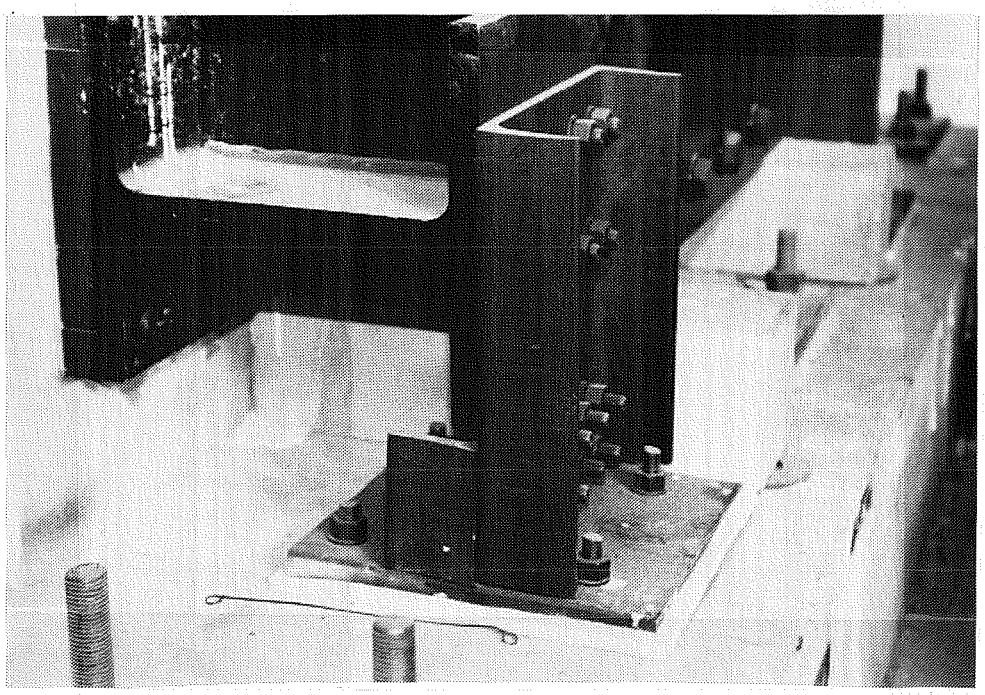

b) Vertical Restraint Detail

Figure 4.10 Completed Post Tensioning Frame

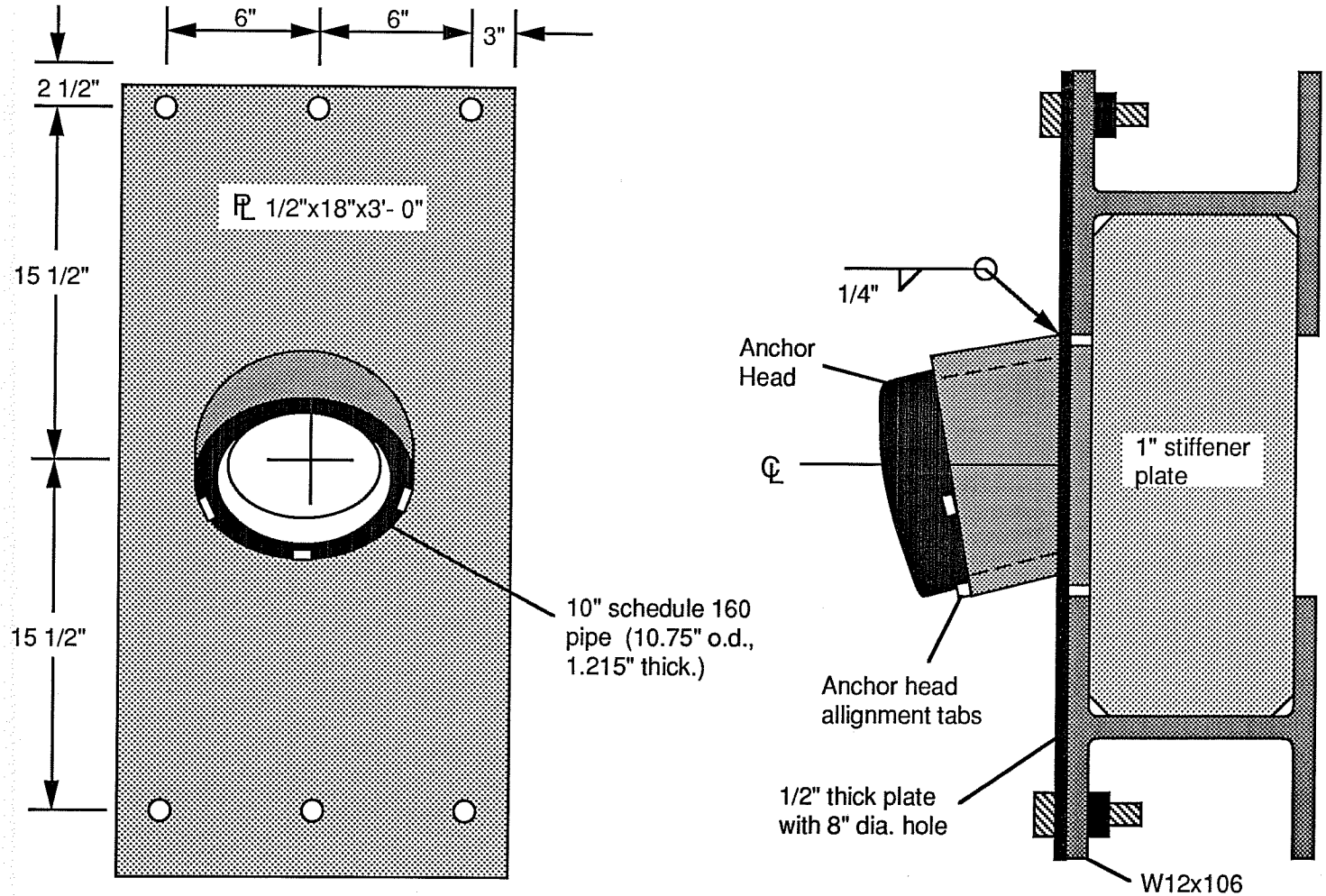

Figure 4.11 Anchor Head Attachment Plate.

holes drilled into the concrete with an embedment depth of 8 inches. This system allowed for easy fit up of the frames onto the concrete buttresses.

The tendon stressing procedure requires a chair for the ram which supports the ram away from the anchor head (see Figure 4.12). This chair allows the wedges to be power seated easily. The chair uses a 2 in. thick plate with 12 - 2 in. diameter holes bored in the pattern of the strand anchorage. This plate is then bolted to a frame of four legs (L3x3x3/8), cut to the desired tendon deviation angle and welded to a 1/2 in. thick plate with an 8 in. hole in the center. This allows the 2 in. plate to be used for all tendon deviation angles since it can be removed and bolted to frames with legs cut to different angles. The chair assembly can then be positioned around the anchor head and bolted to the anchor head attachment plate. To align the ram parallel to the tendon a small plate assembly was made with a six degree angle to match the angle of the holes in the anchor head. This assembly is removable and can be used for each strand to properly align the ram.

Finally, tendon alignment details were designed and bolted to the back of the frames (see Figure 4.13 and 4.14). These components consist of short lengths of aluminum pipe (2 - 3 in.) set into 1 x 7 x 7 in. steel plates. The edges of the aluminum pipes where the tendon was to enter were rounded out to reduce stress concentrations in the tendon. The steel plates were then welded to a section of steel tube (6 x 6 in.) which was cut to the desired tendon deviation angle. The tube was welded to another 1 in. thick plate, with a 5 1/2 in. diameter hole, which bolts to the frame on the opposite side from the anchor head assembly.

4.2.3 Design of the Segment Longitudinal Supports. The longitudinal supports consists of four rigid frames anchored to each buttress. These frames were fabricated using W8x18 steel beams (see Figure 4.15a and 4.16a). The vertical member has a series of holes drilled through the outer flange where the segment support plates are bolted to the frame. These support plates are 1/2 x 6 x 6 in. and can be located to accommodate various tendon angles. The plates are welded to 4 - 5/8 in. diameter threaded rods which attach to the frame. These rods allow the plate, to be adjustable horizontally so the segment can be set into the testing area easily. The longitudinal support frame is attached to the concrete buttress by an

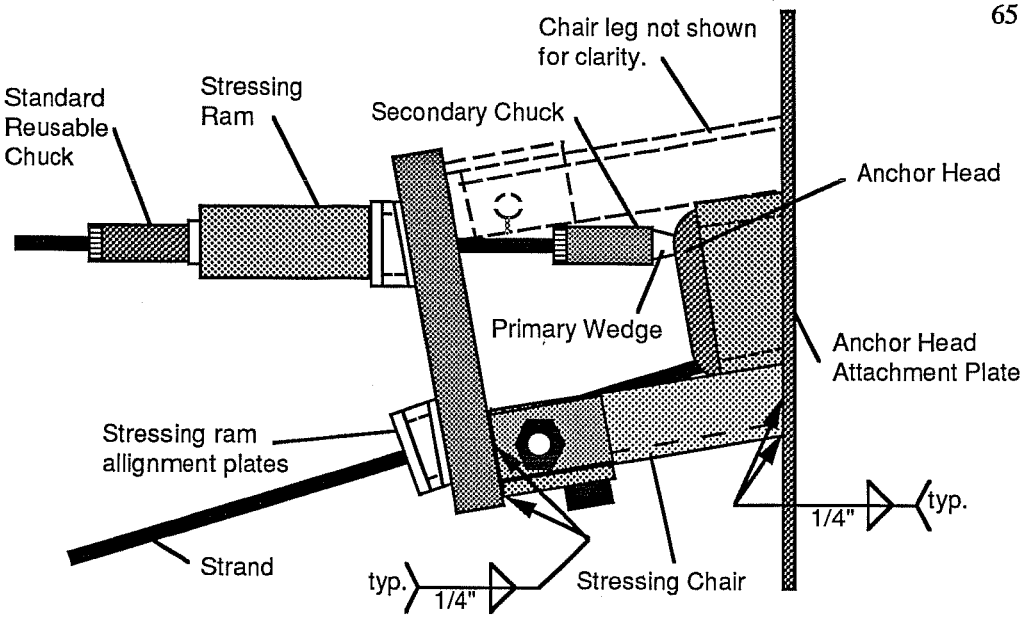

a) Chair Detail.

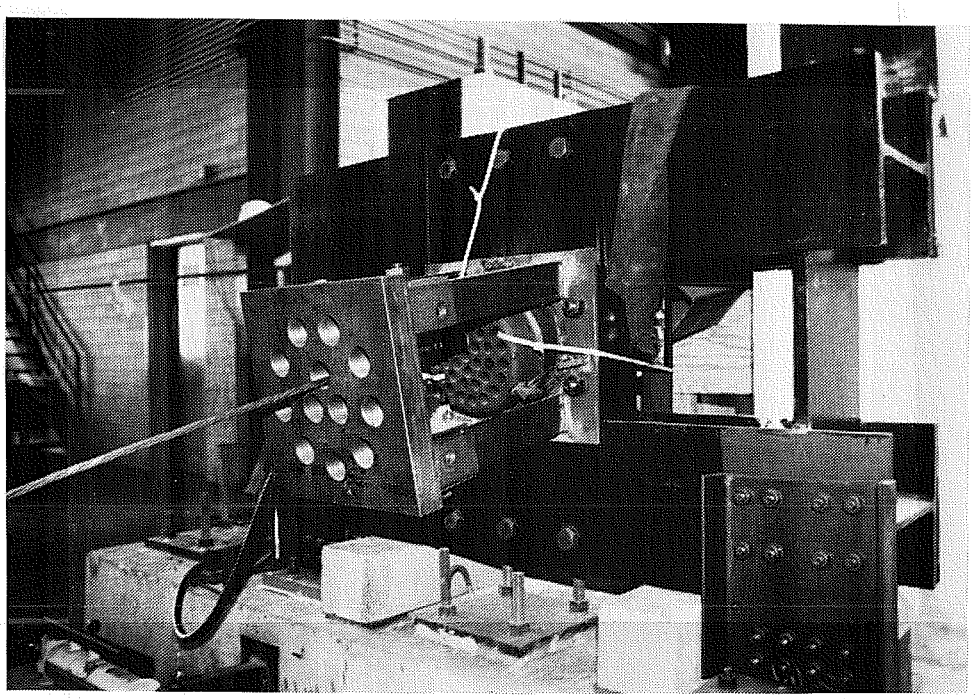

b) Chair Attached to the Anchorage Frame.

Figure 4.12 Chair for the Stressing Ram.

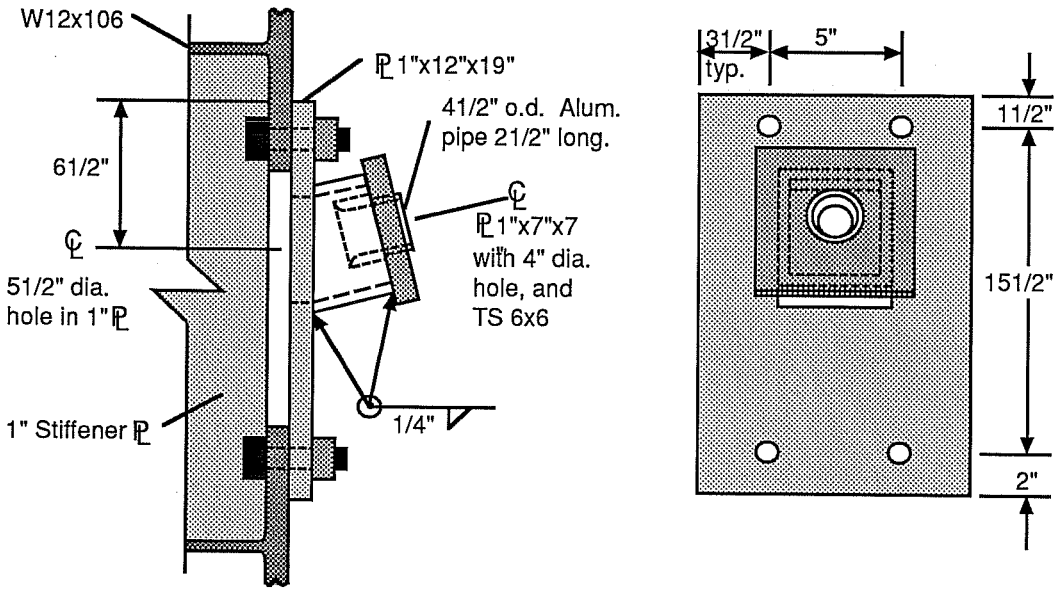

a) Dead End Detail.

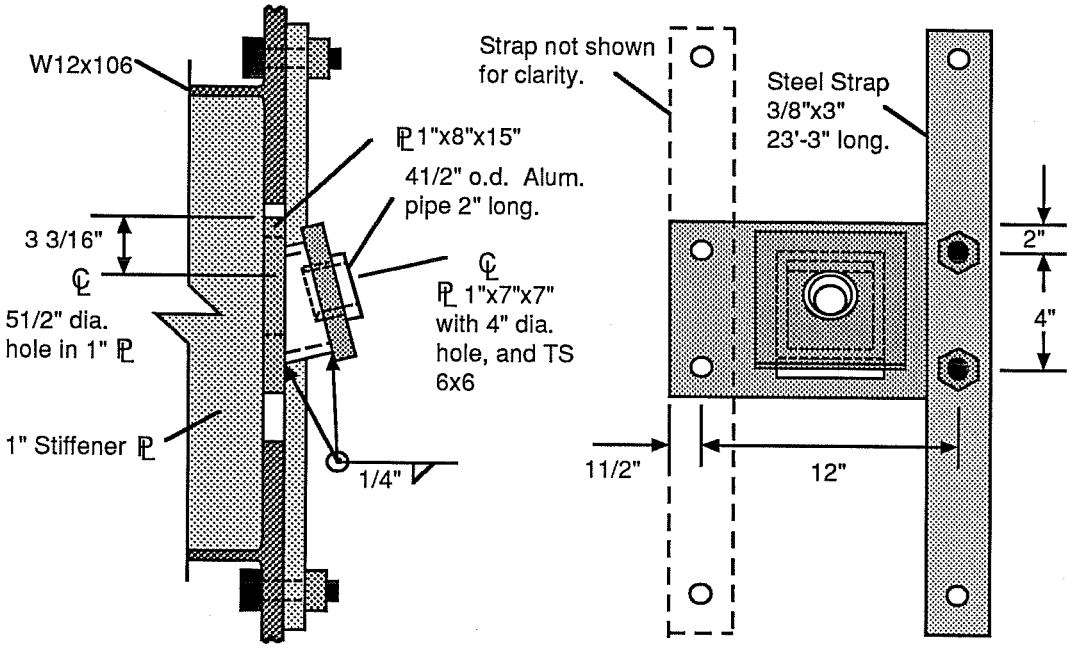

b) Stressing End Detail

Figure 4.13 Alignment Details for External Tendons with 10 degree Deviation Angle.

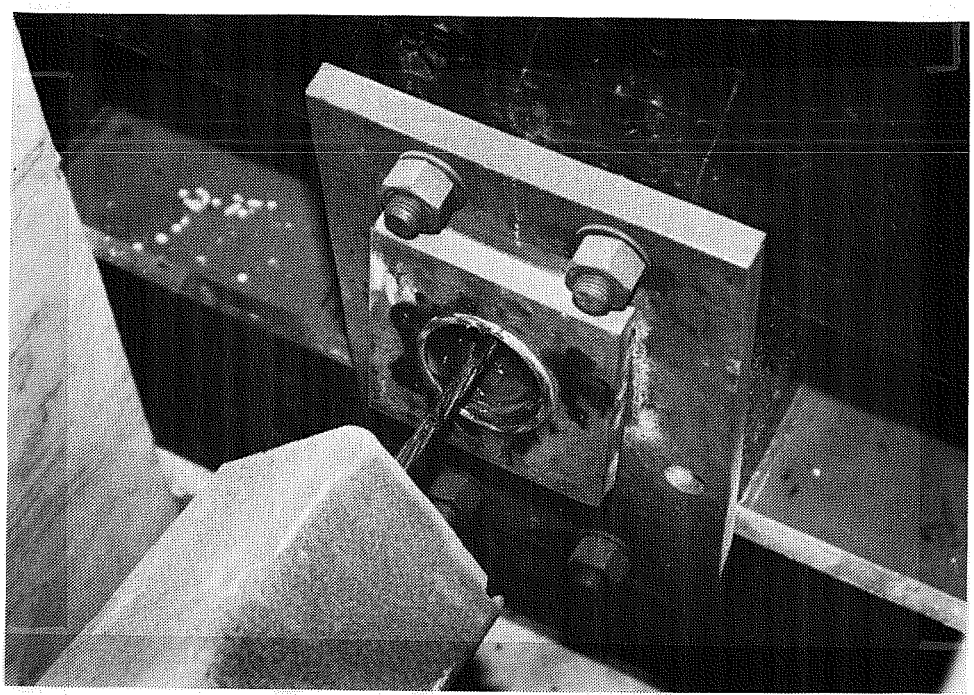

a) Dead End Detail

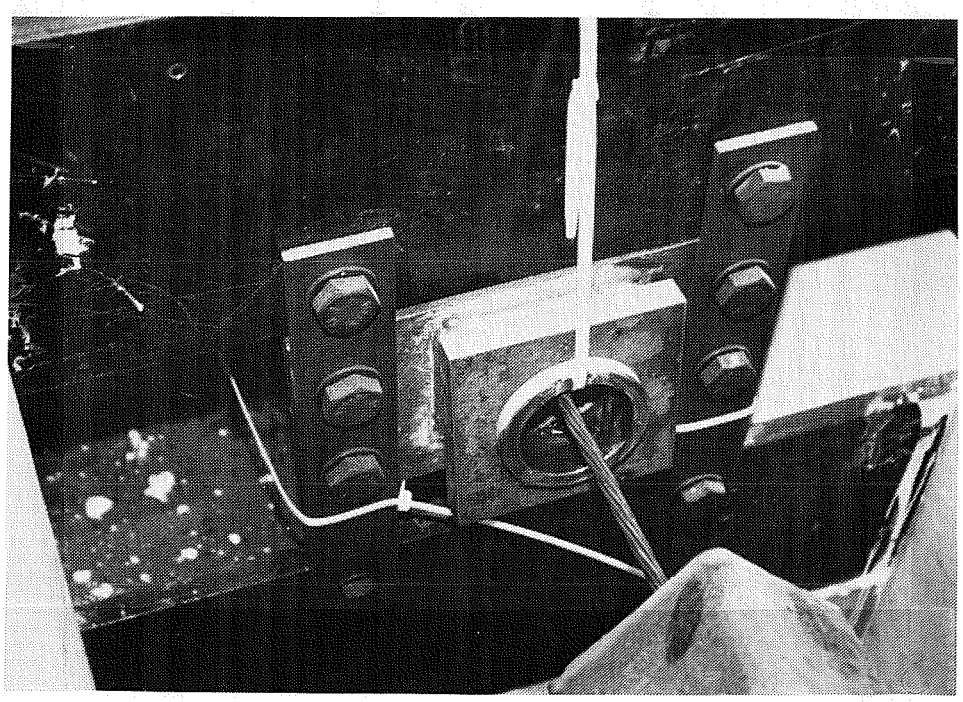

b) Stressing End Detail

Figure 4.14 Assembled Alignment Details.

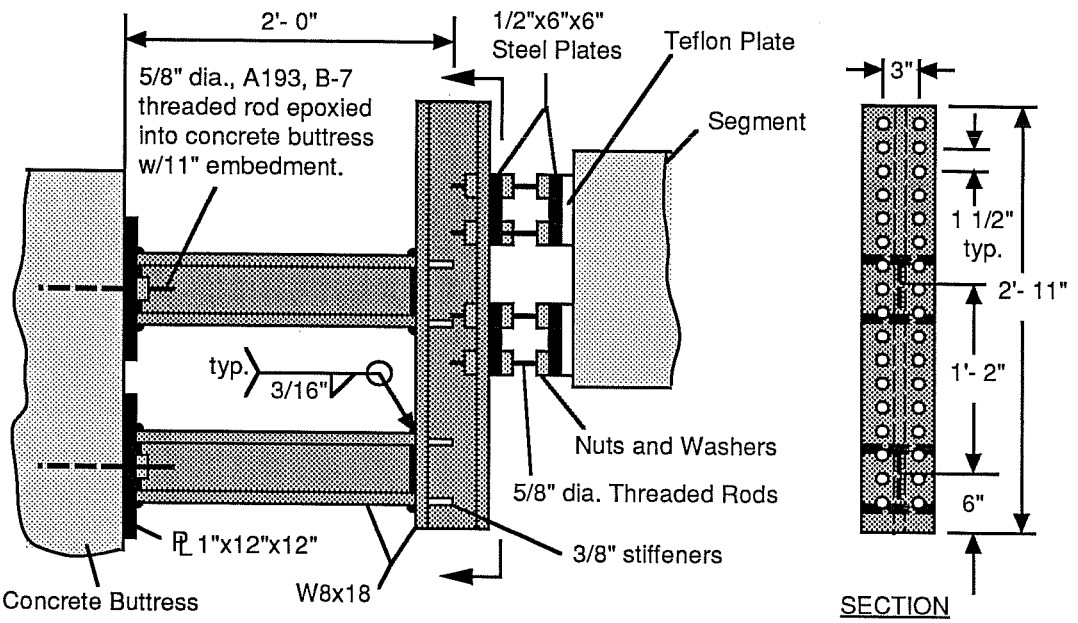

a) Longitudinal Support

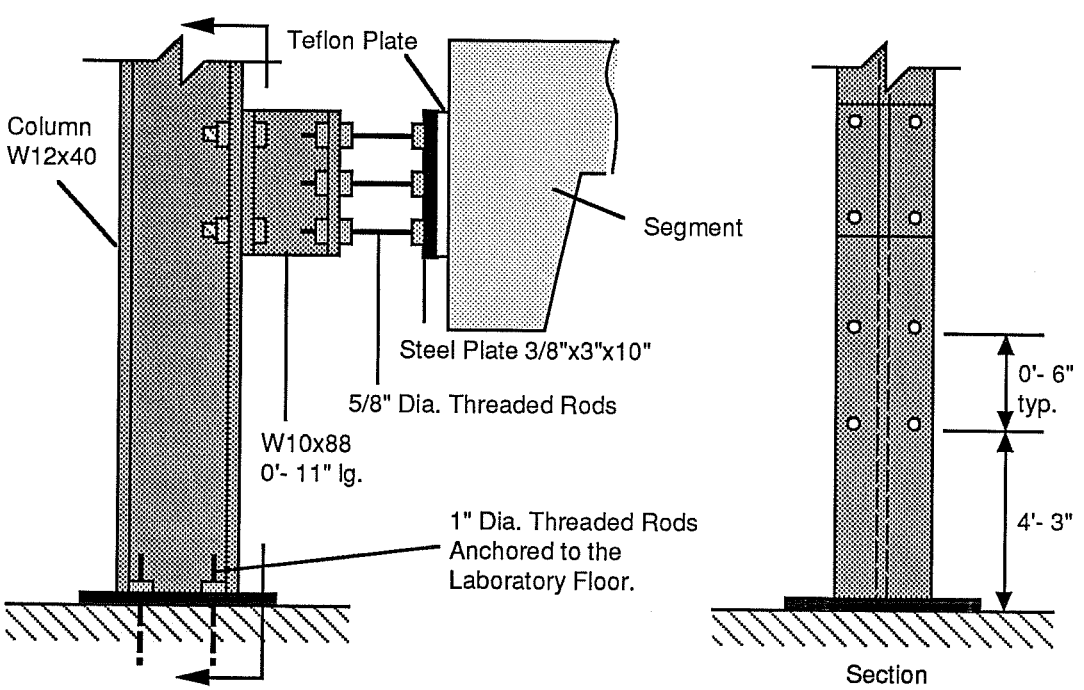

b) Lateral Support

Figure 4.15 Horizontal Supports for Segment.

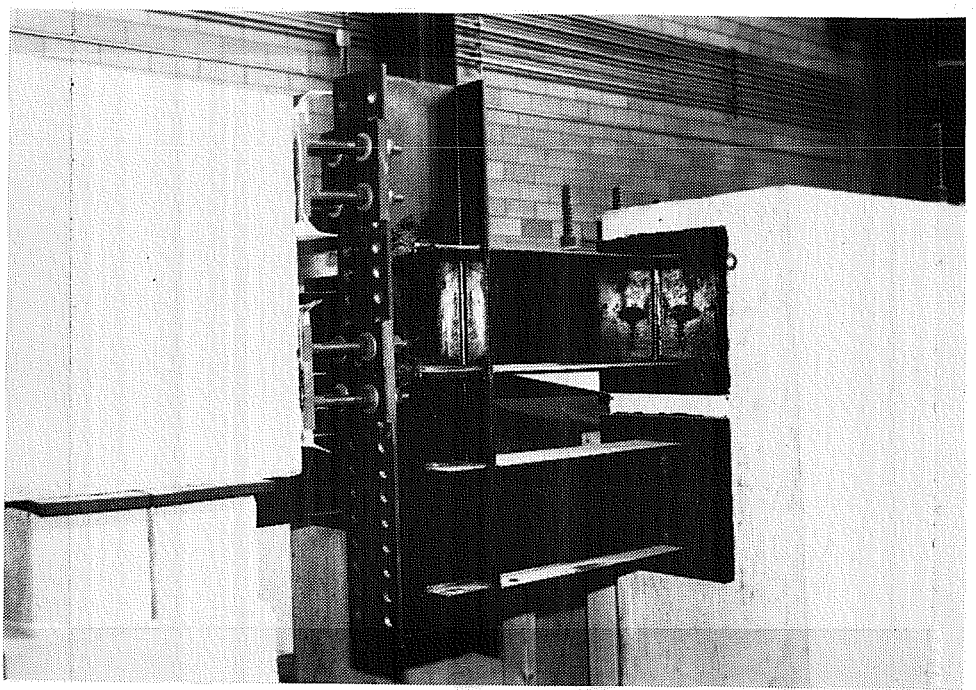

a) Longitudinal Support

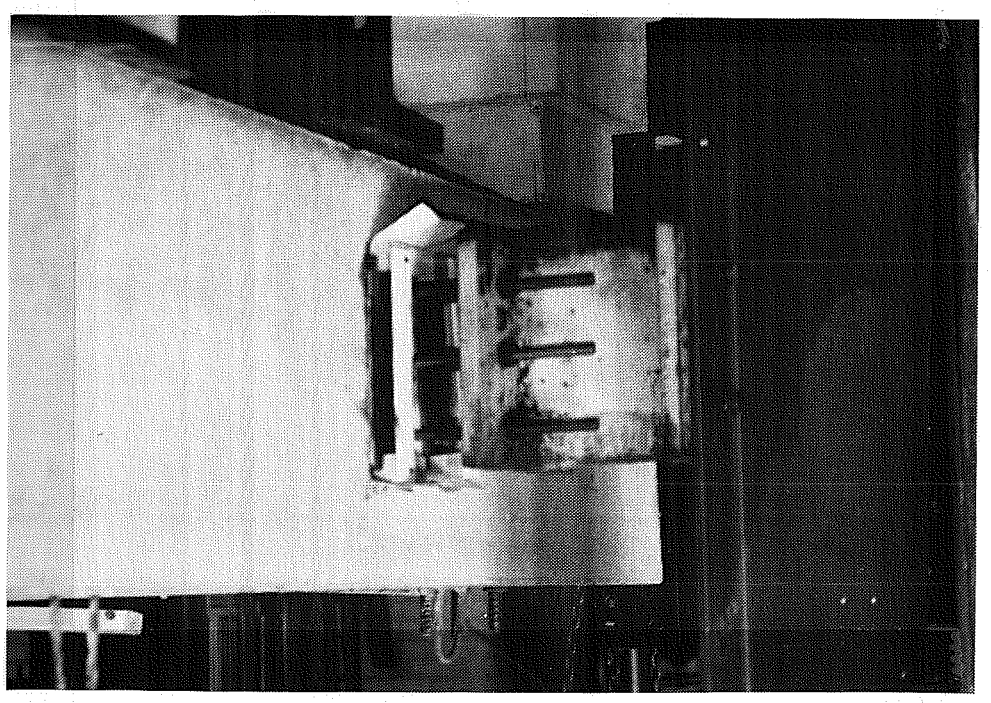

b) Lateral Support

Figure 4.16 Assembled Horizontal Segment Supports

anchor plate. This plate is bolted to two 5/8 in. diameter, A-193, B-7 rods epoxied into holes drilled into the concrete buttress with an embedment depth of 11 inches.

4.2.4 Design of the Segment Lateral Supports. The lateral supports consists of an 11 in. long section of W10x88 bolted to a W12X40 steel column located on each side of the segment (see Figure 4.15b and 4.16b). Two segment support plates, 3/8 x 3 x 10 in., are bolted to these W10 sections with 3 - 5/8 in. diameter threaded rods in a similar fashion as the longitudinal support plates. The W12 columns are anchored to the laboratory floor with 4 - 1 in. diameter rods.

4.2.5 Fabrication and Installation of the Test Setup. All structural steel welding was performed in the laboratory using E70 electrodes. Holes were drilled into the concrete buttresses using a Hilti concrete hammer-drill with a 3/4 in. bit. After the holes were drilled they were cleaned thoroughly by brushing and vacuuming. The threaded rods were then epoxied into the concrete with Sikadur 31 Hi-Mod Epoxy and allowed to set. Hydrostone, a mixture of gypsum cement and water, was used to provide a uniform contact surface for the loading ram base plate, the segment longitudinal support anchor plates, the stressing frame vertical restraint anchor plates, and the stressing frame bearing pads.

Before the stressing frames were attached to the buttresses, the vertical restraint system was installed. A small wooden frame was constructed around the protruding threaded anchor rods and sealed to the concrete base with silicone sealant. Hydrostone was poured into the wooden frame to a depth of about 1/4 inch. Then the anchor plate was fit onto the rods and set into the wet hydrostone. After the hydrostone set, the plate assembly was bolted down. The neoprene pads were then glued onto the stressing frame. The frame was lifted into place by an overhead crane and set onto the concrete blocks. The vertical restraint channels were then bolted on to the frame and to the anchor plate assembly. Hydrostone was poured into the gap between the bearing pads and the concrete buttress after the bottom and sides of the bearing pads were sealed with silicone sealant. While the hydrostone was being poured the frames were repeatedly hit with a mallet to vibrate the pads and ensure a uniform contact surface of hydrostone.

CHAPTER 5
TEST PROGRAM

5.1 Instrumentation

The main objective of the test program is to determine how the fatigue life of the tendon is affected by possible fretting conditions in the deviator. This will be determined by pulsating the entire segment vertically to produce fluctuating stresses in the tendon which passes through the deviator. The number of cycles the segment is pulsated until tendon fracture is initiated is then recorded. The life of the tendon (number of cycles to fracture) can then be compared to the life of typical strand under non-fretting conditions (strand-in-air tests). Therefore, the most important information to be collected is the stress range of the fluctuating tendon stresses and the number of cycles to fracture.

5.1.1 Strain Gages. Strain gages are needed on several of the tendons during the first few tests to determine the actual tendon axial stress. (Although the actual local stresses in the fretting contact zone would be desirable, it is virtually impossible to determine these using any known instrumentation.) These gages should be located outside of the deviator at each end of the segment. By monitoring the gages during stressing and seating, the amount of friction losses across the deviator and losses from wedge seating can be determined. The actual stress in the tendon after losses can be computed from the strain gages before pulsating the segment. Also, by comparing the vertical component of the force in the tendon to the force exerted by the center-hole ram (determined a the load cell), the amount of friction between the segment and the lateral and longitudinal supports can be calculated. Since strain gages typically do not hold up well in fatigue tests, their use during the dynamic testing will be limited. Once a few static cycles are run with strain gages on the tendon, all forces can be accurately calculated by measured ram forces and applied to any additional tests with reduced use of strain gages.

5.1.2 Other Instrumentation. Before testing, linear potentiometers should be attached between the tendon and the segment. These potentiometers are to record the

displacement between the tendon and the segment. Tendon slip in the deviators would result in displacement recorded by the potentiometers. The suggested location of these potentiometers are shown in Figure 5.1. Ram piston displacement should also be monitored by linear potentiometers. These potentiometers would act like a switch, shutting down the system if the ram piston displacement becomes too large. In this way the system would shut down when strand fracture becomes significant enough to cause larger ram displacements. Such a signal would allow the cause of the displacement to be determined.

5.1.3 Test Equipment. The primary test equipment to be used in fatigue testing the tendons is a closed loop servo control system (see Figure 5.1). The hydraulic pressure will be supplied by the laboratory's main hydraulic system. A Pegasus accumulator with a MOOG servo valve controls the hydraulic pressure applied to the ram. A Pegasus control unit with an MTS data display will be used to set the mean load and the fluctuating load levels applied to the specimen and record the number of load cycles. A 200^k load cell between the ram and the concrete segment monitors the force exerted by the ram and continuously relays the information to the control unit. The control unit will automatically adjust these loads to correspond to the preset levels. Therefore, this system will provide controlled loads that are independent of displacement.

Fail-safe mechanisms will be utilized with the test equipment. Several factors which could lead to triggering of these fail-safe mechanisms are:

- Low hydraulic fluid level and high temperature in the pump.
- Loss of electrical power.
- Applied load outside the upper or lower bounds.
- Significant change in ram piston extension.

When any of these factors exceed a preset limit the system and the cycle counter will be shut down. Therefore, the test can run without an operator once it is started and the limits are set.

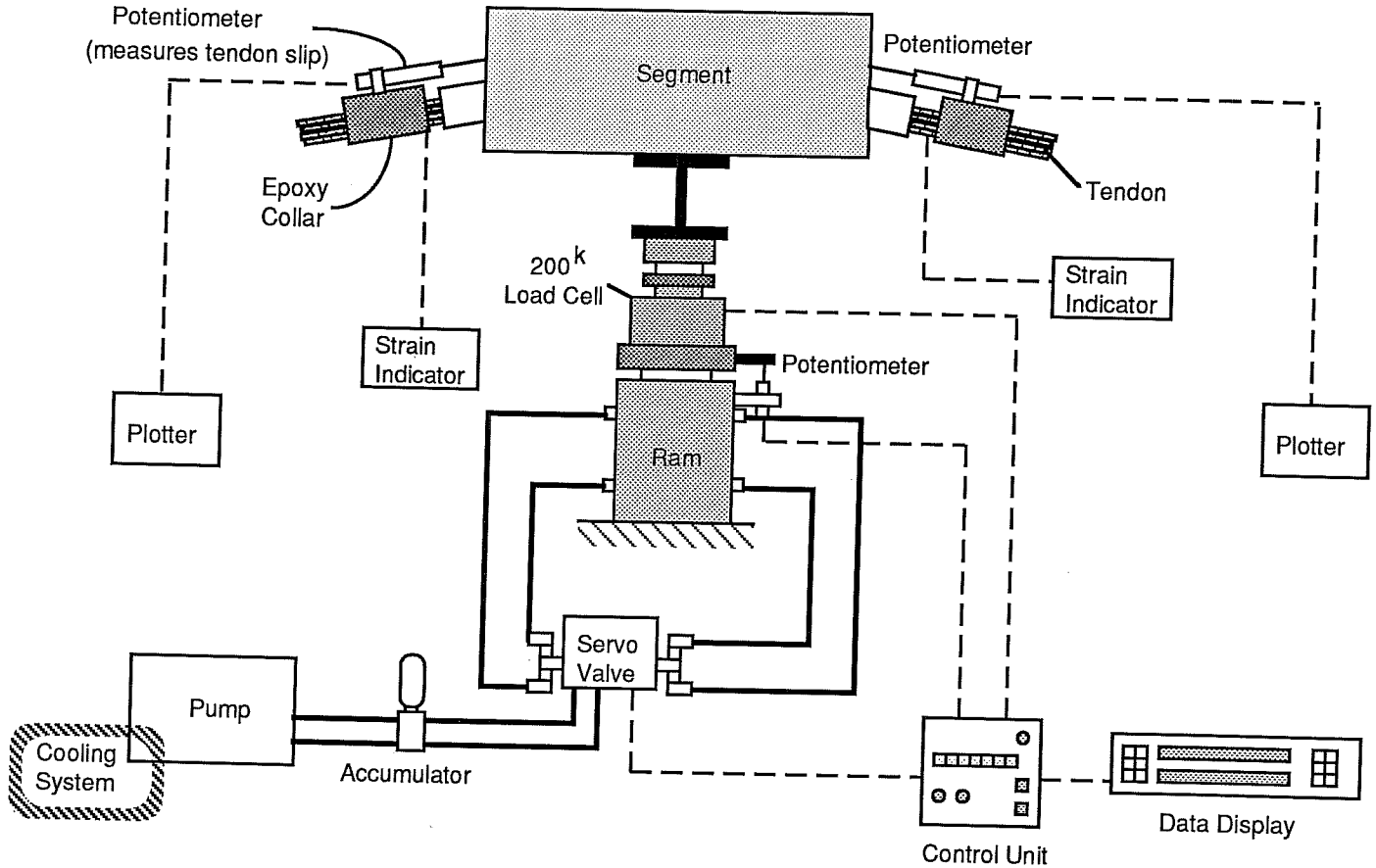

Figure 5.1 Test Equipment.

5.2 Post-Tensioning

5.2.1 Procedure. Before the tendon can be stressed, the segment must be aligned over the load beam and set into place on the stressing supports. Then the lateral and longitudinal support plates must be adjusted to fit tight against the segment. The strands can then be threaded through the anchor heads and the segment deviators with the dead end double-chuck system in place. Care must be taken to maintain proper strand alignment and prevent the strands from twisting or crossing each other. The aluminum alignment pipes should then be coated with grease to help prevent the strands from binding-up in these pipes during the stressing procedure. Once everything is in place the stressing procedure can commence.

Stressing is accomplished by pulling the strand from the live end with a 40^{k} hydraulic ram. This ram sits on a chair assembly and grips the strand using a standard reusable chuck (see Figure 5.2). The strands are stressed individually to a load of 32^{k}. The pressure is sustained until the wedges are power seated. While stressing, care must be taken to avoid crossing the strands in the deviators.

Since the primary wedges use a smaller than ordinary diameter hole for the strand to pass through (see Section 5.2.2.2), they initially protrude about 3/4 in. from the anchor head. If the load is released from the stressing ram into the double-chuck system, the secondary wedges would force the primary wedges about 1/2 in. into the anchor head. This amount of strain change in the tendon would cause large stress losses (about 25-35% of the initial post-tensioning). Therefore, a system was devised to pre-seat the wedges before the load is released from the stressing ram. This system uses a 40^{k} ram on the inner side of the chair that forces the wedge system into the anchor head while the stressing ram maintains the stress in the strand (see Figure 5.2). Once the wedges are seated, using a force of about 31^{k} from the seating ram, the ram is locked off and the pressure sustained. The load is then released from the stressing ram into the double-chuck grip system. Pre-calibrated dial gages will be used to determine the ram force for stressing and seating the tendons.

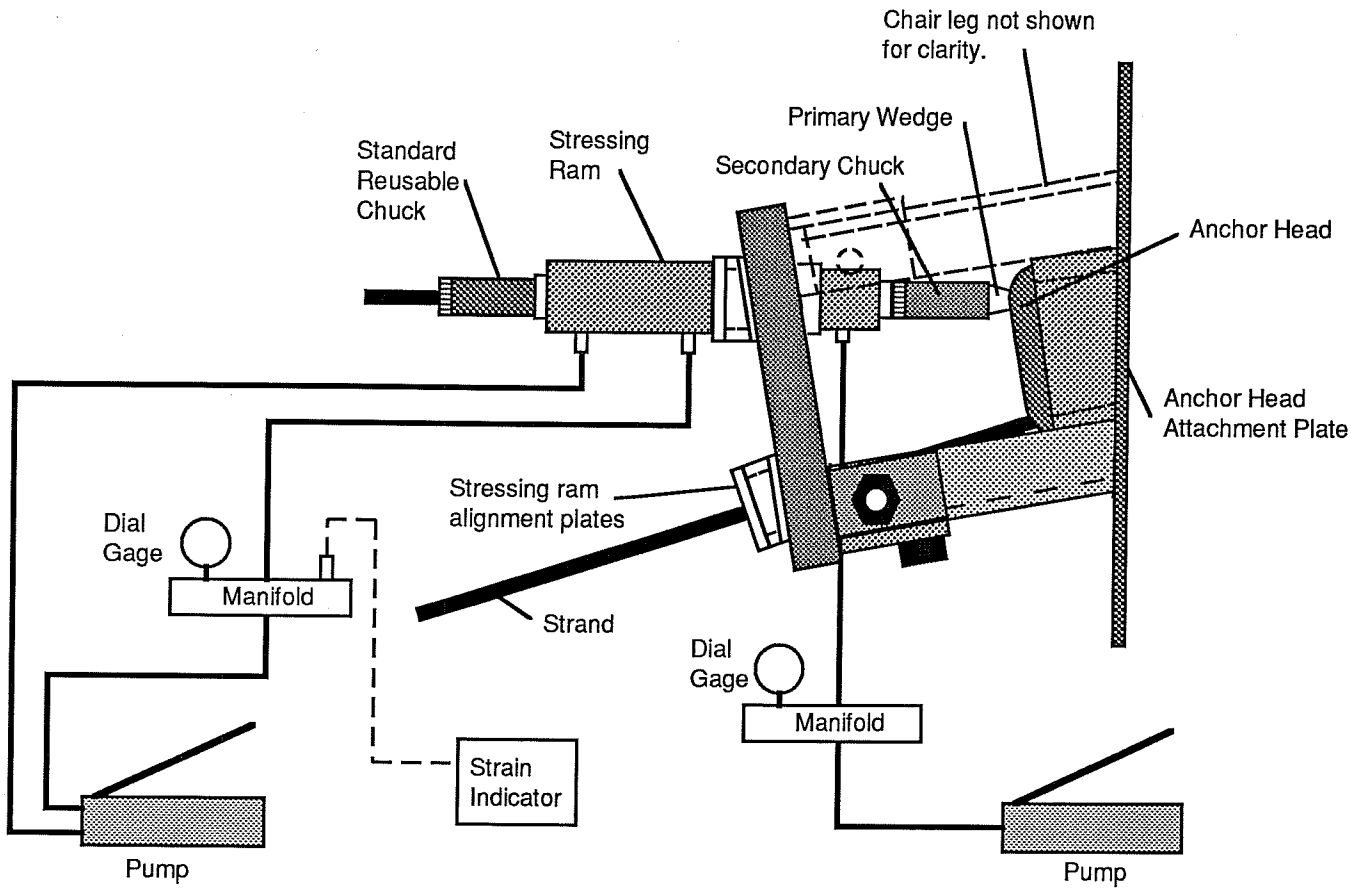

Figure 5.2 Equipment for Post-Tensioning and Seating.

5.2.2 Materials.

5.2.2.1 Prestressing Strand. The tendon consists of 12 - 1/2 in. diameter, Grade 270 (f_{pu} = 270 ksi), low relaxation seven wire strand. This strand complies with ASTM A416 specifications. The ultimate load as determined by the supplier is 43.7 ^{k} ($f_{ult.}$ = 285 ksi) and the modulus of elasticity is 29,100 ksi.

Strand-in-air fatigue tests were performed to determine the fatigue characteristics. The same test setup was utilized that was used in similar tests previously conducted at the laboratory (see Figure 5.3). Several tests were run using Paulson's [25] grip method (aluminum foil with the primary wedges). This method did not work very well as only two of the 20 tests resulted in wire fracture outside of the grip region. Lamb's [17] grip method, using copper wedges, was therefore utilized and performed well. The results of these tests, which did not fail in the grip region, are shown in Figure 5.4. The typical strand-in-air failure zone presented by Paulson [25], based on an evaluation of over 700 fatigue tests, is illustrated with shading. Because of the performance of the copper wedges and the relative simplicity of seating them, these wedges were chosen to be used for the 12 strand tendon.

5.2.2.2 Primary Wedges. The primary wedges were made in the laboratory machine shop from a 1 in. diameter copper bar. These three piece wedges were designed to deform around the strand without producing indentations or significant localized stress concentrations. Therefore, the primary wedges do not use teeth to grip the strand. Instead they rely solely on the secondary chuck to force them into the anchor head. These copper wedges are thicker than the standard wedges but have a smaller diameter hole for the strand to pass through (see Figure 5.5). This configuration results in the primary wedges protruding from the anchor head about 3/4 in. before the double-chuck system picks up the anchorage force. As the tendon force is applied to the double-chuck, the copper wedge deforms around the strand and is forced into the anchor head so that only about 1/4 in. of the wedge protrudes.

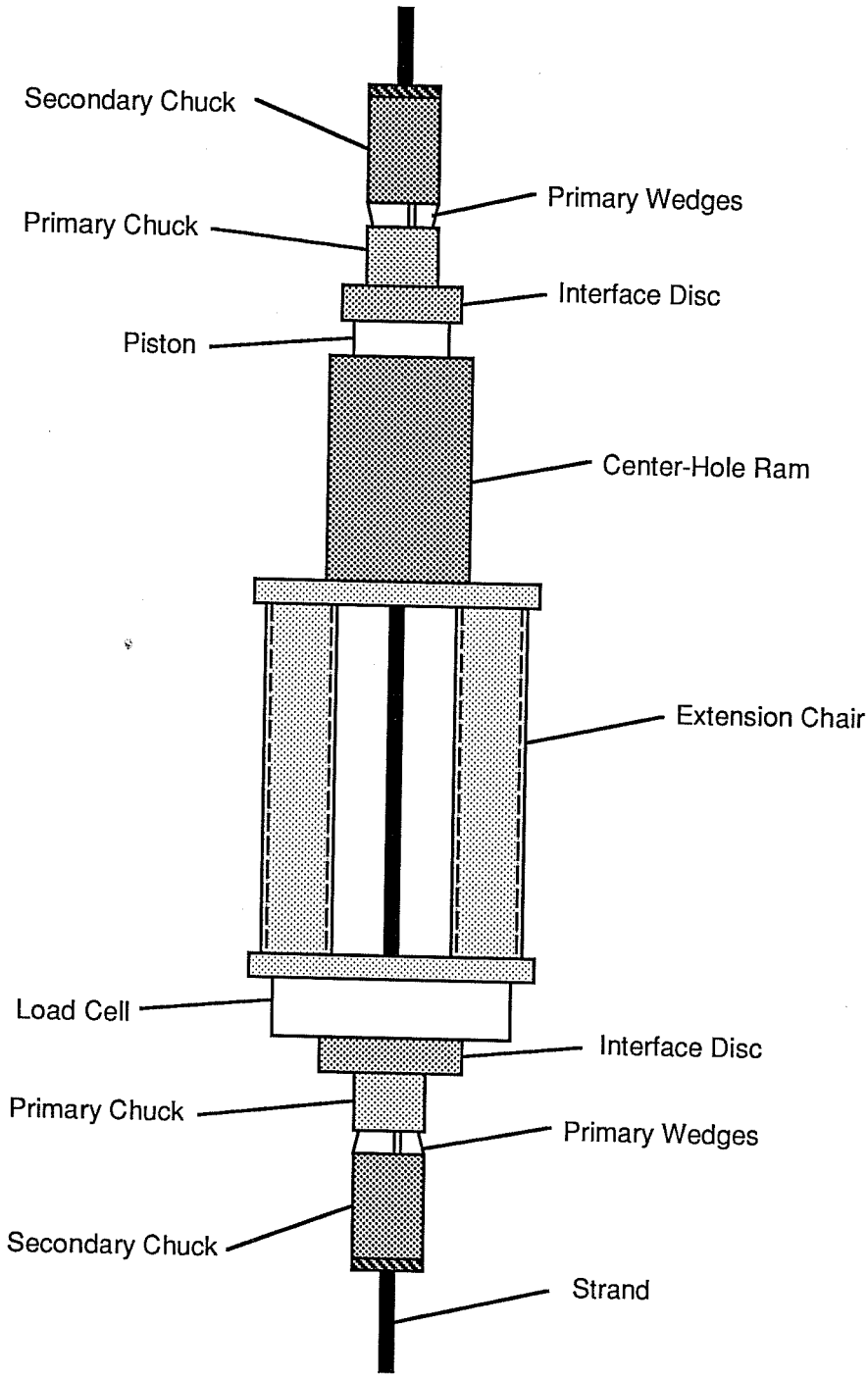

Figure 5.3 Strand-in-Air Test Setup (after Paulson [25])

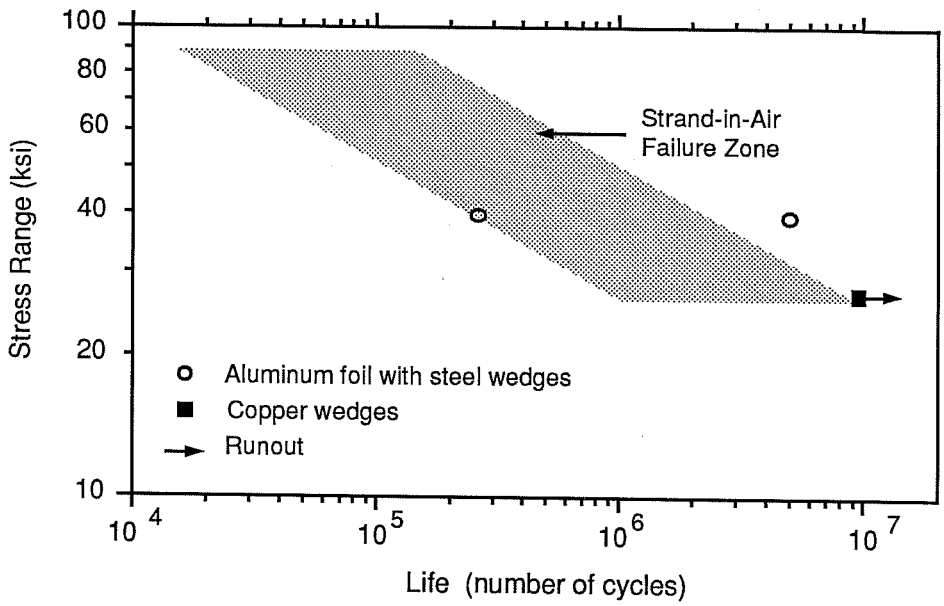

Figure 5.4 Strand-in-Air Test Results

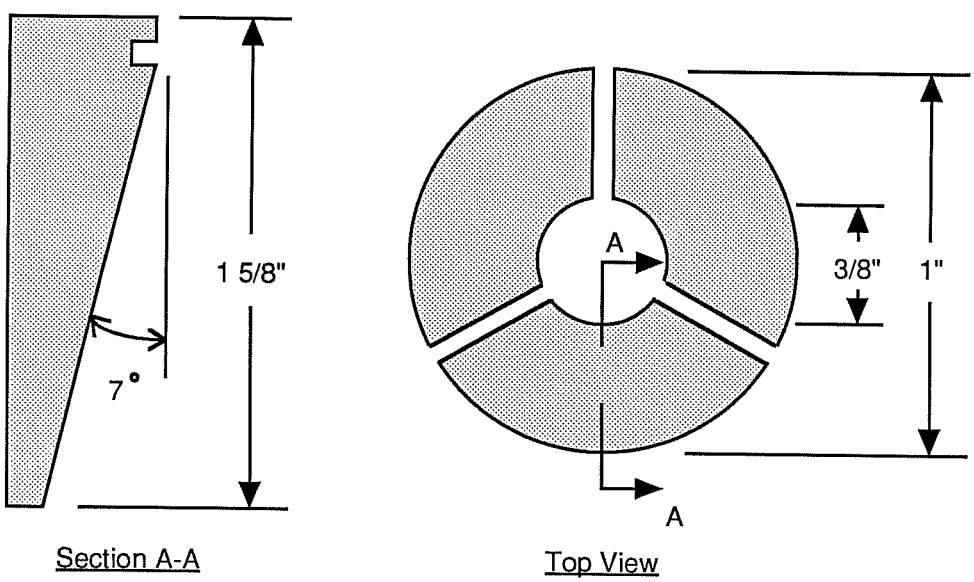

Figure 5.5 Three Piece Copper Wedge Used in the Primary Chuck.

5.2.2.3 Grout. After all of the strands are stressed and seated, the deviators should be grouted. The cement grout mix which was developed from the Texas State Department of Highways and Public Transportation (TSDHPT) is recommended. This mix is:

- 1 bag Portland Cement (Type I, II, or III).
- 5 - 1/2 gallons of water.
- 0.94 lbs Interplast-N expansive admixture.

Grout strengths should be determined at the beginning of each fatigue test from compression tests of standard 2 in. mortar cubes.

A grouting procedure similar to that used by Radloff [27] should be utilized. A short length (about 1.5 feet) of polyethylene tubing should be attached between the two deviator pipes on the inside of the segment. These pipes can be attached using a flexible sleeve which is clamped to the deviator and the polyethylene tube (see Figure 5.6). Similar short lengths of pipe should be attached to the deviator ends on the outside of the segment. Once these tubes are in place, 2 in. thick styrofoam pieces, cut to fit into the tube around the tendon, can be placed in the tube ends and sealed with silicone. The grout injection and outlet ports can then be inserted into the styrofoam and sealed. When the silicone has set sufficiently, the ducts can be grouted using a commercial grouting machine.

5.3 Fretting Fatigue Testing

5.3.1 Dynamic Tests. Once the cement grout in the deviators has reached sufficient strength (about 3 days), the fatigue tests can commence. The segment should be raised by the center-hole ram using the control unit until the maximum tendon stress level is reached. In the first few tests this stress level should be checked against values obtained from the strain gages on the tendon and any necessary adjustments should be made. Subsequent tests can be adjusted by interpolating these values. At this time the stressing support concrete blocks can be removed. The segment should then be lowered until the mean tendon stress level is reached. At this point the span (stress range) can be set with the control unit. The

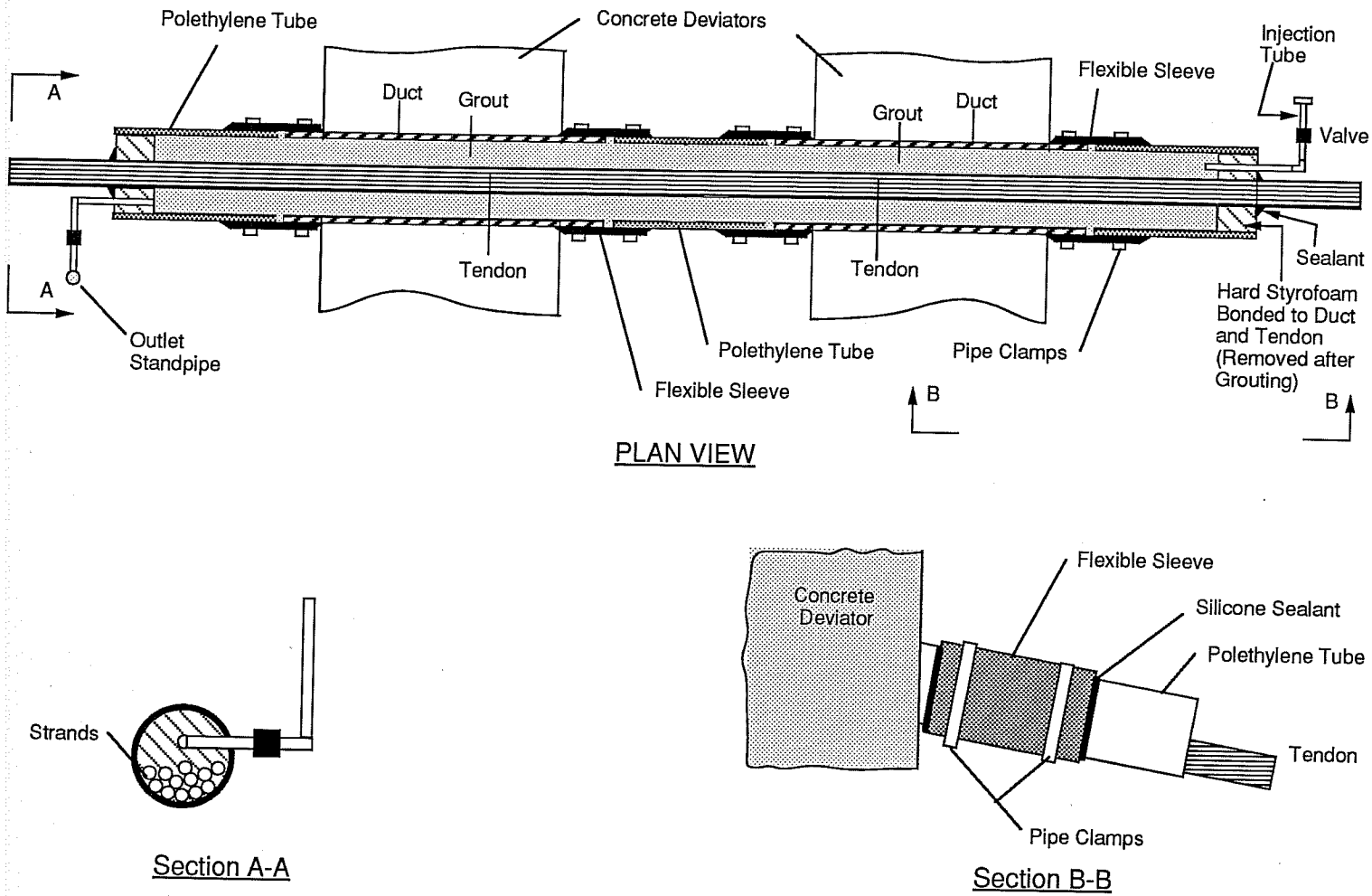

Figure 5.6 Grout Injection Detail (after Radloff [27])

frequency should then be adjusted to allow for the maximum cycles per second the system will allow (about 1 - 3 cps). Once the system is running at the proper levels, all predetermined limits can be set. The test can then be allowed to run without the presence of the operator.

The first test should be run with a tendon stress range of 24 ksi. This high stress range value is useful to "quickly" check the test system and determine if fretting is a problem. A stress range of 24 ksi was chosen because it is approximately the endurance limit for the strand-in-air tests Paulson [25] evaluated and fracture from fretting should occur at this level much more rapidly than it would in the stress range expected in a prototype segmental box-girder (about 1-4 ksi). After the initial test is run and the system is checked out, additional tests should be performed with stress ranges expected in a prototype model.

5.3.2 Static Tests. Whenever the system is shut down through the triggering of one of the fail-safe mechanisms, a static test on the system should be performed. This test involves raising the segment and recording the ram piston displacement and the applied load. By comparing these values to previous values recorded before the start of the dynamic testing, a relative specimen stiffness can be determined. This relative stiffness will be used to determine if any of the strands have fractured signifying the completion of the test.

CHAPTER 6
SUMMARY AND RECOMMENDATIONS

6.1 Summary

External tendon use in segmental concrete box-girder bridge construction is rapidly increasing throughout the United States. These tendons are located outside of the concrete section and the draped tendon profile is maintained by deviator points which provide the only positive attachment to the structure other than the anchorage zones. The placement of these tendons outside of the concrete section can provide substantial economic savings by creating a more efficient web section and less congestion in the reinforcement cage. However, since this technology has been in use for a relatively short period of time, there are some uncertainties about the long term performance of these tendons in a structure that will experience extensive cyclic loads.

Calculated and measured stress ranges for external tendons in typical bridge applications are very low, often only 1 - 4 ksi. These values are well below the endurance limit of prestressing strand. This is one of the reasons there has been little research performed on the study of external tendons under cyclic loading. Therefore, research on fatigue of post-tensioned internal tendons was examined for insight to the possible behavior of external tendons. This research has shown that internal tendons in cracked post-tensioned beams exhibit reduced fatigue life due to a condition known as fretting fatigue.

Fretting fatigue is the reduction of fatigue life due to surface damage caused by relative slip between two materials under a high contact force. The conditions required for fretting to occur in the tendons are found in typical post-tensioned beam details. These include fluctuating axial stress in the tendon, metal-to-metal contact (tendon-to-duct, strand-to-strand, or wire-to-wire contact) under high contact stresses, shear stresses between the contacting surfaces, and relative slip between the tendon and the duct or between the individual strands or wires. These conditions are also found in the deviator regions of post-tensioned external tendons.

The deviator points, typically metal ducts, drastically change the angle of the tendon producing high contact forces. As the tendon is stressed it is pulled across the deviator creating shear stresses resulting from the friction between the tendon and the duct. As the segment encounters typical traffic loading, the tendon stress will fluctuate and experience minute slip in these deviator regions. The combination of these conditions leads to the possibility of fretting fatigue in post-tensioned external tendons used in box-girder construction even though the calculated axial stress ranges are very low.

This research was primarily directed towards the development and construction of a testing apparatus for examining and quantifying this potential for fretting fatigue in external tendons. The main components of this apparatus consists of post-tensioning and anchorage frames attached to concrete buttresses, a concrete deviator segment with two deviation points, and a loading and restraining system. The system is designed for testing a full scale tendon (12 - 1/2 in. diameter, 7-wire strands) stressed to $0.75f_{pu}$ and a maximum fluctuating tendon stress of 24 ksi.

The testing procedure involves pulsating the deviator segment vertically to introduce fluctuating stresses in the post-tensioned tendon. This method was chosen because it closely simulates the load path of a prototype bridge model. The loading system is a closed loop system with several fail-safe mechanisms to allow the test to run without the presence of the operator. The conclusion of the test is determined from one of two conditions. The first is fracture of multiple wires in one or more strands which should result in a substantial loss of stiffness in the specimen. This would be signified by a sudden change in the loading ram piston displacement which will shut down the system. After the system shuts down, a static load test is required to verify if there was a significant loss of stiffness in the specimen. The second condition for test completion would occur when the number of tendon load cycles reaches a preset limit without multiple wire fracture. This condition would indicate that fretting fatigue does not significantly affect the tendon fatigue life.

6.2 Recommendations

The following are recommendations for testing external tendons, using the system developed and constructed in this research program, in order to determine the effect of fretting fatigue on external tendons. This recommended program depends largely on anticipated results of the tests and may have to be altered during the actual tests.

a) Use a tendon stress range of 24 ksi to "quickly" check the testing system and determine if the fatigue life of the tendon is affected by fretting.

b) Run several tests near the expected tendon stress range found in a prototype model (1 - 4 ksi). These tests should be run to a maximum of 6 million load cycles.

c) If fretting does not affect the fatigue life of the tendons in this stress range, tests should be run at longer stress ranges to determine where it does affect the tendon life.

d) If fretting does affect the fatigue life of the tendons in this stress range a sufficient number of tests to obtain a reliable data base should be performed. Additional tests should then be performed altering the deviator details in an effort to eliminate the fretting condition. This could include, but is not limited to, the use of plastic deviator ducts, deviator ducts with flared ends, epoxy coated strands, or grease-filled deviators.

APPENDIX A

Segment Design Calculations

MAXIMUM TENDON FORCES

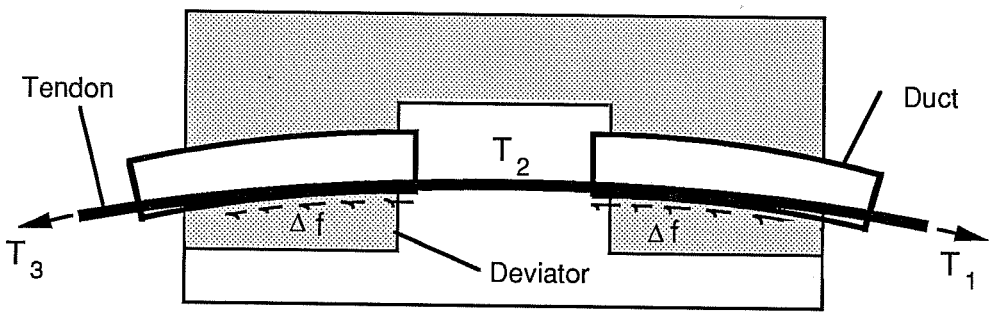

Area of 0.5" dia. strand, $A_s = 0.153\ in^2$

Low relaxation strand, $f_{pu} = 270$ ksi

Number of strands per tendon = 12

Tendon Tension During Post-Tensionining

$T_1 = 0.75f_{pu} \bullet \#\text{ of strands} \bullet A_s$

$= 372$ kips

$\mu = 0.5$ $\quad K = 0.0002$

$L = 2.0$ ft.

$T_2 = T_1 e^{-(\mu\alpha + KL)}$

$= 341$ kips $\quad \alpha = 10$ degrees (0.175 rad.)

$= 356$ kips $\quad \alpha = 5$ degrees (0.087 rad.)

$T_3 = T_2 e^{-(\mu\alpha + KL)}$

$= 312$ kips $\quad \alpha = 10$ degrees

$= 341$ kips $\quad \alpha = 5$ degrees

Tendon Tension During Testing

Specimen is raised to induce additional stress of 24 ksi maximum.

$T_1 = 372 + 24(12)(0.153) = 416^k$

$T_3 = 312 + 24(12)(0.153) = 356^k$ (10 deg.)

$= 341 + 24(12)(0.153) = 385^k$ (5 deg.)

TENDON REACTIONS ON DEVIATORS

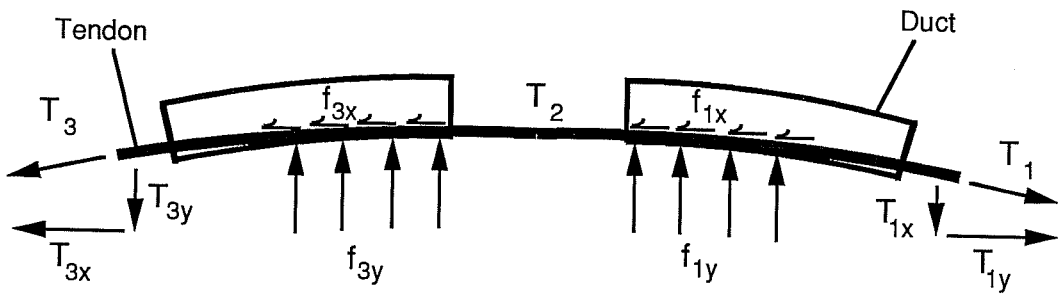

Maximum loads on the specimen occur with the maximum tendon deviation angle, 10 degrees.

Reactions During Stressing:

$T_1 = 372^k$, $T_2 = 341^k$, $T_3 = 312^k$, $L = 24''$

$f_{1y} = T_{1y} / L$
$= 2.71$ k/in

$f_{3y} = T_{3y} / L$
$= 2.25$ k/in

$f_{1x} = (T_{1x} - T_2) / L$
$= 1.04$ k/in

$f_{3x} = (T_2 - T_{3x}) / L$
$= 1.42$ k/in

Reactions During Testing: Assume that since the ducts are grouted the portion of the tendon between the ducts will not elongate (T_2 does not change). This is a worst case scenario for calculating the reactions during testing.

$T_1 = 416^k$, $T_2 = 341^k$, $T_3 = 356^k$, $L = 24''$

$f_{1y} = 3.01$ k/in

$f_{3y} = 2.58$ k/in

$f_{1x} = 2.86$ k/in

$f_{3x} = -0.42$ k/in

DESIGN FORCES FOR DEVIATOR

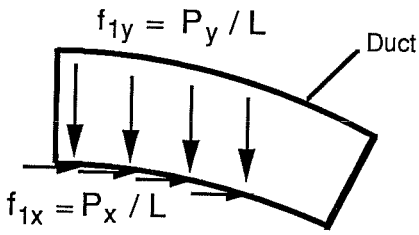

(maximum during testing)

$P_{x\,(max)} = f_{1x} L$
$= 69^k$

$P_{y\,(max)} = f_{1y} L$
$= 72^k$

DEVIATOR REINFORCEMENT DESIGN

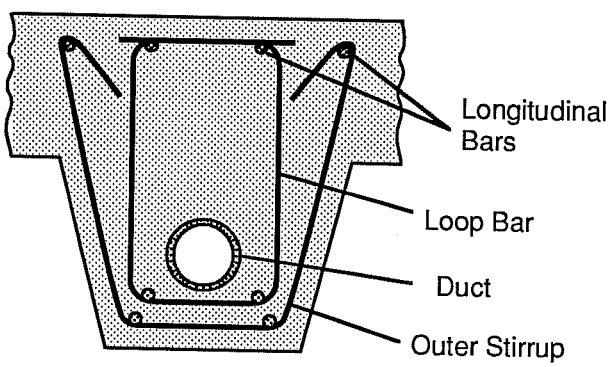

Load Factor (LF) = 1.26

ϕ = 0.90 (Tension)

ϕ = 0.85 (Shear)

f_y = 60 ksi

f'_c = 5000 psi

Direct Tension Reinforcement: (loop bar design)

$F_u = \phi(A_s)(f_y)$ $\quad F_u = LF(P_y)$

$A_s = LF(P_y) / (\phi f_y) = 1.68\ in^2$

Use # 3 bar, $A_b = 0.11\ in^2$

# of loops, $N_l = A_s / (2A_b)$
$= 7.6$ bars

Use: 8 - # 3 loop bars and stirrups per deviator.

Shear Friction Reinforcement: (stirrup check)

$\phi V_n = \phi(A_{vf})(f_y)(\mu)$
$= 126^k$ $\quad < 0.2f'_cA_c = 326^k$
$< 0.8A_c = 269^k$

$A_{vf} = 2(8)(0.11) = 1.76\ in^2$

$\mu = 1.4$ (monolithic)

$A_c = 16(24) = 384\ in^2$

$V_u = LF(P_{x(max)}) = 87^k$

$\phi V_n = 126^k > V_u = 87^k$ Stirrups are adequate.

BOX SEGMENT REACTIONS FOR STRESSING SUPPORT CONDITIONS

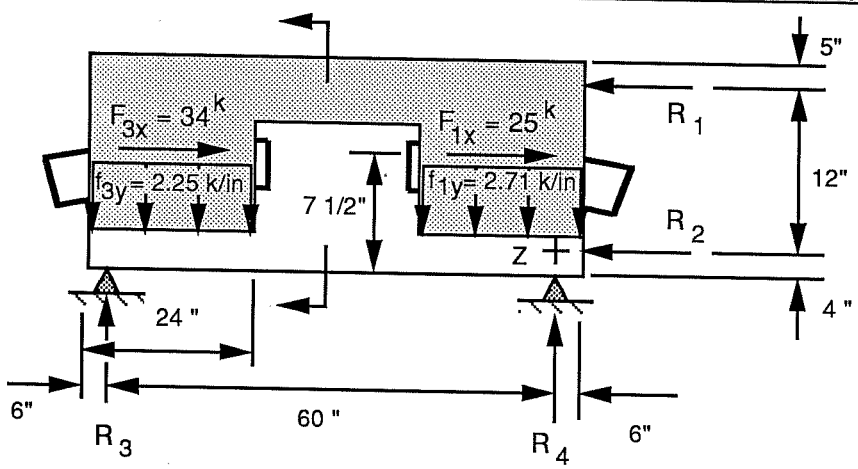

Reaction Calculation:

The stiffness of the supports are much lower than the segment stiffness. Therefore, supports are considered to act like springs which only displace axially. Assume a horizontal and vertical displacement (u and v respectively), and a rotation (θ).

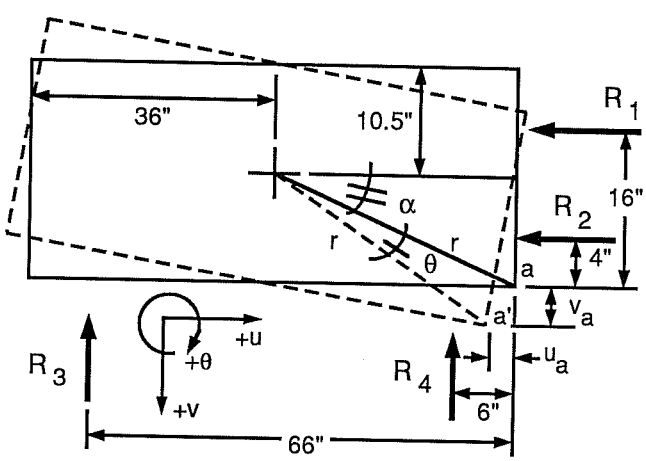

Displacements at the support points are related to the displacement of the lower corner point of the segment, point (a). Assume small rotation angles (θ).

$\alpha = \tan^{-1}(10.5 / 36) = 16.26°$

$r = (10.5^2 + 36^2)^{1/2} = 37.5"$

Find displacements at the lower corner due to a small rotation, θ (point a to a´):

$u_a = r\cos(\alpha + \theta) - r\cos(\alpha) \approx 0$ [for small rotations ($\alpha >> \theta$), $\alpha + \theta \approx \alpha$]

$v_a = r\sin(\alpha + \theta) - r\sin(\alpha) \approx 0$

Displacement at supports due to rotation (θ) only: [for small rotations ($\tan\theta$) = θ]

$$u_{\theta 1} = u_a + (16 + v_a)\tan\theta = 16\theta \qquad v_{\theta 3} = v_a - (66 + u_a)\tan\theta = -66\theta$$

$$u_{\theta 2} = u_a + (4 + v_a)\tan\theta = 4\theta \qquad v_{\theta 4} = v_a - (6 + u_a)\tan\theta = -6\theta$$

Total Displacement at Supports:

$$u_1 = u + u_{\theta 1} = u + 16\theta \qquad v_3 = v + v_{\theta 3} = v - 66\theta$$

$$u_2 = u + u_{\theta 2} = u + 4\theta \qquad v_4 = v + v_{\theta 4} = v - 6\theta$$

Static Equilibrium Equations:

$\Sigma F_u = 0$: $\quad 34 + 25 - R_1 - R_2 = 0 \qquad R_1 + R_2 = 59^k$

$\Sigma F_v = 0$: $\quad 2.25(24) + 2.71(24) - R_3 - R_4 = 0 \qquad R_3 + R_4 = 119^k$

$\Sigma M_z = 0$: $\quad$ Moments taken about point z.

$$(34 + 25)(7.5 - 4) + R_3(60) = 2.25(54)(24) + 2.71(24)(6) + R_1(12)$$

$$5R_3 - R_1 = 258.3^k$$

Reaction Equations: $\quad (k_1 = k_2$, and $k_3 = k_4)$

$$R_1 = u_1k_1 \qquad R_2 = u_2k_1 \qquad R_3 = v_3k_3 \qquad R_4 = v_4k_3$$

Combine reaction equations and equilibrium equations. Then substitute for u_i and v_i.

$$u_1k_1 + u_2k_1 = 59^k$$

$$v_3k_3 + v_4k_3 = 119^k \qquad 5v_3k_3 - u_1k_1 = 258.3^k$$

$$(k_1u + 16k_1\theta) + (k_1u + 4k_1\theta) = 59^k \quad \Rightarrow \quad k_1u + 10\theta = 29.5^k$$

$$(k_3v - 66k_3\theta) + (k_3v - 6k_3\theta) = 119^k \quad \Rightarrow \quad k_3v - 36\theta = 59^k$$

$$(5k_3v - 330k_3\theta) - (k_1u + 16k_1\theta) = 258.3^k \quad \Rightarrow \quad 5k_3v - k_1u - 16k_1\theta - 330k_3\theta = 258.3^k$$

Solve for u, v and θ :

$$\begin{bmatrix} k_1 & 0 & 10k_1 \\ 0 & k_3 & -36k_3 \\ -k_1 & 5k_3 & -16k_1 - 330k_3 \end{bmatrix} \begin{bmatrix} u \\ v \\ \theta \end{bmatrix} = \begin{bmatrix} 29.5^k \\ 59.5^k \\ 258.3^k \end{bmatrix}$$

Reduces to:

$$\begin{bmatrix} k_1 & 0 & 10k_1 \\ 0 & k_3 & -36k_3 \\ 0 & 0 & 1.2k_1 + 30k_3 \end{bmatrix} \begin{bmatrix} u \\ v \\ \theta \end{bmatrix} = \begin{bmatrix} 29.5^k \\ 59.5^k \\ 1.942^k \end{bmatrix}$$

See following page:

$k_1 = 5230$ k/in

$k_3 = 6900$ k/in

$\theta = 9.11 \times 10^{-6}$ $\quad$ $v = 8.95 \times 10^{-3}$ in $\quad$ $u = 5.55 \times 10^{-3}$ in

Substitute u, v and θ into local displacement equations to find displacement at each support:

$u_1 = 5.55 \times 10^{-3} + 16(9.11 \times 10^{-6}) = 5.70 \times 10^{-3}$ in.

$u_2 = 5.55 \times 10^{-3} + 4(9.11 \times 10^{-6}) = 5.59 \times 10^{-3}$ in.

$v_3 = 8.95 \times 10^{-3} - 66(9.11 \times 10^{-6}) = 8.35 \times 10^{-3}$ in.

$v_4 = 8.95 \times 10^{-3} - 6(9.11 \times 10^{-6}) = 8.90 \times 10^{-3}$ in.

Substitute local displacements into force equations:

$R_1 = 0.00570(5230) = 29.8^k$

$R_2 = 0.00559(5230) = 29.2^k$

$R_3 = 0.00835(6900) = 57.6^k$

$R_4 = 0.00890(6900) = 61.4^k$

Calculate maximum moment and shear:

(Max. moment is located 42" from R_3 support, max. shear is located at the R_4 support.)

$M_{max} = R_3(42) - 2.25(24)(36) - 34(10.5 - 7.5) = 373.2^{in\text{-}k}$

$V_{max} = R_4 - 2.71(6) = 45.1^k$

A conservative segment design is desired since the strength of the segment is not being tested. Maximum moments and shear will be used for the reinforcement design although they do not occur at the same location. This is conservative.

STIFFNESS FACTORS FOR SEGMENT SUPPORTS

Longitudinal Supports: Assume top and bottom supports have the same stiffness ($k_1 = k_2$). The stiffness, k_1, is calculated as the sum of the stiffness for two supports (one on each side of the segment).

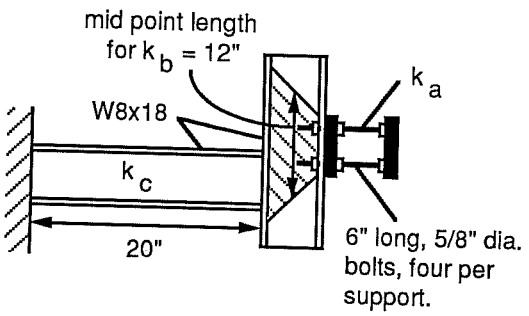

$$1/k_1 = 1/k_a + 1/k_b + 1/k_c$$

$$k_i = E_i A_i / L_i$$

Bolt Group (k_a): $E = 29000$ ksi, $L = 6"$

$A = \#$ bolts(area of bolt)

$= 4(2)(.3068) = 2.45 \text{ in}^2$

$k_a = 29000(2.45)/(6) = 11{,}842$ k/in

W8x18 Web (k_b): $E = 29000$ ksi, $L = 6.625"$

$A = (\text{width of eff. web})(t_w)$

$= 12(2)(.23) = 5.52 \text{ in}^2$

$k_b = 29000(5.52)/(6.625) = 24{,}163$ k/in

W8x18 Leg (k_c): $E = 29000$ ksi,

$L = 20"$

$A = 5.26(2) = 10.52 \text{ in}^2$

$k_c = 29000(10.52)/(20) = 15{,}254$ k/in

$$1/k_1 = 1/11842 + 1/24163 + 1/15254 = 0.000191 \qquad \underline{k_1 = 5230 \text{ k/in}}$$

Vertical Supports: The segment is supported vertically on elastomeric bearing pads 1/2" x 9" x 12". Modulus of Elasticity (E) was interpolated from the stress-strain curves for elastomeric pads given in AASHTO provisions [1] between a range of stress from 100 to 500 psi. The stiffness of each pad is assumed equal ($k_3 = k_4$). There are two pads per support (one on each side of the segment).

$$E = (500 - 100) / (0.035 - 0.01) = 16000 \text{ psi} \qquad A = 9(12) = 108 \text{ in}^2$$

$$\underline{k_3 = 2(16)(108) / (0.5) = 6900 \text{ k/in}}$$

BOX SEGMENT REINFORCEMENT DESIGN - STRESSING

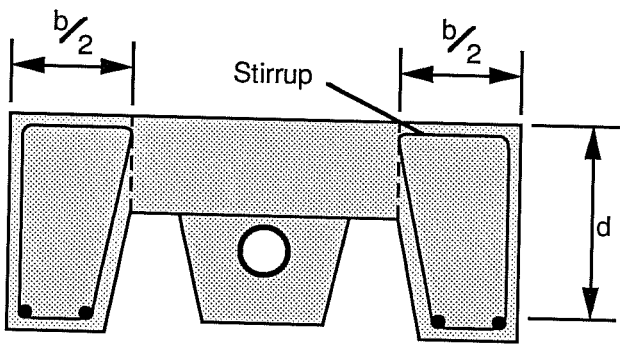

$f'_c = 5000$ psi

$f_y = 60$ ksi

$b = 22$ "

$d = 18$ "

$M_u = 1.26(373.2) = 470^{\text{in-k}}$

$V_u = 1.26(45.1) = 57^{k}$

$\beta_1 = 0.80$

Bending Reinforcement:

$\rho_b = \beta_1 (0.85 f'_c)(87000) / f_y (87000 + f_y) = 0.0335$

$\rho_{min} = 200 / f_y = 0.0033$

$A_s \leq 0.75 \rho_b bd = 9.96 \text{ in}^2$

$A_s \geq \rho_{min} bd = 1.32 \text{ in}^2$

Use 4 - # 6 bars (2 in each web), $A_s = 1.76 \text{ in}^2$

$a = A_s f_y / (0.85 f'_c b) = 1.13$ "

$M_n = A_s f_y (d - a/2) = 1841^{\text{in-k}}$

$$\phi M_n > M_u$$

$$\phi M_n = 1657^{\text{in-k}} > M_u = 470^{\text{in-k}}$$

<u>4 -# 6 bars are more than adequate.</u>

Shear Reinforcement: Use # 3 stirrup bars.

$V_c = 2\sqrt{f'_c}\, b_w d = 56^k$ $\phi V_c = 47.6^k$ $b_w = 18''$

Minimum $A_v = 50\, b_w\, s / f_y$

Minimum $s = A_v f_y / (50\, b_w)$ $< d/2$

$= 4(0.11)(60000) / (50)(18)$ $< (18 / 2)$

$= 29''$ $\not< 9''$

Therefore, minimum s = 9 "

$\phi V_c = V_u + V_s$ $V_s = 57 - 47.6 = 9.4^k$

$V_s = A_v f_y d / s$

$s = A_v f_y d / V_s$

$= 4(0.11)(60)(18) / (9.4)$

$= 50.6''$ $\not< 9''$

Therefore, use s = 9 "

BOX SEGMENT REACTIONS FOR TESTING SUPPORT CONDITIONS

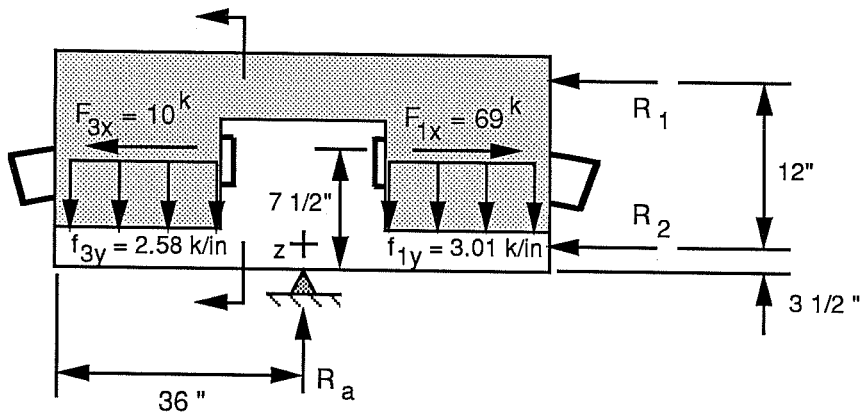

$R_a = (3.01 + 2.58)(24) = 134^k$

Moments are taken about point z to calculate the longitudinal reactions, R_1 and R_2.

$R_1 = [(3.01 - 2.58)(24)^2 + (69 - 10)(7.5 - 3.5)] / 12$
$= 40.3^k$

$R_2 = 59 - 40.3 = 18.7^k$

Design shear and moment are calculated using the higher of the two deviators loads.

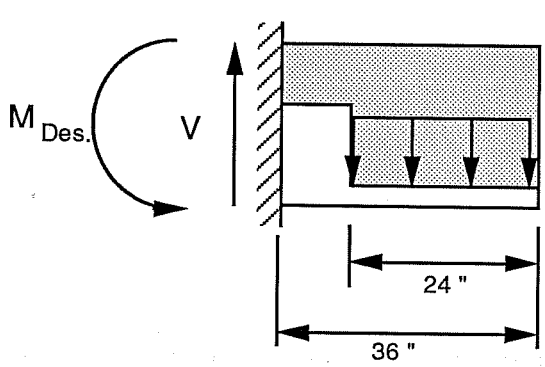

$V_{max} = 3.01(24) = 72^k$

$M_{max} = 3.01(24)(24) = 1734^{in\text{-}k}$

BOX SEGMENT REINFORCEMENT DESIGN - TESTING

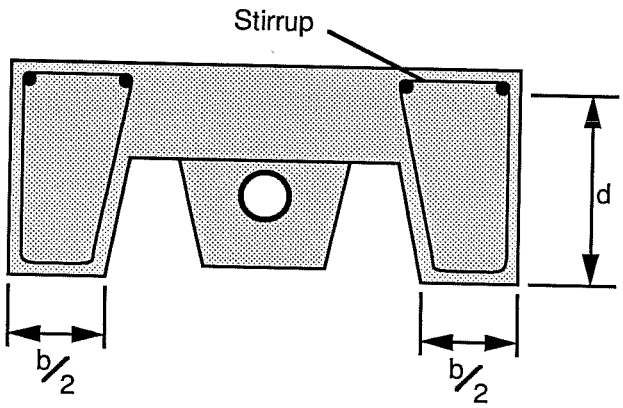

f'_c = 5000 psi

f_y = 60 ksi

b = 18 "

d = 18 "

M_u = 1.26(1632) = 2056 in-k

V_u = 1.26(68) = 86 k

Bending Reinforcement:

$\rho_b = 0.0335$

$A_s \leq 8.14 \text{ in}^2$

$\rho_{min} = 0.0033$

$A_s \geq 1.07 \text{ in}^2$

Use 4 - # 7 bars (2 each web), $A_s = 2.40 \text{ in}^2$

a = 1.88 "

$\phi M_n = \phi A_s f_y (d - a/2)$

$= 2211$ in-k $> M_u = 2056$ in-k

4 - # 7 bars are adequate.

Shear Reinforcement: Use # 3 U stirrups.

$\phi V_c = 47.6$ k

Minimum s = 9 "

$V_s = 86 - 47.6 = 38.4$ k

$s = A_v f_y d / V_s$

$= 12.4 " \not< 9 "$

Therefore use s = 9 "

LATERAL REINFORCEMENT DESIGN

Strut and Tie Method

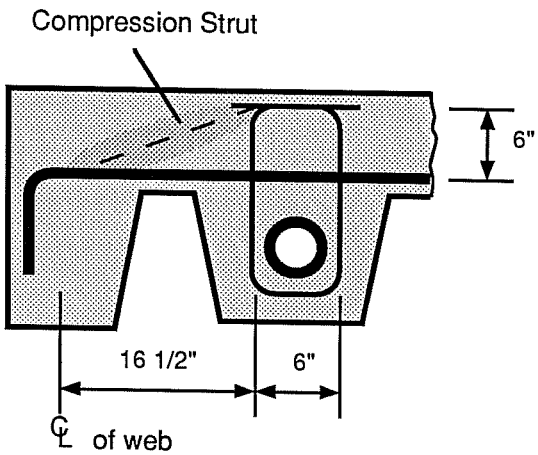

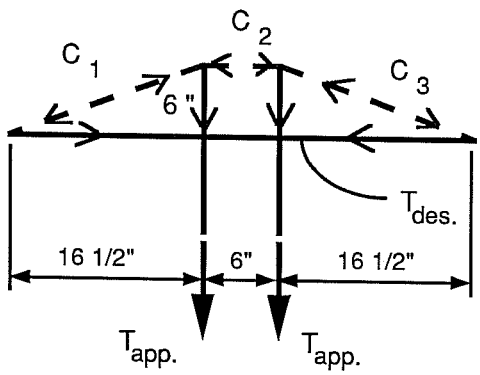

$T_{app.}$ = Vertical load on one deviator / number of legs per loop bar

$= 72 / 2 = 36^{k}$

$T_{des.} = 36\ (16.5 / 6) = 99^{k}$ $\qquad$ $T_u = LF\ (T_{des.}) = 125^{k}$

$T_u = \phi f_y A_s$ $\qquad$ $A_s = T_u / \phi f_y$ $\qquad$ $A_s = 125 / (0.90)(60)$

$= 2.31\ in^2$

Each deviator load is assumed to act over half of the segment length (3 ft.).

$$A_s = 2.31 / 3 = 0.77\ in^2/ft$$

<u>Use 2 - # 6 bars per foot, (A_s = 0.88 in^2/ft).</u>

Use hooked bars with a 90 degree bend and an extension of $12d_b$ (9 ") at each end. Also, for ease of cage construction use s = 6 " for shear reinforcement in the web instead of 9 ". This will allow the lateral reinforcement to be tied to the web shear reinforcement.

APPENDIX B

Test Setup Design Calculations

LOADING FOR TEST APPARATUS DESIGN

Load Beam (P):

P = Vertical component of tendon tension + Segment Weight

Vertical tendon load $= (T_1 + T_3)_{max} \sin\alpha$ (from Appendix A)

for 5 degrees: $= (416 + 385) \sin 5 = 70^k$

for 10 degrees: $= (416 + 356) \sin 10 = 134^k$

Segment weight = Volume of segment x 150 pcf (Volume = 32 ft^3)

$= 32\ (0.15) = 4.8^k$

$P_5 = 70 + 4.8 = 75^k$ $P_{10} = 134 + 4.8 = 140^k$

Stressing and Anchorage Frames (F_x & F_y): F_x and F_y are taken as the maximum tendon force components possible for the deviation angles.

$F_x = T_1 \cos\alpha = 416 \cos 5$
$= 414^k$

$F_y = T_1 \sin\alpha = 416 \sin 10$
$= 72^k$

Longitudinal Supports (R_1 & R_2): R_1 and R_2 were calculated in Appendix A for the stressing and testing support conditions.

Stressing: $R_1 = 29.8^k$, $R_2 = 29.2^k$

Testing: $R_1 = 40.3^k$, $R_2 = 18.7^k$

All of the steel framing components were designed based on the AISC, LRFD manual [2]. The elastomeric bearing pads were designed based on the AASHTO provisions [1]. The anchor plate assemblies were designed based on the Design Guide for Steel-to-Concrete Connections [7].

LOAD BEAM DESIGN

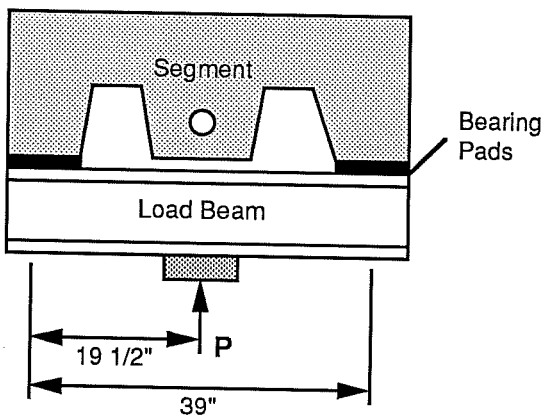

$LF = 1.26,\ \phi_b = 0.9,\ \phi_v = 0.9$

$\underline{\alpha = 5 \text{ deg.}}$

$P_u = P_5\,(LF) = 94.5^{\,k}$

$M_u = P_u\,(L) / 4 = 921^{\,in\text{-}k}$

$V_u = P_u / 2 = 47.3^{\,k}$

$\underline{\alpha = 10 \text{ deg.}}$

$P_u = P_{10}\,(LF) = 176.4^{\,k}$

$M_u = P_u\,(L) / 4 = 1720^{\,in\text{-}k}$

$V_u = P_u / 2 = 88.2^{\,k}$

$\underline{\alpha = 5 \text{ degrees:}}$ (Use W8 x 48)

width - thickness ratios λ: flange: $b/t < \lambda_p = 65 / \sqrt{F_y}$

$5.1 < 10.83$

web: $h_c / t_w < \lambda_p = 640 / \sqrt{F_y}$

$12.4 < 107$

LTB: $L_b / r_y < \lambda_p = 300 / \sqrt{F_{y\,t}}$

$39 / 2.10 = 19 < 50$

Bending:

Since $\lambda < \lambda_p$, then $M_n = M_p = Z\,F_y$

$\phi M_n = 0.9(59.8)(36) = 1938^{\,in\text{-}k} > M_u = 921^{\,in\text{-}k}$

Shear:

$h / t_w < 187\sqrt{k/F_{yw}} \qquad k = 5$

$12.4 < 69.7$

therefore: $\phi V_n = 0.9\,(0.6)\,F_{yw}\,A_w = 86.8^{\,k} > V_u = 47.3^{\,k}$

<u>W8 x 58 is OK</u>

Stiffener Check: (Load applied at the center of the beam will control.)

Local web yielding: $(N = 8",\ \phi = 1.0)$

$R_n = (5k + N)\,F_{yw}\,t_w = 267^{\,k}$

$\phi R_n = 267^{\,k} > P_u = 94.5^{\,k}$

Web Crippling: ($N = 8", \phi = 0.75$)

$$R_n = 135\, t_w^2 \left[1 + 3\,(N / d)\,(t_w / t_f)^{1.5} \right] \sqrt{F_y t_f / t_w} = 629^{k}$$

$$\phi R_n = 472^{k} > P_u = 94.5^{k}$$

Sidesway Web Buckling: (Loaded flange is not restrained against rotation.)

$(d_c / t_w) / (l / b_f) = 2.53 > 1.7$ N.A.

Stiffeners are not required.

α = 10 degrees: (Use W12 x 65)

$b / t = 9.9 < \lambda_p = 10.83$ $h_c / t_w = 24.9 < \lambda_p = 107$

$L_b / r_y = 13 < \lambda_p = 50$

Bending: ($\lambda < \lambda_p$) $\phi M_n = 0.9(96.8)(36) = 3136^{in\text{-}k} > M_u = 1720^{in\text{-}k}$

Shear: $h / t_w = 24.9 < 187\sqrt{k/F_{yw}} = 69.7$

$$\phi V_n = 0.9\,(0.6)\,F_{yw} A_w = 86.8^{k} > V_u = 47.3^{k}$$

W12 x 65 is OK

Stiffener Check: (Use same equations as for α = 5 degrees.)

Local web yielding: ($N = 8", \phi = 1.0$)

$$\phi R_n = 204^{k} > P_u = 176.4^{k}$$

Web Crippling: ($N = 8", \phi = 0.75$)

$$\phi R_n = 311^{k} > P_u = 176.4^{k}$$

Sidesway Web Buckling: (Loaded flange is not restrained against rotation.)

$(d_c / t_w) / (l / b_f) = 7.50 > 1.7$ N.A.

Stiffeners are not required.

Elastomeric Bearing Pad Design for Load Beam: Service Load Design.

α = 5 degrees: $R = P_5 / 2 = 37.5^k$

Compressive Stress: Non-reinforced $\sigma_c \leq 800$ psi

$\sigma_c = R / (L\,W) \leq 800$ psi W = 8" L = 9"

520 psi < 800 psi

$S = (L\,W) / [\,2t\,(L + W)\,] = 2.12 / t$

Use Hardness = 70: G = 160 - 260 psi (Use G = 160 psi)

$\sigma_c \leq G\,S / \beta$ β = 1.8 for non-reinforced pad

$t \leq (2.12\,G) / (\sigma_c \beta) = 0.363"$

Use plain pad 1/4" x 8" x 9"

Rotation:

$L\alpha_L + W\alpha_W \leq 2\Delta_c$ $S = 2.12 / 0.25 = 8.5$

α_L = rotation of the beam perpendicular to the longitudinal axis at the support.

α_W = rotation of the beam parallel to the longitudinal axis at the support.

$\Delta_c = \Sigma\, \epsilon_{ci}\, t_i$ $\epsilon_{ci} = 0.027$ (from AASHTO stress-strain curves)

$= 0.0068"$

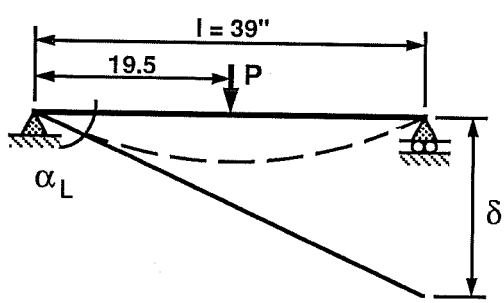

$\alpha_W = 0$

$\delta = P_5\, l^3 / 16EI$ E = 29000 ksi

$\alpha_L = \delta / l$ I = 228 in^4

$= 0.00054$

$L\alpha_L + W\alpha_W = 0.0049" < 2\Delta_c = 0.0135"$ OK

Shear Deformation: (Assume $\Delta T = 80^\circ$ F)

Coefficient of thermal expansion of beam, $\alpha_t = 6.5 \times 10^{-6}$

$T = \Sigma\, t_i > 2\Delta_s$ $\qquad \Delta_s = \alpha_t \Delta T\, l = 0.021"$

$T = 0.25" > 2\Delta_s = 0.041"$ $\qquad$ <u>OK</u>

Shear Force: (Use G = 260 psi for maximum shear force)

$F_s = G\,A\,\Delta_s / T = 1572$ lb. $\qquad A = L\,W$

$F_{allowable} = \mu\, R = 7500$ lb. $\qquad \mu = 0.20$

$F_s = 1572$ lb. $< F_{all.} = 7500$ lb. $\qquad$ <u>OK</u>

Stability: $T < W/5$

$T = 0.25 < W/5 = 1.6"$ $\qquad$ <u>OK</u>

Stiffeners for Beam:

$b_f / 2t_f \leq \sqrt{F_y/3.4\sigma_c}$

$5.1 \not\leq 4.5$ $\qquad$ <u>N.G.</u>

<u>$\therefore$ Need Stiffeners. Use 3/8" thick stiffener plates each side of web.</u>

<u>α = 10 degrees:</u> $\qquad R = P_{10} / 2 = 70^k$

Compressive Stress: Non-reinforced $\sigma_c \leq 800$ psi

$\sigma_c = R / (L\,W) \leq 800$ psi $\qquad W = 12" \qquad L = 9"$

648 psi < 800 psi

$S = (L\,W) / [\,2t\,(L + W)\,] = 2.57 / t$

Use Hardness = 70: G = 160 - 260 psi (Use G = 160 psi)

$\sigma_c \leq G\,S / \beta$ $\qquad \beta = 1.8$ for non-reinforced pad

$t \leq (2.57\,G) / (\sigma_c \beta) = 0.353"$

<u>Use plain pad 1/4" x 9" x 12"</u>

Rotation:

$L\alpha_L + W\alpha_W \leq 2\Delta_c$ $\qquad$ $S = 2.57 / 0.25 = 10.3$

α_L = rotation of the beam perpendicular to the longitudinal axis at the support.

α_W = rotation of the beam parallel to the longitudinal axis at the support.

$\Delta_c = \Sigma\, \epsilon_{ci}\, t_i$ $\qquad$ $\epsilon_{ci} = 0.028$ (from AASHTO stress-strain curves)

$= 0.0070"$

$\alpha_W = 0$

$\delta = P_{10}\, l^3 / 16EI$ $\qquad$ $E = 29000$ ksi

$\alpha_L = \delta / l$ $\qquad$ $I = 533\ in^4$

$= 0.00086$ $\qquad$ $l = 39"$

$L\alpha_L + W\alpha_W = 0.0078" < 2\Delta_c = 0.014"$ $\qquad$ <u>OK</u>

Shear Deformation: (Assume $\Delta T = 80°$ F)

Coefficient of thermal expansion of beam, $\alpha_t = 6.5 \times 10^{-6}$

$T = \Sigma\, t_i > 2\Delta_s$ $\qquad$ $\Delta_s = \alpha_t \Delta T\, l = 0.021"$

$T = 0.25" > 2\Delta_s = 0.041"$ $\qquad$ <u>OK</u>

Shear Force: (Use G = 260 psi for maximum shear force)

$F_s = G A \Delta_s / T = 2359$ lb. $\qquad$ $A = L W$

$F_{allowable} = \mu R = 14{,}000$ lb. $\qquad$ $\mu = 0.20$

$F_s = 2359$ lb. $< F_{all.} = 14{,}000$ lb. $\qquad$ <u>OK</u>

Stability: $T < W/5$

$T = 0.25 < W / 5 = 2.4"$ $\qquad$ <u>OK</u>

Stiffeners for Beam:

$b_f / 2t_f \leq \sqrt{F_y / 3.4\sigma_c}$

$9.9 \not< 4.0$ $\qquad$ <u>N.G.</u>

<u>∴ Need Stiffeners. Use 3/8" thick stiffener plates each side of web.</u>

DESIGN OF STRESSING AND ANCHORAGE FRAMES

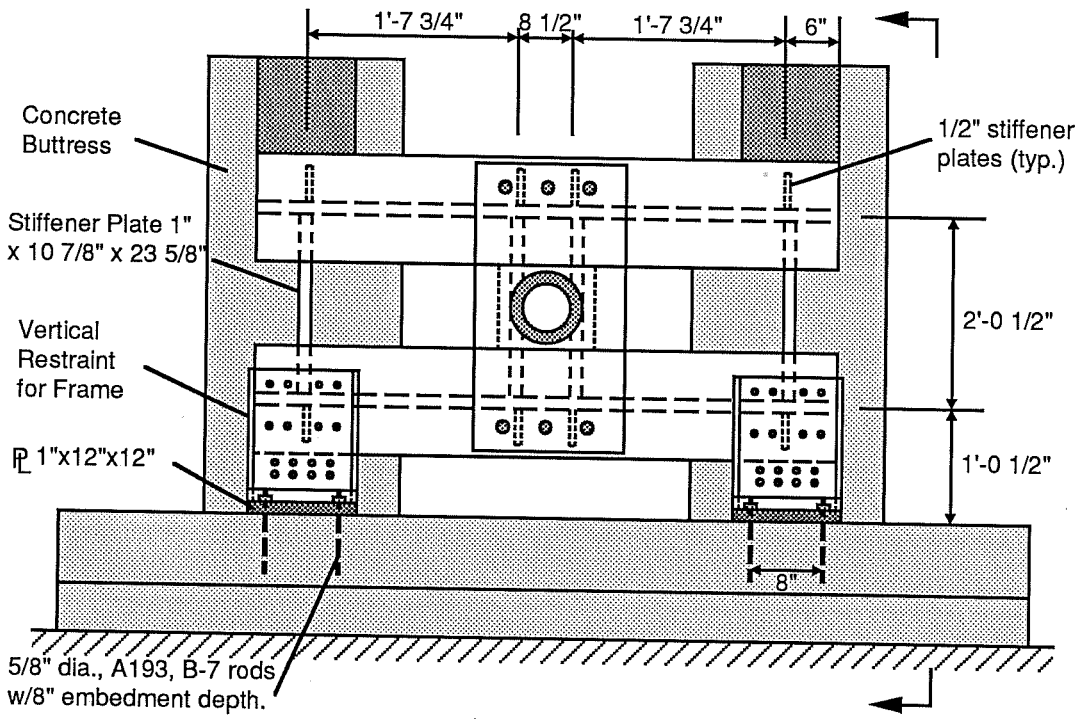

a) Elevation

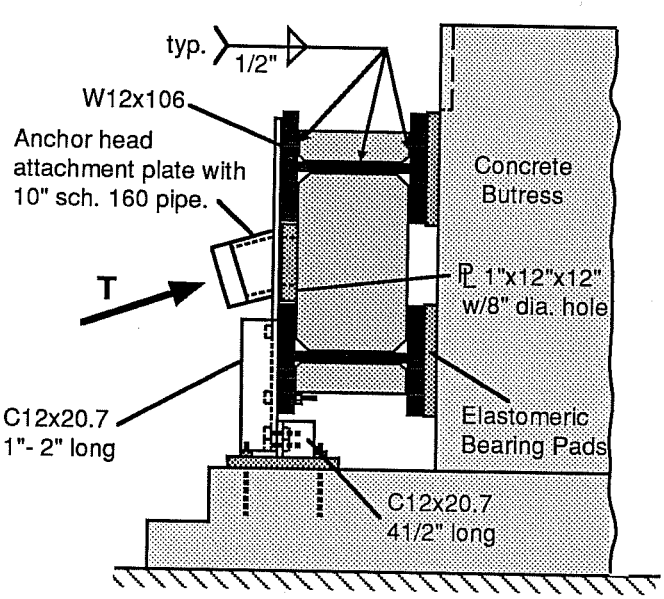

b) Section

$T = 416^{k}$

$LF = 1.26$

$T_x = T \cos \alpha$

$= 72^{k} \quad (\alpha = 5)$

$T_y = T \sin \alpha$

$= 414^{k} \quad (\alpha = 10)$

Check Anchor Head Attachment Plate Assembly:

10" Schedule 160 Pipe: $l_{max} = 3.0"$ $A = 19.4 \text{ in}^2$ $d_o = 10.75"$ $t = 1.215"$

$F_y = 36$ ksi (conservative)

$r^2 = I/A$ $I = \pi (d_o^4 - d_i^4) / 64 = 250 \text{ in}^4$

$r = 3.59$ $kl/r = 2.39$ $\phi F_{cr} = 30.59$ ksi (LRFD, Chapter 6, Table 3-36)

$P_u = LF\,T = 524^k < \phi\, A\, F_{cr} = 593^k$ OK

1/2" x 18" x 3'-0" Plate With 8" Diameter Hole:

The W12 x 106 and the 1" stiffener plates fully support the anchor head attachment plate in the horizontal direction by bearing. The vertical load is transfered from the anchor head attachment plate to the W12 x 106 through the bolts. Therefore the plate and bolts must be designed for this load.

Plate: Assume the vertical force acts like tension across the plate.

$P = T \sin\alpha = 72^k$ $A_g = 9 \text{ in}^2$ $A_n = (18 - 8)(1/2) = 5 \text{ in}^2$

Fracture: $\phi = 0.75$

$P_u < \phi\, F_u\, A_n$

$91^k < 217.5^k$

Yield: $\phi = 0.90$

$P_u < \phi\, F_y\, A_g$

$91^k < 292^k$ OK

Bolts: A325 friction connection, 3 - 1" dia. bolts per end.

$P_b = P / 6 = 12$ k/bolt (Slip critical - Service load check)

$\phi P_n = 13.4^k$ (LRFD, Chapter 5, Table 1-D)

$P_b = 12^k < \phi P_n = 13.4^k$ OK

Spacing of 6" and edge distance of 3" are well above that required.

Check Stressing and Anchorage Frame:

The horizontal force component from the tendon is applied through the anchor head attachment plate and the 1" x 12" x 12" filler plate into the two middle 1" stiffener plates. These stiffener plates carry the load to the W12 beams and cause them to deflect together in strong axis bending. These beams are treated as having pinned supports (elastomeric bearing pads). The vertical force component is transfered from the anchor head to the W12 beams through the bolts. These beams are treated as having pinned supports (1" stiffener plate for the top W12 beam, and C12 for the bottom W12 beam). The 1" stiffener plates near the end of the beams will transfer the vertical reaction from the top W12 beam to the C12 attached to the bottom W12 beam.

Check 1" x 10 7/8" x 1'-11 5/8" Stiffener Plates:

Because the load is applied through a round area (10" pipe), the load on the middle stiffener plates is modeled as a distributed load, w, and two point loads, P_x. The 1" stiffener plate support conditions were modeled as pinned. The end 1" stiffener plates are designed to carry the vertical reaction from the upper W12 beam.

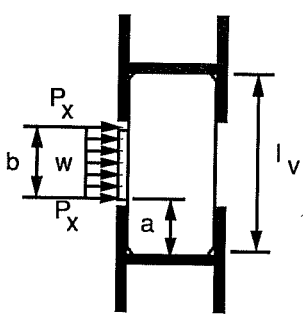

$l_v = 23.6"$ $\quad a = 5.8"$ $\quad b = 12"$

$P_x = T_x / 8 = 51.75^k$

$w = (T_x / 4) / b = 8.62$ k/in

$R_x = P_x + w\,b / 2 = 103.5^k$

$M_{max} = R_x\,a + (R_X - P_x)\,(b/2) / 2 = 756$ in-k

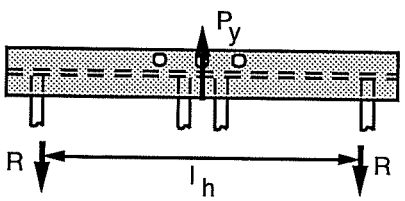

$l_h = 48"$

$P_y = T_y / 2 = 36^k$

$R = P_y / 2 = 18^k$

$M_z = P_y\,l_h / 4 = 432$ in-k

Check Middle Plates:

Bending: (ϕ = 0.90)

for rectangular sections: $L_b / r_y < \lambda_p = 3750 \sqrt{J A} / M_p$

L_b = 23.6" (consv.) $r_y = t \sqrt{1/12}$ = 0.29" $J = d t^3 / 3 = 3.625 \text{ in}^4$

$A = 10.875 \text{ in}^2$ $M_p = Z F_y$ = 1064 in-k $Z = (t b^2) / 4$

$L_b / r_y = 81 < \lambda_p = 139$ $\therefore M_n = M_p$

$M_u = LF\, M_{max}$ = 952 in-k $< \phi M_p$ = 958 in-k <u>OK</u>

Shear: (ϕ = 0.90)

$V_u = LF\, R_x = 130^k$

$h / t_w < 187 \sqrt{k/F_{yw}}$ k = 5

10.9 < 69.7 therefore: $\phi V_n = \phi (0.6) F_y A_w$

$\phi V_n = 211^k > V_u = 130^k$ <u>OK</u>

Check Welds: Treat welds as lines.

$F_w = 0.6 F_{EXX}$ = 42 ksi Use E70 Electrode ϕ = 0.75

A_w = 10.875" (2) + 4" (4) = 37.75 in

Shear on weld: $V = V_u / A$ = 3.44 k/in

$V < \phi F_w t_{eff}$ $t_{eff} = \sqrt{0.5}\, t_{weld}$

$t_{weld} > V / \phi F_w \sqrt{0.5}$ = 0.44" <u>Use 1/2" Weld</u>

Check End Plates:

Tension:

$P_u = LF\, R = 22.7^k$ $\phi P_n = \phi F_y A_g$ $A_g = 10.875 \text{ in}^2$

$P_u = 22.7^k < \phi P_n = 352^k$ <u>OK</u>

Check Welds: 1/2" weld is OK by comparison of reactions from middle plates.

Check W12 x 106 Beams:

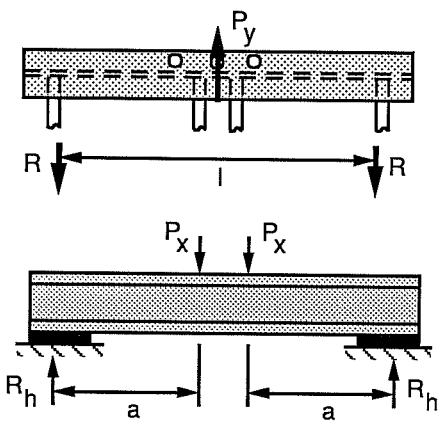

$l = 48"$

$P_y = T_y / 2 = 36^k$

$R_v = P_y / 2 = 18^k$

$M_z = P_y l_h / 4 = 432$ in-k

$P_x = T_x / 4 = 103.5^k$

$R_h = P_x = 103.5^k$

$M_y = a R_h = 2044$ in-k

$a = 19.75"$

Bending: (Biaxial, $\phi = 0.90$)

flange: $b/t < \lambda_p = 65 / \sqrt{F_y}$

$6.2 < 10.8$

web: $h_c / t_w < \lambda_p = 640 / \sqrt{F_y}$

$15.9 < 107$

LTB: $L_b / r_y < \lambda_p = 300 / \sqrt{F_{yt}}$

$19.75 / 3.11 = 6.35 < 50$

$\lambda < \lambda_p \therefore M_n = M_p$

$M_{uz} = LF\, M_z = 544$ in-k

$M_{uy} = LF\, M_y = 2575$ in-k

$\phi M_{nz} = \phi Z_y F_y = 2443$ in-k

$\phi M_{ny} = \phi Z_x F_y = 5314$ in-k

$P_u = 0$ (axial load) $\qquad P_u / \phi P_n < 0.2$

$\therefore M_{uz} / \phi M_{nz} + M_{uy} / \phi M_{ny} \leq 1.0$

$0.71 < 1.0$ <u>OK</u>

Shear: ($\phi = 0.90$)

Weak Axis: $h / t_w = 12.4 < 187\sqrt{k/F_{yw}} = 69.7 \quad (k = 5)$

$\phi V_n = 2\, \phi\, (0.6)\, F_y A_f = 470^k > V_u = LF\, R_v = 22.7^k$ <u>OK</u>

Strong Axis: $h / t_w = 15.9 < 187\sqrt{k/F_{yw}} = 69.7 \quad (k = 5)$

$\phi V_n = \phi\, (0.6)\, F_y A_w = 153^k > V_u = LF\, R_h = 130^k$ <u>OK</u>

Design Elastomeric Bearing Pads:

Compressive Stress: Non-reinforced $\sigma_c \leq 800$ psi

$\sigma_c = R / (L\,W) \leq 800$ psi W = 12" L = 12"

720 psi < 800 psi

$S = (L\,W) / [\,2t\,(L + W)\,] = 3.0 / t$

Use Hardness = 70: G = 160 - 260 psi (Use G = 160 psi)

$\sigma_c \leq G\,S / \beta$ β = 1.8 for non-reinforced pad

$t \leq (3.0\,G) / (\sigma_c \beta) = 0.370"$

Try plain pad 5/16" x 12" x 12"

Rotation:

$L\alpha_L + W\alpha_W \leq 2\Delta_c$ S = 3.0 / 0.3125 = 9.6

α_L = rotation of the beam perpendicular to the longitudinal axis at the support.

α_W = rotation of the beam parallel to the longitudinal axis at the support.

$\Delta_c = \Sigma\,\epsilon_{ci}\,t_i$ $\epsilon_{ci} = 0.029$ (from AASHTO

= 0.009" stress-strain curves)

$\alpha_L = 2P_x\,l^2 / 16EI = 0.0011$ (consv.) E = 29000 ksi I = 933 in^4

$\alpha_W = \alpha_L = 0.0011$ (consv.)

$L\alpha_L + W\alpha_W = 0.026" \not< 2\Delta_c = 0.018"$ <u>N.G.</u>

Use steel reinforced pad: (β = 1.4 outer layers, β = 1.8 inner layers)

$t \leq (3.0\,G) / (\sigma_c \beta)$

$t_o \leq 0.48$ outer layer use t_o = 5/16" $S_o = 9.6$

$t_i \leq 0.67$ inner layer use t_i = 3/8" $S_i = 8.0$

$\epsilon_{co} = 0.029$ $\epsilon_{ci} = 0.031$

$\Delta_c = \Sigma\,\epsilon_c\,t = 2\,\epsilon_{co}\,t_o + N\,\epsilon_{ci}\,t_i < 0.026$ N = No. of inner layers.

$N = (0.026 - 0.018) / (0.012) = 0.7$ Use one inner layer.

Reinforcement: (Sheet metal plates)

$R > 1700\ t_{avg}$ $\qquad t_{avg} = (t_o + t_i) / 2 = 0.344"$

$R = t_r F_t$ $\qquad t_r$ = thickness of reinforcement

$t_r > 1700\ t_{avg} / F_t$ $\qquad F_t$ = Allowable stress in tension.

$t_r > 0.016"$ $\qquad = 0.5\ F_y = 37{,}000$ psi (consv.)

Use 20 gauge (t = 0.036")

Shear Deformation: (Assume $\Delta T = 80°$ F)

Coefficient of thermal expansion of beam, $\alpha_t = 6.5 \times 10^{-6}$

$T = \Sigma\ t > 2\Delta_s$ $\qquad \Delta_s = \alpha_t \Delta T\ l = 0.025"$

$T = 1.0" > 2\Delta_s = 0.05"$ $\qquad$ <u>OK</u>

Shear Force: (Use G = 260 psi for maximum shear force)

$F_s = G\ A\ \Delta_s / T = 936$ lb. $\qquad A = L\ W$

$F_{allowable} = \mu\ R = 20{,}700$ lb. $\qquad \mu = 0.20$

$F_s = 936$ lb. $< F_{all.} = 20{,}700$ lb. $\qquad$ <u>OK</u>

Stability: $T < W / 3$

$T = 1.0 < W / 3 = 4.0"$ $\qquad$ <u>OK</u>

<u>Use bearing pad 1" thick with 2 steel reinforcing plates.</u>

Stiffeners for Beam:

$b_f / 2t_f \leq \sqrt{F_y / 3.4\sigma_c}$

$6.2 \not< 3.83$ $\qquad$ <u>N.G.</u>

<u>∴ Need Stiffeners. Use 1/2" thick plates opposite side of web from the 1" stiffener plates.</u>

Check Vertical Supports:

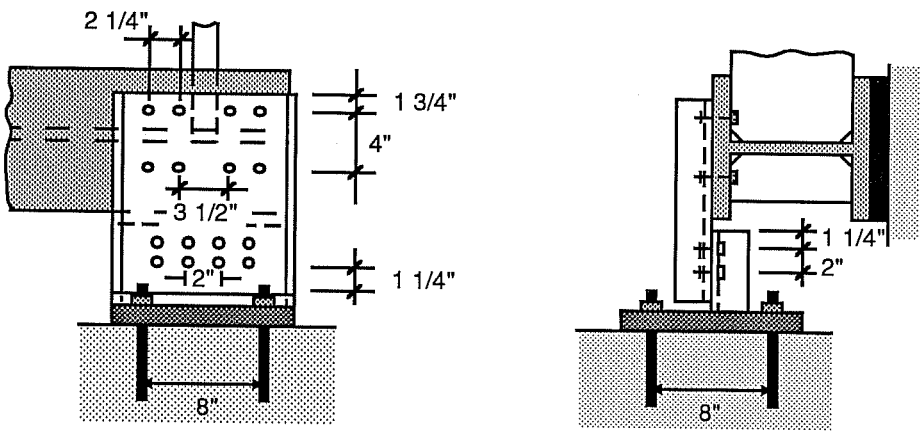

Check 5/8" bolts: Oversize Holes, d_h = 13/16"

Slip critical connection - service load design.

$\phi\ V_n$ = 4.60 k/bolt (LRFD, Chapter 5, Table 1-D)

$V = 36 / 8 = 4.5$ k/bolt $< \phi\ V_n = 4.60$ k/bolt <u>OK</u>

Check C12 x 20.7: $P_u = LF\ P = 45.4^k$

Yielding: $\phi = 0.90$

$\phi\ P_n = \phi\ F_y A_g$ $A_g = T_{C12}\, t_w = 9.75(0.282) = 2.75\ in^2$

$P_u = 45.4^k < \phi\ P_n = 89.1^k$

Fracture: $\phi = 0.75$

$\phi\ P_n = \phi\ F_u A_n$ $A_n = t_w\,(T_{C12} - 4d_h) = 1.83\ in^2$

$P_u = 45.4^k < \phi\ P_n = 79.7^k$ <u>OK</u>

Check Weld: $\phi = 0.75$ $F_{EXX} = 70$ ksi

Treat welds as lines.

$\phi\ F_w = \phi\ (0.6)\ F_{EXX}\ t_e$ $t_e = 0.707 t_w$

$P_u = 45.4^k < \phi\ F_w A_w$ $A_w = 2T_{C12} = 19.5"$ (consv.)

$t_w > P_u / 0.318\ F_{EXX} A_w = 0.104"$

<u>Use 1/4" weld.</u>

Check Anchor Rods:

Use A193 B-7 threaded rods with an embedment depth of 8", F_u = 120 ksi.

Tension: $T = T_u / 4 = 11.34$ k/rod

$T < \phi A_s F_u$

$11.34^k < 0.75 (0.226) (120) = 20.3^k$

Embedment: 8" embedment is sufficient to develop the strength of the epoxy. Sikadur 31, Hi-Mod epoxy was used (compressive strength = 11,000 psi).

Anchor Plates: 1" x 12" x 12"

Bending: $\phi_b = 0.90$

$M_u = T_u s / 4 = 90.7$ in-k

$m_{ut} = M_u / 12 = 7.56$ in-k/in

$m_{ut} = 7.56$ in-k/in $< 0.25 \phi_b F_y t^2 = 8.10$ in-k/in

<u>Plate 1" x 12" x 12" with 4 - 5/8" diameter A193 B-7 threaded rods with an embedment depth of 8" is adequate.</u>

DESIGN OF LONGITUDINAL SUPPORTS FOR THE DEVIATOR SEGMENT

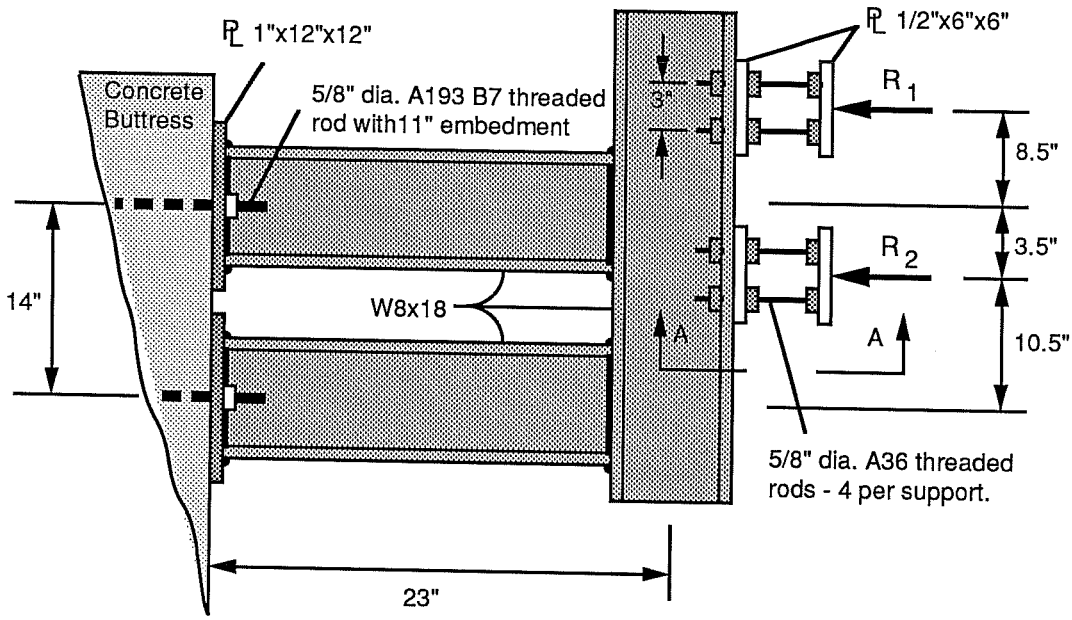

Check Bolt Assembly:

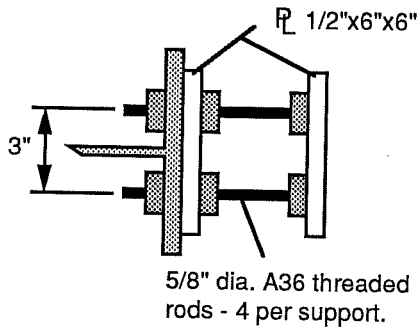

Section A-A

$R_{max.} = R_1 = 40.3$ kips / 8 bolts

LF = 1.26 $\quad$ l = 5.5"

r = d / 4 =0.156" $\quad$ k = 2.0

kl/r = 70.4

ϕF_{cr} = 23.57 ksi (LRFD Chpt. 6, Table 3-36)

$F_u = LF\ (R_1 / 8) / A_{bolt}$

$F_u = 20.7$ ksi $< \phi F_{cr} = 23.57$ ksi

4 - 5/8" dia. bolts per supt. assembly is OK

Check Support Frame:

Frame analysis was performed using the finite element program MICROFEAP. The input and output data for this program are shown on the following two pages. The frame was analyzed for the testing support condition reactions only ($R_1 = 40.3^k$ & $R_2 = 18.7^k$), because they produce the largest stresses in all components of the support. Factored loads were used.

LONGITUDINAL SUPPORT ANALYSIS

```
==================================================
     MICROFEAP-P1          DATE: 11-18-1990
PROJECT  : Longitudinal Support
AUTHORITY: FERGUSON LABORATORY
==================================================
```

```
      ***********************************
      *                                 *
      * STRUCTURE DATA *
      *                                 *
      ***********************************
```

COORDINATE DATA (in) **BOUNDARY DATA**

NODE	1-COOR	2-COOR	1-B	2-B	3-B
1	0.00	0.00	L	L	L
2	0.00	14.00	L	L	L
3	22.00	-6.00			
4	22.00	0.00			
5	22.00	10.50			
6	22.00	14.00			
7	22.00	22.50			
8	22.00	29.00			

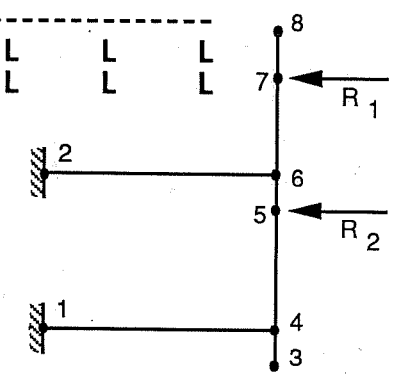

ELEMENT DATA

ELEM	1-NODE	2-NODE	HINGE	MATERIAL
1	1	4		1
2	2	6		1
3	3	4		1
4	4	5		1
5	5	6		1
6	6	7		1
7	7	8		1

MATERIAL DATA

MATE	E-MODULUS (lb/in^2)	AXIAL-AREA (in^2)	INERTIA (in^4)
1	2.900D+07	5.260D+00	6.190D+01

LOAD CASE #1 : Testing Load - 10 deg. deviation
VOLUME LOAD DATA

ELEM	1-DENSITY (lb/in^3)	2-DENSITY (lb/in^3)
ALL	0.000D+00	-2.830D-01

LOAD CASE #1 : Testing Load - 10 deg. deviation
NODAL FORCE DATA

NODE	1-FORC (lb)	2-FORC (lb)	3-FORC (lb-in)
5	-9.350D+03	0.000D+00	0.000D+00
7	-2.015D+04	0.000D+00	0.000D+00

```
****************************
*                          *
* COMBINATION *
*                          *
****************************
```

STRESS COMBINATION <2D-FRAME SYSTEM>
LOAD FACTOR : 1.26

ELEM	MA HINGE	SECTION (in)	AXIAL F. (lb)	SHEAR (lb)	MOMENT (lb-in)
1	1	0.00	5.7476D+03	-3.2755D+03	6.9304D+04
		22.00	5.7476D+03	-3.3168D+03	-3.2124D+03
2	1	0.00	-4.2918D+04	3.4237D+03	2.2450D+04
		22.00	-4.2918D+04	3.3825D+03	9.7318D+04
3	1	0.00	-1.8325D-03	1.5625D-02	-1.5625D-02
		6.00	1.1252D+01	1.5625D-02	1.5625D-01
4	1	0.00	3.3281D+03	5.7476D+03	-3.2123D+03
		10.50	3.3478D+03	5.7476D+03	5.7137D+04
5	1	0.00	3.3477D+03	1.7529D+04	5.7137D+04
		3.50	3.3543D+03	1.7529D+04	1.1849D+05
6	1	0.00	-2.8135D+01	-2.5389D+04	2.1581D+05
		8.50	-1.2193D+01	-2.5389D+04	-3.7500D-01
7	1	0.00	-1.2205D+01	-6.2500D-02	-5.6250D-01
		6.50	-1.3640D-02	-6.2500D-02	1.2500D-01

Check W8 x 18 (Vertical Elements 3 - 7): $M_{max.} = 216$ in-k $V_{max.} = 25.4^k$ $F_{axial} = 0^k$

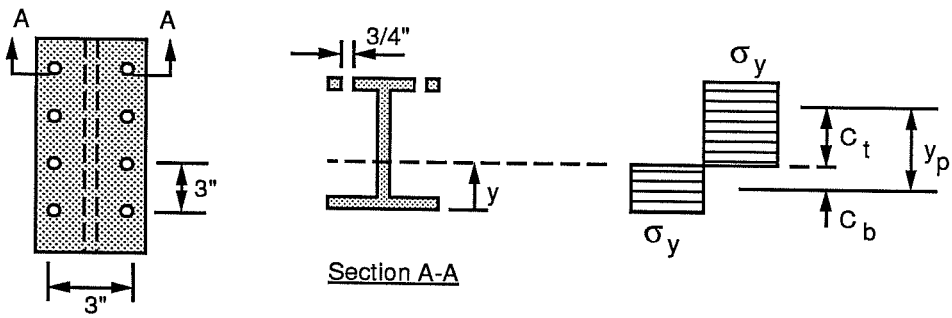

Elevation

$A = A_{W8x18} - 2(0.75)t_f = 4.765 \text{ in}^2$

$y = (A/2 - b_f t_f) / t_w + t_f = 3.156"$

$$C_t = \frac{t_f [b_f - 2(0.75)] (d - y - t_f/2) + t_w [(d - y - t_f)^2] /2}{(A / 2)} = 3.548"$$

$$C_b = \frac{t_f b_f (y - t_f/2) + t_w [(y - t_f)^2] /2}{(A / 2)} = 2.560"$$

$y_p = C_t + C_b = 6.108"$ $\qquad M_p = y_p \sigma_y A/2 = 524$ in-k

Bending: ($\phi = 0.90$)

flange: $b/t < \lambda_p = 65 / \sqrt{F_y}$

$8.0 < 10.8$

web: $h_c / t_w < \lambda_p = 640 / \sqrt{F_y}$

$29.2 < 107$

$M_u = 216$ in-k $< \phi M_n = 472$ in-k

LTB: $L_b / r_y < \lambda_p = 300 / \sqrt{F_{yt}}$

$35 / 1.23 = 28.5 < 50$

$\lambda < \lambda_p \therefore M_n = M_p$

OK

Shear: ($\phi = 0.90$)

$h / t_w < 187 \sqrt{k/F_{yw}}$ $\quad k = 5$

$29.9 < 69.7$

therefore: $\phi V_n = \phi (0.6) F_{yw} A_w = 36.4^k > V_u = 25.4^k$ OK

Stiffener Check (at member connections, nodes 4 and 6):

Compression Flange:

node 4: $C = 42.9^k$ $M = 97.3$ in-k

$C_f = C (A_f / A) + M / 8 = 26.3^k$

Local web yielding: ($N = t_f$, $\phi = 1.0$)

$R_n = (2.5k + N) F_{yw} t_w = 18.2^k$

$\phi R_n = 18.2^k \not> C_f = 26.3^k$ Stiffeners are required.

Provide stiffeners: Stiffeners must extend at least one half of the web depth. Therefore, use stiffener plate 3/8" x 2 1/2" x 3 3/4" long. Stiffeners are required on each side of web of the vertical members where the flanges of the horizontal members are attached. Stiffeners should be fully welded.

Web Crippling: Stiffeners are provided - need not be checked.

Sidesway Web Buckling: (Loaded flange is not restrained against rotation.)

$(d_c / t_w) / (l / b_f) = 4.32 > 1.7$ ($l = 35"$) N.A.

Tension Flange: (Stiffeners are provided)

node 6: $T = 5.75^k$ $M = 3.21$ in-k

$T_f = T (A_f / A) + M / 8 = 2.30^k$

Local Flange Bending: Loads are relatively small and stiffeners are provided. Flange and web are adequately stiffened.

Stiffener Check (at applied load points, $P_u = (LF\ R_{max}) / 2 = 25.4^k$):

Local web yielding: (N = width of plate = 6", $\phi = 1.0$)

$R_n = (5k + N) F_{yw} t_w = 80.7^k$

$\phi R_n = 80.7^k > R_{max.} = 25.4^k$

Web Crippling: ($N = 6''$, $\phi = 0.75$)

$$R_n = 135\, t_w^2 \left[1 + 3\,(N / d)\,(t_w / t_f)^{1.5} \right] \sqrt{F_y t_f / t_w} = 119.4^k$$

$$\phi R_n = 89.6^k > R_{max.} = 25.4^k$$

Sidesway Web Buckling: (Loaded flange is not restrained against rotation.)

$(d_c / t_w) / (l / b_f) = 4.32 > 1.7$ $\quad$ ($l = 35''$) $\quad$ <u>N.A.</u>

Compression Buckling of the Web: ($\phi = 0.90$)

$$\phi R_n = \phi\ 4100\, t_w^3 \sqrt{F_y} / d_c = 40.7^k > 25.4^k$$

<u>Stiffeners are not required.</u>

<u>Check W8 x 18 (Horizontal Elements 1 & 2):</u>

Bending: $M_{ux} = 97.3$ in-k $\quad M_{uy} = 0$ in-k $\quad P_u = 42.9^k$ (compression)

$\phi_c P_n = \phi_c A_g F_{cr}$ $\quad$ $kl/r = 2.0\,(22) / 1.23 = 35.8$

$= 150.4^k$ $\quad$ $\phi_c F_{cr} = 28.6$ ksi (LRFD Chpt. 6, Table 3-36)

$P_u / \phi_c P_n = 0.29 > 0.2$ $\quad$ therefore, use eqn. H1-1a.

$\phi_b = 0.90$ $\quad$ $\lambda < \lambda_p \quad \therefore M_n = M_p = 612$ in-k

$$P_u / \phi P_n + (8/9)\,(M_{ux} / \phi_b M_{nx} + M_{uy} / \phi_b M_{ny}) < 1.0$$

$$0.47 < 1.0$$

Shear: ($V_u = 3.4^k$, $\phi = 0.90$)

$h / t_w < 187 \sqrt{k / F_{yw}}$ $\quad k = 5$

$29.9 < 69.7$

therefore: $\phi V_n = \phi\ (0.6)\, F_{yw} A_w = 36.4^k > V_u = 3.4^k$ $\quad$ <u>OK</u>

Check Welded Connections of W8 x 18: (Treat weld as a line.)

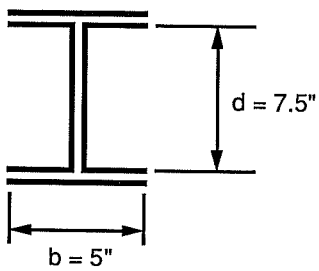

Loads: (members 1 & 2)

negative load signifies compression

$F_{A1} = 5.75^{k}$ $\quad F_{A2} = -42.9^{k}$

$F_{v1} = 3.28^{k}$ $\quad F_{v2} = 3.38^{k}$

$M_1 = 69.3$ in-k $\quad M_2 = 97.3$ in-k

$F_w = 0.6\ F_{EXX}$ Use E70 Electrode

$= 42$ ksi

$\phi = 0.75$

$S = 2bd + d^2 / 3 = 93.8\ in^2$ $\qquad A = 2(b + d) = 35.0$ in

Reactions at member 2 end, are in compression; therefore, reactions from member 1 will govern.

Tension on weld: $T = F_{A1} / A + M_1 / S = 0.90$ k/in

Shear on weld: $V = F_{v1} / A = 0.09$ k/in (negligible)

$T < \phi\ F_w\ t_{eff}$ $\qquad t_{eff} = \sqrt{0.5}\ t_{weld}$

$t_{weld} > T / \phi\ F_w \sqrt{0.5} = 0.040"$

<u>Use 3/16" weld.</u>

Check Anchor Rods and Plates:

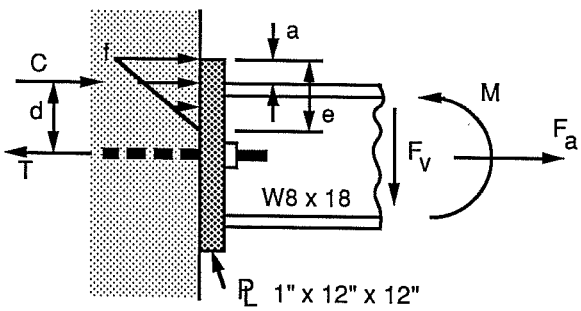

Max. factored reactions - node 1.

$F_a = 5.75^k \quad F_v = 3.28^k$

$M = 69.3$ in-k

$d = d_{beam} / 2 + t_{weld} = 4.26"$

$C = M / d = 16.3^k$

$T = (F_a + M / d) / 2 = 11.0^k$

$V = F_v / 2 = 1.64^k$

Anchor Rods: Use A193 B-7 threaded rods with an embedment depth of 11", $F_u = 120$ ksi.

Tension: $T < \phi A_s F_u$

$11.0^k < 0.75\ (0.226)\ (120) = 20.3^k$

Shear: $V < \phi \mu C$

$1.64^k < 0.65\ (0.40)\ (16.3) = 4.24^k$ Shear resisted by friction.

Embedment: 8" embedment is sufficient to develope the strength of the epoxy. However, 11" embedment was used to insure adequate bond in a horizontal hole. Sikadur 31, Hi-Mod Gel epoxy was used (compressive strength = 11,000 psi).

Anchor Plates: 1" x 12" x 12" (Use $h_{pl} = 12"$, $w_{pl} = 8"$)

Bending - at face of flange: $\phi_b = 0.90$

$a = h_{pl}/2 - d = 1.74"$ $\quad e = 3a = 5.22"$

$C = 1/2\ f\ e\ w_{pl}$ $\quad f = 2\ C / e\ w_{pl} = 0.780$ ksi

$m_{ut} = f\ a^2 / 2 = 1.18$ in-k/in (conservative)

$m_{ut} < 0.25\ \phi_b\ F_y\ t^2$

1.18 in-k/in < 8.10 in-k/in

Shear: $\phi_v = 0.90$

$$v_{ut} = V / 8 = 0.41 \text{ k/in}$$
$$v_{ut} = 0.41 \text{ k/in} < \phi_v (0.6 F_y) t^2 = 19.44 \text{ k/in}$$

Concrete Bearing: $\phi_p = 0.70$, $f'_c = 5000$ psi

$$C < \phi_p \, 0.85 f'_c A_1 \sqrt{A_2/A_1} \qquad \sqrt{A_2/A_1} \leq 2$$

A_1 = loaded area $\qquad A_2$ = Concrete area $\qquad$ Use $A_2 / A_1 = 1.0$

$$A_1 = e \, w_{pl} = 41.76 \text{ in}^2$$
$$C = 16.3^k < 124^k$$

<u>Plate 1" x 12" x 12" with 2 - 5/8" diameter A193 B-7 threaded rods with an embedment depth of 11" is adequate.</u>

REFERENCES

1. American Association of State Highway and Transportation Officials, Standard Specifications for Highway Bridges, Fourteenth Edition, Washington D.C., 1989.

2. American Institute of Steel Construction, Manual of Steel Construction, Load and Resistance Factor Design, First Edition, USA, 1986.

3. Beaupre, R.J., "Deviation Saddle Behavior and Desigm for Externally Post-Tensioned Bridges," Unpublished M.S. Thesis, The University of Texas at Austin, August, 1988.

4. Beaupre, R.J., Powell, L.C., Breen, J.E., and Kreger, M.E., "Deviation Saddle Behavior and Design for Externally Post-Tensioned Bridges," The University of Texas at Austin, Center for Transportation Research, Research Report 365-2, July 1988.

5. Bill, R.C., "Review of Factors that Influence Fretting Wear," Materials Evaluation Under Fretting Conditions, ASTM STP 780, American Society for Testing and Materials, 1982, pp. 165-182.

6. Carter, L.C., "Deviator Behavior in Externally Post-Tensioned Bridges," Unpublished M.S. Thesis, The University of Texas at Austin, August, 1987.

7. Cook, R.A., Doerr, G.T., Klingner, R.E., "Design Guide for Steel-To-Concrete Connections," The University of Texas at Austin, Center for Transportation Research, Research Report 1126-4F, March 1989.

8. Diab, J.G., "Fatigue Tests of Post-Tensioned Concrete Girders," Unpublished M.S. Thesis, The University of Texas at Austin, December 1988.

9. Eibl, J., and Voss, W.,"Zwei Autobahnbrucken mit externer Vorspannung (Two Motorway Bridges with External Prestressing)," Beton und Stahlbetonbau (84), 1989, Heft 11.

10. Eibl, J., "Externally Prestressed Bridges," External Prestressing in Bridges, ACI SP-120, 1990, pp. 375-387.

11. Eibl, J., "On Some External Prestressed Bridges in Germany," Federation Internationale De La Precontrainte, Eleventh Congress, Hamburg, 1990.

12. Foo, M.H., and Warner, R.T., "Fatigue Tests on Partially Prestressed Concrete Beams," Presented at the NATO Advanced Research Workshop, Paris, France, June 18-22, 1984.

13. Georgio, T., "Fretting Fatigue in Post-Tensioned Concrete Girders," Unpublished M.S. Thesis, The University of Texas at Austin, December 1988.

14. Hindi, A., "Enhancing the Strength and Ductility of Post-Tensioned Segmental Box-Girder Bridges," PhD Dissertation The University of Texas at Austin, December, 1990.

15. Jartoux, P., LaCroix, R., "Development of External Prestressing, Evolution of the Technique," Federation Internationale De LaPrecontrainte, 11th Congress, Hamburg, 1990.

16. Krueger, F.E., "Fretting Failures," Metals Handbook, Vol. 10, American Society for Metals, 8th Edition, pp. 154-160.

17. Lamb, J.L., and Frank, K.H., "Development of a Simple Fatigue Resistant Stay Cable Anchorage," The University of Texas at Austin, Center for Transportation Research, Research Report 384-1F, November 1985.

18. Lin, T.Y., and Burns, N.H., Design of Prestressed Concrete Structures, John Wiley & Sons, New York, 1981, pp. 87-125.

19. MacGregor, R.J.G., "Evaluation of Strength and Ductility of a Three-Span Externally Post-Tensioned Box Girder Bridge Model," PhD. Dissertation, The University of Texas at Austin, December, 1988.

20. MacGregor, R.J.G., Kreger, M.E., and Breen, J.E., "Strength and Ductility of a Three-Span Externally Post-Tensioned Segmental Box Girder Bridge Model," External Prestressing in Bridges, ACI SP-120, 1990, pp.315-338.

21. Muller, H.H., "Fatigue Strength of Prestressing Tendons," Betonwerk und Fertigteiltechnik, December 1986, pp. 804-808.

22. Oertle, J., Thurlimann, B., and Esslinger, V., "Versuche zur Reibermudung einbetonierter Spannkabel (Fretting Fatigue Tests of Post-Tensioning Tendons)," Institut fur Baustatik und Konstruktion, ETH Zurich (Swiss Federal Institute of Technology), Report 8101-2, October 1987.

23. Oertle, J., and Thurlimann, B., "Reibermudung einbetonierter Spannkabel (Fretting Fatigue of Post-Tensioning Tendons)," Festschrift Christian Menn zum 60. Geburtstag, Institut fur Baustatik und Konstruktion, ETH Zurich (Swiss Federal Institute of Technology), 1986, pp. 33-38.

24. Overman, T.R., Breen, J.E., and Frank, K.H., "Fatigue Behavior of Pretensioned Concrete Girders," The University of Texas at Austin, Center for Transportation Research, Research Report 300-2F, November 1984.

25. Paulson, C., Frank, K.H., and Breen, J.E., "A Fatigue Study of Prestressing Strand," The University of Texas at Austin, Center for Transportation Research, Research Report 300-1, April 1983.

26. Powell, L.C., Breen, J.E., and Kreger, M.E., "State of the Art for Externally Post-Tensioned Bridges with Deviators," The University of Texas at Austin, Center for Transportation Research, Research Report 365-1, June 1988.

27. Radloff, B.J., "Bonding of External Tendons at Deviators," Unpublished M.S. Thesis, The University of Texas at Austin, December, 1990.

28. Rignon, C., and Thurlimann, B., "Fatigue Tests on Post-Tensioned Concrete Beams," Report 8101-1, Institut fur Baustatik und Konstruktion, ETH Zurich (Swiss Federal Institute of Technology), May 1985.

29. Trinh, J., "Fatigue Resistance of Post-Tensioned Cables in Partial Prestressing," Federation Internationale De La Precontrainte, Eleventh Congress, Hamburg, 1990.

30. Virlogeux, M., "Non-Linear Analysis of Externally Prestressed Structures," Federation Internationale De La Precontrainte, Eleventh Congress, Hamburg, 1990.

31. Waterhouse, R.B., Fretting Fatigue, Applied Science Publishers Ltd., London, 1981, 240 pp.

32. Waterhouse, R.B., "Occurrence of Fretting in Practice and Its Simulation in the Laboratory," Materials Evaluation Under Fretting Conditions, ASTM STP 780, American Society for Testing and Materials, 1982, pp. 3-16.

33. Wharton, M.H., Taylor, D.E., and Waterhouse, R.B., "Metallurgical Factors in the Fretting Fatigue Behavior of 70/30 Brass and 0.7% Carbon Steel," Wear, Vol. 23, 1973, p. 251.

34. Wollman, G.P., "Fretting Fatigue of Multiple Strand Tendons in Post-Tensioned Concrete Beams," Unpublished M.S. Thesis, The University of Texas at Austin, December, 1988.

35. Wollman, G.P., Yates, D.L., Breen, J.E., and Kreger, M.E., "Fretting Fatigue in Post-Tensioned Concrete," The University of Texas at Austin, Center for Transportation Research, Research Report 465-2F, November 1988.

36. Yates, D.L., "A Study of Fretting Fatigue in Post-Tensioned Concrete Beams," Unpublished M.S. Thesis, The University of Texas at Austin, December 1987.

VITA

Cliff Raymond Hall was born in Blue Island, Illinois on October 29, 1962 to Robert and Karolyn Hall. After graduating from Thornridge High, Dolton, Illinois in June 1980, he attended The University of Illinois at Champaign/Urbana where he earned the degree of Bachelor of Science in Engineering in May 1984. During the following three years he was employed as a structural engineer at Sargent and Lundy Engineers, Chicago, Illinois. On August 17, 1985, he was married to Alesia Traci Gilcrease. In September of 1987, he started working as a civil engineer at Smith Engineering Consultants, McHenry, Illinois. He entered The Graduate School of The University of Texas at Austin in August 1988. In December 1990, he joined Greiner, Inc. as a structural engineer.

Permanent Address: 12712 Hampton Park Blvd.
Tampa, Florida 33624

This thesis was typed by Cliff R. Hall.